# EXTRACTION OF CALCIUM CARBONATE FROM WASTE EGGSHELLS AS FILLERS IN COMPOSITES

A Thesis Submitted to the College of
Graduate and Postdoctoral Studies
In Partial Fulfillment of the Requirements
For the Degree of Master of Science
In the Department of Mechanical Engineering
University of Saskatchewan
Saskatoon

By

GAURANG GOLAKIYA

## PERMISSION TO USE

In presenting this thesis in partial fulfillment of the requirements for a postgraduate degree from the University of Saskatchewan, I agree that the Libraries of this University may make it freely available for inspection. I further agree that permission for copying of this thesis in any manner, in whole or in part, for scholarly purposes may be granted by Professor Duncan Cree who supervised my thesis work or, in their absence, by the Head of the Department or the Dean of the College in which my thesis work was done. It is understood that any copying or publication or use of this thesis or parts thereof for financial gain shall not be allowed without my written permission. It is also understood that due recognition shall be given to me and to the University of Saskatchewan in any scholarly use which may be made of any material in my thesis.

Requests for permission to copy or to make other uses of materials in this thesis/dissertation in whole or part should be addressed to:

Head of the Department of Mechanical Engineering
University of Saskatchewan
57 Campus Drive
Saskatoon, Saskatchewan S7N 5A9
Canada

OR

Dean
College of Graduate and Postdoctoral Studies
University of Saskatchewan
116 Thorvaldson Building, 110 Science Place
Saskatoon, Saskatchewan S7N 5C9
Canada

## ABSTRACT

Large amounts of eggs are consumed in different forms around the world, which results in a massive amount of eggshells. These eggshells can end up in landfills, rivers or coastal waters which can impact public health, contamination of water resources and pollute the environment. Furthermore, in recent years, special focus is given to industrial sectors that are sources of pollution to the environment.

Mineral limestone, which is made of calcium carbonate ($CaCO_3$) is used as filler materials for polymer composites to reduce the cost and improve certain properties. On the other hand, eggshells contain high amounts of $CaCO_3$ with some organic membranes but are generally considered as a waste. In this study, to utilize waste eggshell as an alternative to limestone, thermal and chemical treatments are investigated to produce purified eggshell powder.

Polymer composites were made using bio-epoxy resin with different amounts of eggshell, purified eggshell and limestone fillers (5, 10 and 20 wt. %). Trace analysis of fillers, microscopic morphology, thermal and mechanical properties of fabricated composites are evaluated.

The filler powders were sieved using 20 and 32 μm size standard sieves. The particle size analysis using ImageJ software showed average particle diameters of 11.2 and 23.8 μm for 20 and 32 μm sieved powders, respectively possibly due to the presence of some lower particle sizes as a result of grinding. Eggshell powder had a higher weight loss when heated to 850 °C for 2 h than pure limestone powder due to the removal of organic membranes. Eggshell powder had a lower density than purified eggshell and limestone particles due to the presence of low density membrane. Composites with eggshell fillers absorbed higher water than composites with purified eggshell and limestone filler due to the presence of organic membrane in eggshell. Inductively coupled plasma mass spectrometry (ICP-MS) analysis showed $87.5 \pm 0.5$ wt. % of $CaCO_3$ content in pure eggshell, which increased to $95.0 \pm 0.5$ wt. % in purified eggshell due to the absence of organic membrane as a result of thermal and chemical treatments. Scanning electron microscopic (SEM) analysis of fractured surfaces showed a flat and mirror-like surface for bio-epoxy, which became rougher when loaded with eggshell fillers. Tensile, flexural and Charpy impact strengths decreased as the filler content was increased for all fillers. However, tensile and flexural modulus improved significantly and showed maximum values at 20 wt. % for all three fillers. Thermogravimetric

analysis (TGA) analysis showed higher weight losses between 300-550 °C for eggshell powder than purified eggshell and limestone due to the decomposition of the organic membranes. Economic analysis for an egg breaking plant in Lethbridge, Alberta showed that approximately 705,000 kg of $CaCO_3$ could be produced annually by recycling waste eggshell.

This research not only presents a way to reduce waste eggshell, but also shows a method to purify them for use as bio-epoxy composite filler materials. Bio-epoxy composites with eggshell fillers could be used in applications with higher tensile and flexural modulus with reduced cost such as plastic chairs, tables, skateboards, glass frames, boats, bicycles and toys.

## ACKNOWLEDGEMENTS

Throughout this study, I have been inspired by so many individuals who supported me. I would like to thank every single one of them.

I am deeply grateful to my supervisor, Prof. Duncan Cree, for giving me the opportunity of studying a master's degree and also, for his patient guidance, supports and motivations throughout of master study. I would also like to express my deep gratitude to Prof. Akindele G. Odeshi and Prof. Shafiq Alam for their valuable suggestions and guidance given as committee members.

I would also like to offer my special thanks to Prof. Carey Simonson and Prof. Ike Oguocha for the courses they offered which would definitely help me to become a successful engineer.

I would like to express my very great appreciation to Dr. Majid Soleimani for all his advice and suggestions regarding this study as well as the helps and training on the use of lab equipment.

I cannot omit mentioning my friends, Parth Borad, Vishnu Mistry, Asad Hatia, Jignesh Golakia, Jay Patel, Parth Jivani, Maaz Muhammad, Stephen Owuamanam and Wilson Navas for being my best memories.

Finally, I wish to thank my parents and my family for their endless love, supports, understandings and encouragement throughout my life.

## DEDICATION

This work is dedicated to my lovely parents, the roots of my life,

Mr. Madhavjibhai Golakiya and Mrs. Ushaben Golakiya.

## TABLE OF CONTENTS

## LIST OF TABLES

## LIST OF FIGURES

## LIST OF NOMENCLACTURES AND SYMBOLS

| | |
|---|---|
| $b$ | Flexural sample width (mm) |
| $d$ | Flexural sample thickness (mm) |
| $D_f$ | Degree of freedom |
| DSC | Differential scanning calorimeter |
| TGA | Thermogravimetric analysis |
| MMC | Metal matrix composites |
| PMC | Polymer matrix composite |
| CMC | Ceramic matrix composite |
| FRC | Fiber reinforced composites |
| $E_f$ | Flexural modulus (GPa) |
| $E_a$ | Impact energy (J) |
| $E_i$ | Energy absorbed per unit area ($J/m^2$) |
| BE | Bio-epoxy |
| ES | Eggshell |
| PES | Purified eggshell |
| LS | Limestone |
| $L$ | Length of support span (mm) |
| $L_o$ | Gauge length (mm) |
| $m$ | Slope of the load-deflection curve |
| $MS$ | Mean square |
| $P$ | Flexural load (N) |
| RH | Relative humidity |
| RT | Room temperature (23 °C) |
| SEM | Scanning electron microscope |
| $SS$ | Sum of squares |
| $T_g$ | Glass transition temperature ( ℃) |
| $v_f$ | Volume fraction of filler |
| $v_m$ | Volume fraction of matrix |
| $W_f$ | Weight fraction of filler |
| $W_m$ | Weight fraction of matrix |

| | |
|---|---|
| $m_a$ | Weight in air |
| $m_{cw}$ | Weight in liquid |
| $\rho_c$ | Density of composite (g/cm$^3$) |
| $\rho_m$ | Density of matrix (g/cm$^3$) |
| $\rho_f$ | Density of filler (g/cm$^3$) |
| $\rho_d$ | Density of liquid (g/cm$^3$) |
| $\sigma_f$ | Flexural strength (MPa) |
| $E_f$ | Flexural modulus of elasticity |

# CHAPTER 1
# INTRODUCTION

## 1.1 Overview

All over the world, agricultural wastes are some of the most emerging problems in food industries due to economic and environmental factors. However, this issue could become an opportunity for the bio-friendly society if new uses for these waste materials can be redeveloped. To protect the quality of the environment, research has focused on effective methods to properly manage agricultural wastes. A general waste hierarchy chart is shown in Figure 1.1 which outlines the most to least favored option for managing waste materials [1,2]. Making new products is one option which requires virgin materials and energy. Therefore, to limit the requirement of new products, waste must be minimized. The second option is to reuse waste materials. Households produce more and more waste and disposal to landfill sites are filling up. Various types of wastes could be reused, recycled and channeled towards valuable and utilizable products. To achieve sustainability, utilization of waste materials in new products is a priority [3].

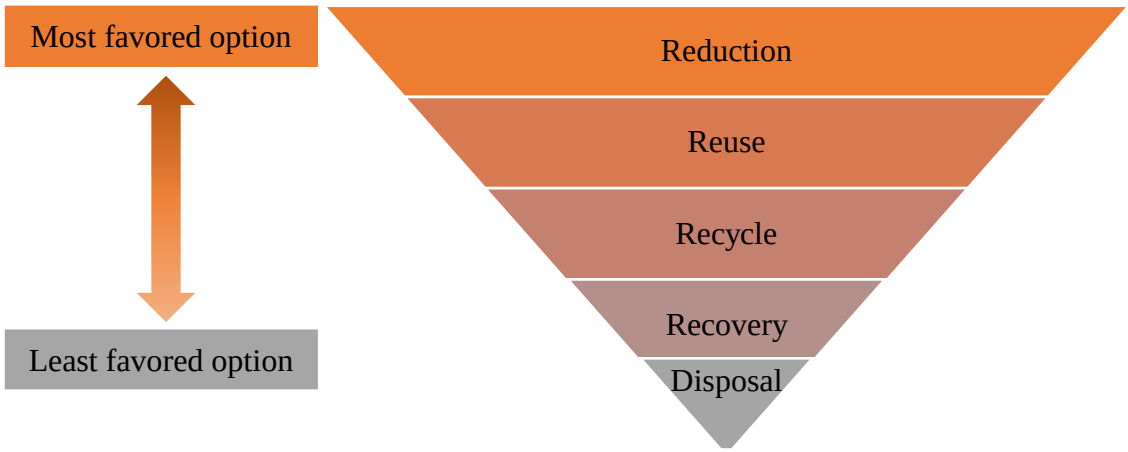


Figure 1.1 The waste hierarchy chart

Chicken eggs are extensively used in food processing plants. Currently, eggs are being used to make a variety of products such as cakes, salad dressings and quiches, whose production results in several daily tons of eggshell waste as a by-product and incur considerable disposal costs throughout the world. Eggshell contain high amounts (around 92 -95 %) of calcium carbonate ($CaCO_3$) but are generally discarded to landfills at a cost of $100,000 per year for one egg processing plant in United States [4][5]. About 8 million tons of eggshell waste is generated

annually worldwide and disposed as waste in landfill without any pretreatment which has been declared a source of organic pollution [6–8]. The eggshell accounts for approximately 10 wt. % of the total egg which could be recuperated and used in a variety of applications.

It is well known that composite materials are attracting interest in many applications and in particular within the plastic industry due to low cost, lightweight and improved mechanical properties. In the present review, eggshell waste are considered as a platform for new biomaterials [9,10]. Eggshell polymer composites can be used in machine components, plastic toys, electronic packaging, automotive and aerospace parts. According to the literature, a variety of composite material were produced using these waste eggshell for different applications such as enhancement of thermal conductivity of polyaniline material [11], absorbent material in active packaging [12], and heterogeneous catalyst in biodiesel production [13]. This highlighted an interest to further investigate and widen the possible uses of eggshell for new, lower cost green materials [14,15]. Eggshell have been used as filler materials for different polymer matrices, however, to the best of the author's knowledge, no research has been conducted on the purification of eggshell for use as fillers in bio-epoxy composites.

In previous studies, it was found that eggshell powders had physical, chemical and a crystalline structure similar to commercial limestone [16]. In this study, thermal and chemical treatments were performed on eggshell powder to remove organic membrane and to produce purified eggshell powder. A solution mixing technique was used to manufacture bio-epoxy composites with different filler loadings. Physical properties, density, and water absorption, mechanical properties such as tensile and flexural strengths/modulus and Charpy impact strengths and thermal property glass transition temperature were evaluated at different filler percentages. This research showed eggshell could be used as an alternative to replace commercial calcium carbonate fillers in bio-epoxy composites.

### 1.2 Research objectives

The goal of this research is to develop a combined thermal and chemical treatment to purify eggshell waste in order to fabricate and characterize bio-epoxy composites. To achieve this goal the following objectives are proposed:

1. To develop a heat and chemical treatment for removal of eggshell membranes from the eggshell.

2. To develop a bio-epoxy composite, using pure eggshell, purified eggshell and mineral limestone powder as filler materials.

3. To determine the effects of particle size and filler contents on the mechanical and thermal performance of the composite materials.

The major contribution of this research is to provide a way to purify and reuse waste eggshell for bio-epoxy composites and to evaluate mechanical and thermal properties of bio-epoxy/eggshell composites.

### 1.3 Thesis organization

This thesis consists of five chapters. Chapter 1 contains an overview of the topic, objectives and research contributions. A comprehensive literature review on eggshell polymer composites, its fabrication methods and properties are discussed in Chapter 2. Materials and experimental procedures to achieve the objectives are presented in Chapter 3. In the Chapter 4, the results of experiments from this work are presented and discussed. Finally, conclusions from the analysis of the tests results and some suggestions for future work are summarized in Chapter 5.

# CHAPTER 2
# LITERATURE REVIEW

Nowadays, bio-epoxy composites have gained significant recognition in different engineering applications due to their superior quality such as low shrinkage, strong mechanical properties, resistance to corrosive liquids and environments, good performance at elevated temperatures, and good adhesion to substrates. Different fillers such as wood, silica, calcium carbonate and talc have been used in the composite industry to improve specific properties or to reduce the cost of the final product by saving raw material or a mixture of both. Waste eggshell contain about 92-95 % limestone [17]. Limestone is a carbonate sedimentary mineral containing impurities, and is processed to produce pure limestone powder [18]. Comparison of waste eggshell and limestone as a filler in bio-epoxy composites have been reviewed and included in this chapter.

## 2.1 Composite materials

A composite is a material composed of two or more distinct phases (matrix phase and dispersed phase) and having significantly different properties from those of any of the individual phases. The objective is to produce a new superior material from both materials without compromising on the weakness of either. Composites can be classified based on the matrix material or the structure of the filler/reinforcement material. Detail classification of composite materials are shown in Figure 2.1. Composites based on matrix type are classified as metal matrix composites (MMC), polymer matrix composites (PMC) or ceramic matrix composites (CMC). Composite materials can also be classified based on the type of reinforcing materials: fiber or particles reinforced composites.

The primary function of the matrix is to transfer stresses between fillers/reinforcements and to protect them from environmental damage. Whereas the filler material in a composite functions as a load-bearing component [19]. The overall performance of composites depends on several factors such as fiber and resin type, filler/resin volume fraction, fiber structure, and fiber-matrix compatibility [20]. Fillers could be naturally available materials such as wood, bone, flax, grass or eggshells which are relatively cheaper but have lower mechanical properties than artificially produced materials. Artificial composite are made from stiffer and stronger fillers such as glass, carbon nanotubes, carbon, aramid or boron. They are very popular in high stress application such as aeronautical and military components because of their advance mechanical properties [21].

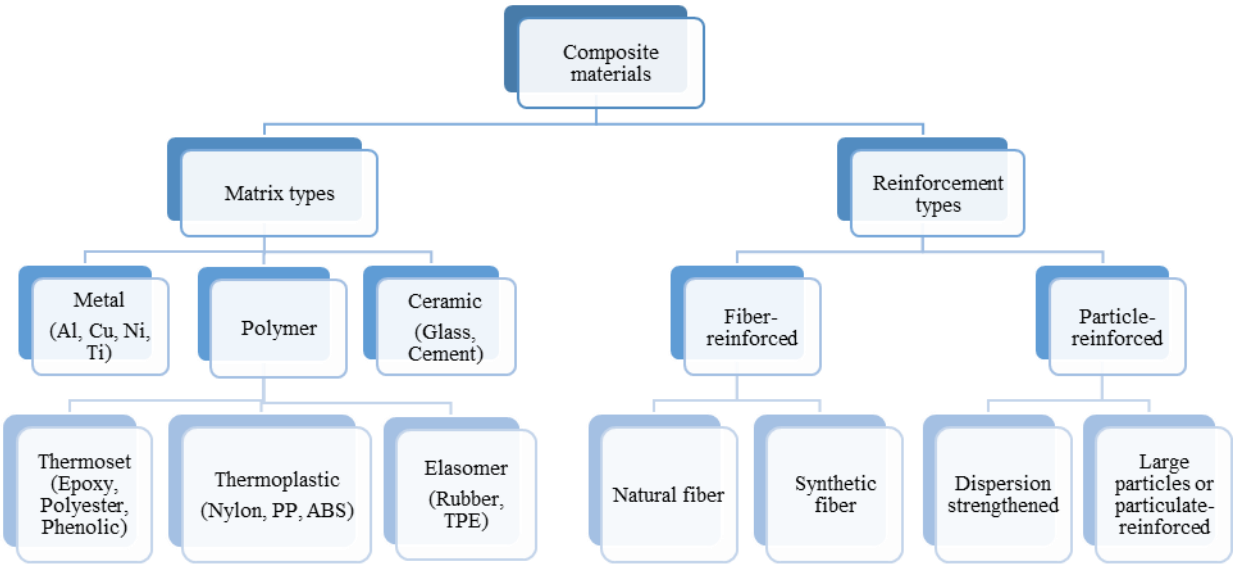


Figure 2.1 Classification of composite materials

### 2.1.1 Matrix types

The matrix in a composite binds the fiber reinforcements, transfers load between fibers and gives the component its net shape. Generally, composite matrices are divided into three groups: Metal matrix composites (MMC), Polymer matrix composites (PMC) and Ceramic matrix composites (CMC).

#### 2.1.1.1 Metal matrix composites (MMC)

MMCs usually consists of low-density materials for their matrix such as magnesium or aluminum with reinforcing ceramic materials such as silicon carbide or graphite. The reinforcement could be in the form of continuous fibers, short fibers, particles or whiskers. Compared to pure metals, MMCs offer high specific strength and stiffness, greater wear and tear resistance and can have higher operating temperatures. In addition, MMCs have the opportunity to modify their specific properties by changing the reinforcement diameters, orientation and distribution for specific applications. However, MMCs also have some disadvantages compared to pure metals such as higher fabrication costs, lower ductility and toughness [22]. Presently, MMCs are defined in two main groups. One consists of very high performance composites formed with expensive continuous fiber reinforcements along with costly processing methods which limits their current

markets to military and aerospace applications [23]. The second group consists of relatively inexpensive reinforcements producing low performance composites. Different techniques and methods in powder metallurgy [24] and surface coating [25] are being developed to enhance mechanical and thermal properties while decreasing the overall cost of MMCs [26].

#### 2.1.1.2 Polymer matrix composite (PMC)

PMCs are composed of a polymer (resin) matrix combined with a variety of short or continuous reinforcement materials. Polymers have low density and good chemical resistance compared to pure metals. However, the matrix of PMCs is typically the weak link which can usually be overcome by the addition of suitable reinforcement materials.

PMC products are increasing each year due to advantages such as low cost and simple fabrication methods with government legislation driving the pressure of recycling [27]. A PMC matrix is defined based on the recycling route of the plastic: thermosets or thermoplastics. Thermoset resins include polyester, epoxy, phenolic, vinyl-ester and polyamide, which creates extensive cross-links when cured. Unlike thermosets, thermoplastics consist of long, discrete chains, which can weaken rapidly and be transferred to a viscous liquid with increased temperature [28]. Examples of thermoplastics that can be recycled are nylon, acrylic, acrylonitrile butadiene styrene (ABS), polypropylene and polylactic acid (PLA). Thermoplastics are generally weaker then thermosets due to a lack of three-dimensional cross-links. However, under high stress conditions thermosets may undergo plastic deformation.

#### 2.1.1.3 Ceramic matrix composite (CMC)

Conventional precipitation and dispersion hardened metal alloys work efficiently at normal temperature. However, these materials may coarsen and become thermally unstable at higher temperatures resulting in a decline in mechanical strength [29]. CMCs combine ceramic fibers embedded in a ceramic material which has a benefit of high strength and stability at elevated temperature. CMCs offer low density, high hardness and superior thermal and chemical resistance. They are very popular and considered as a lightweight replacements for metallic super alloys in applications such as gas turbines for aerospace, maritime propulsion and other “hot-zone” structures [30].

### 2.1.2 Reinforcement types

A reinforcement is a material added to a matrix to impart specific properties of the base material. Broadly, composites based on reinforcement materials are classified into two groups: fiber reinforced composites (FRC) and particle reinforced composites (PRC).

#### 2.1.2.1 Fiber reinforced composites (FRC)

FRCs are materials used in advanced engineering applications because of their high stiffness and high-strength properties [31]. The performance of FRCs are significantly dependent on position and orientation of fibers [32]. FRCs are classified based on the source of fibers: synthetic fibers and natural fibers. Synthetic fibers are developed artificially and further classified as organic (aramid/Kevlar, polyethylene, aromatic polyester) and inorganic fibers (glass, boron, carbon and silica carbide). Synthetic fibers are more durable than natural fibers and possess superior thermomechanical properties mainly used in advanced systems such as high efficiency turbines, hypersonic aircraft and rocket nozzles. Natural fibers include fibers from animals (silk, wool and hair), cellulose (leaf, seed, fruit, wood, stalk and grass) and minerals (asbestoses). Unlike synthetic fibers, natural fibers are composed of biodegradable polymers which tend to produce environment friendly composites [33]. Generally, natural fibers have a lower cost, are lighter but have lower mechanical properties as compared to synthetic fibers. Depending on the targeted application, natural fiber based composites may be acceptable [34,35].

#### 2.1.2.2 Particle reinforced composites (PRC)

Generally, PRCs are popular due to their low cost, ease of production and forming abilities. PRCs are similar to FRCs but consist of reinforced particles or fillers to enhance the property of the resin instead of short or long fibers. In the literature, the terms particle reinforcement and particle filler are not used interchangeable. A reinforcement always leads to improvements in properties, while a filler may or may not increase the properties but does reduce the cost since fillers are cheaper than the polymer resins. If the particles are used to enhance the property of the resin then they are referred to as reinforcement particles whereas if particles are added to the matrix to produce cost effective composites, then the particles are referred to as fillers. For example, wood, hair, calcium carbonate, and kaolins are defined as fillers. Talc, mica and silica are generally treated as non-

fibrous reinforcements while fibrous reinforcements includes all glass fiber variants, carbon, boron, ceramic, aramid, and stainless steel fibers [36]. Particles can be in any size or shape, however they are generally spherical, ellipsoidal, polyhedral or irregular in shape. Particles could be used in their original form or sometimes they can be surface treated to be made compatible with the matrix. For instance, Wu *et al.* [37] showed hydrophilic particles can be converted into hydrophobic particles by a surface treatment which yielded better tensile and impact strengths for polymer composites due to lower particle agglomeration and better particle-matrix interaction. To improve the dispersion of eggshell particles in a polymer matrix, Ghabeer *et al.* [38] treated eggshell with stearic acid and results showed that treated particles in the polypropylene matrix had better thermal behaviors compared to composites containing untreated particles.

### 2.2 Limestone

Limestone is formed by the accumulation of sediments on the sea floor. These sediments gradually transformed into limestone minerals and are composed of over 50 % carbonate minerals. Depending on the type of limestone minerals, calcium carbonate can be extracted by various industrial processes such as the lime soda process, the calcium chloride process and the carbonation process [18]. Limestone is usually gray in color, but may also be found as brown, yellow or white color. There are three main components in limestone mineral: calcite or aragonite, dolomite and impurities. Both calcite and aragonite have different crystal forms of calcium carbonate but have the same chemical formula $CaCO_3$. Dolomite is a carbonate mineral that often forms from calcite. When liquids rich in magnesium carbonate ($MgCO_3$) pass through limestone minerals, the $CaCO_3$ reacts with $MgCO_3$, and forms dolomite ($CaMg(CO_3)_2$). Impurities in the form of sand grains, silt or mud are found in limestone minerals. These materials eroded from nearby lands and washed into the sea by rivers to be mixed with lime muds, shells, corals, etc. $CaCO_3$ has many industrial processes as it is used as a raw material in Portland cement, mining, paper and glass manufacturing. In addition, calcium is an important micronutrient and several commercial drugs (antacids and calcium supplements) are made from pulverized limestone.

## 2.3 Eggshell

An eggshell is the outer covering of a hard-shelled chicken egg, which consists mostly of $CaCO_3$ with some proteins and other minerals [39]. Detail chemical composition of the eggshell and its structure are discussed further.

### 2.3.1 Chemical composition of chicken eggshell

Eggshell is a strong bio-filler candidate as it contains a high percentage of calcium carbonate; it is available in bulk quantities and is inexpensive. According to the chemical analysis, eggshell contains about 92-95 % calcium carbonate with 5-7 % organic membranes [17]. Large amounts of eggshell are generated everyday around the world. Most of them are passed through egg breaking industries in which eggshell are broken and converted to various liquid egg products. New methods are being developed to recycle, reuse and to form new materials with minimum costs. According to statistics Canada, in 2016, Canada's annual egg production was 747.7 million dozen (or 8.97 billion eggs) [40] which includes eggs for consumption, rejected and hatching. Approximately 30 % of eggs are sent to egg-breaking industries, which is around 2.7 billion eggs, a significant amount of limestone waste. For instance, an average egg weights approximately 60-70 g depending upon the size of egg, and an empty eggshell represents 10-11 wt. % [41]. Therefore, around 17,500 tonnes (175,00,000 kg) of calcium carbonate could be produced from eggshell annually. Consequently, for every 100 million eggs that are discarded, 650 tonnes (650,000) of high grade calcium carbonate could be produced. This would provide an additional profit of $97,500 to egg breaking plants based on an approximate commercial limestone powder value of $150 per tonne [4]. Utilization of eggshell as a filler material in polymer composites not only provides a cost-effective way of recycling this solid waste but also reduces its environmental effects significantly. More importantly, waste eggshell have been used as an alternative source of mineral limestone for various applications such as $CO_2$ sorbents [42], low-cost solid catalyst for biodiesel production [43], ceramic wall tile paste [44], eggshell in adsorbents for defluoridation of drinking water [45], and bio-fillers in polymer composites [46].

### 2.3.2 Egg structure

The eggshell consists of different layers positioned in a well-organized structure, which grows in various segments of the hen's oviduct [17]. A number of different proteins (soluble and insoluble), minerals and fibers are deposited during the process of eggshell formation which is later used up by the developing embryo. The eggshell is mainly composed of three parts: shell, albumen and yolk as shown in Figure 2.2. The inner part yolk is surrounded by albumen layers that are covered by the hard eggshell. The outer eggshell layer is composed of a thin film layer called cuticle, a limestone layer and two shell membranes (inner and outer membranes).

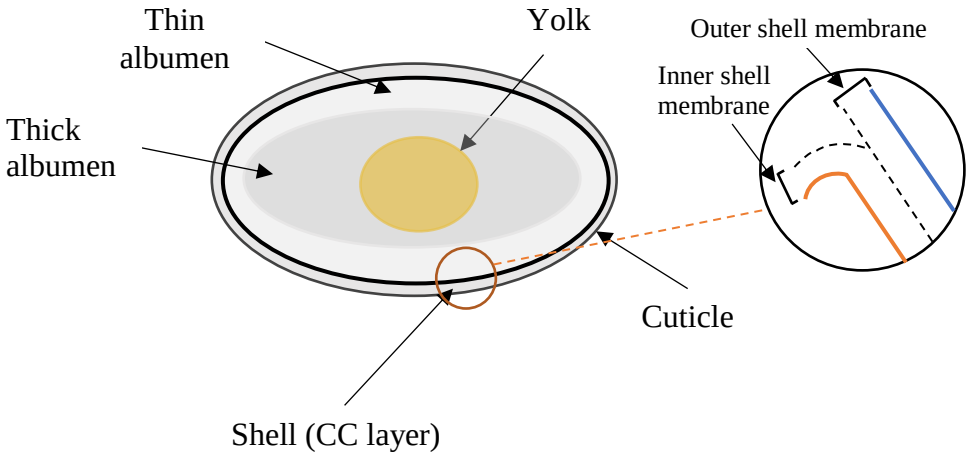


Figure 2.2 Egg structure and its different components

The cuticle is the outer most layer measuring about 10 to 20 µm thick and prevents moisture and bacterial penetration to a certain extent [47,48]. Matthes *et al.* [49] suggested the cuticle could be removed from the shell easily by soaking eggs in either weak acid solutions or just by washing with water. Around 95 % of the eggshell consist of inorganic limestone substance, 3.3 % protein and 1.6 % water [17]. The eggshell membranes are composed of inner and outer membranes with thicknesses of 50 µm and 15 µm, respectively. Maxwell *et al.* [50] identified different types of collagen proteins, amino and carboxylic acids in both inner and outer layers of the membrane. The egg albumen portion consists of a thin and thick albumen which covers the yolk in the center of the egg. The yolk is mainly made of protein and lipids which consists of yellow yolk (around 98 %) and white yolk (around 2 %).

### 2.3.3 Global egg production

According to "Atlas of the Global Egg Industry" [51], in 2011, total world egg production reached a volume of 65.0 million tonnes. Figure 2.3 shows a detailed pattern on a by country basis of egg production by tonnes (T) where 76-78 % of the total production was concentrated in 15 countries. Furthermore, between 1971 to 2011, the total egg production growth was 225 %, which is expected to follow the same trend for the next few decades as the global population is expected to increase from 6.9 billion to 8.0 billion from 2010 to 2025, respectively or by 16.10 %. In 2011, the top egg producing country was China with 24.1 million tonnes (around 37.20 % of the global production volume). This is followed by the USA with 5.4 million tonnes (8.28 % of global egg production), India with 3.5 million tonnes (5.38 %) as well as Japan and Mexico with 2.5 million tonnes each with 3.79 % of the global production.

| 1971 | | | 1991 | | | 2011 | | |
|---|---|---|---|---|---|---|---|---|
| **COUNTRY** | **PRODUCTION (1,000 T)** | **SHARE (%)** | **COUNTRY** | **PRODUCTION (1,000 T)** | **SHARE (%)** | **COUNTRY** | **PRODUCTION (1,000 T)** | **SHARE (%)** |
| USA | 4,126 | 20.4 | China | 7,589 | 20.8 | China | 24,149 | 37.2 |
| USSR | 2,486 | 12.3 | USSR | 4,478 | 12.3 | USA | 5,419 | 8.3 |
| Japan | 1,800 | 8.9 | USA | 4,114 | 11.3 | India | 3,490 | 5.4 |
| China | 1,584 | 7.8 | Japan | 2,498 | 6.9 | Japan | 2,483 | 3.8 |
| Germany | 1,165 | 5.8 | Brazil | 1,315 | 3.6 | Mexico | 2,459 | 3.8 |
| United Kingdom | 879 | 4.3 | India | 1,210 | 3.3 | Russia | 2,284 | 3.5 |
| France | 647 | 3.2 | Mexico | 1,141 | 3.1 | Brazil | 2,037 | 3.1 |
| Italy | 588 | 2.9 | Germany | 922 | 2.5 | Indonesia | 1,166 | 1.8 |
| Spain | 494 | 2.4 | France | 918 | 2.5 | Ukraine | 1,064 | 1.6 |
| Poland | 396 | 2.0 | Italy | 715 | 2.0 | France | 840 | 1.3 |
| Brazil | 355 | 1.8 | Netherlands | 646 | 1.8 | Spain | 830 | 1.3 |
| Mexico | 350 | 1.7 | Spain | 641 | 1.8 | Turkey | 810 | 1.2 |
| Canada | 333 | 1.6 | United Kingdom | 634 | 1.7 | Germany | 777 | 1.2 |
| India | 308 | 1.5 | Thailand | 482 | 1.3 | Iran | 741 | 1.1 |
| Netherlands | 265 | 1.3 | Republic of Korea | 422 | 1.2 | Italy | 737 | 1.1 |
| **15 countries** | **15,776** | ***78.1** | **15 countries** | **27,724** | ***76.0** | **15 countries** | **49,286** | **75.8** |
| **World** | 20,206 | 100.0 | **World** | 36,453 | 100.0 | **World** | 65,003 | 100.0 |

Figure 2.3 Top 15 leading egg producing countries in 1971, 1991 and 2011 [51]

## 2.4 Particulate filled polymer composites

Mechanical performance of materials have been improved by dispersing particles in ceramic, metal and polymer matrices. To overcome the weakness of pure polymers such as low stiffness and low strength, particulate micro/nano fillers such as silica ($SiO_2$), alumina ($Al_2O_3$), glass and limestone are often added to polymer based composites [52,53]. Properties of polymer composites can be

strongly controlled by changes in filler characteristics and amounts [54,55]. Depending on the size of particles, they are classified into two groups: dispersion strengthen composites and large particle or particulate reinforced composites.

Dispersion strengthen composites are common in metals where small particles in the range of 10 to 100 nm in diameter are added to the matrix material. These particles resist matrix deformation and produces materials that are harder and stronger. Whereas, the particles in large particle reinforced composite are generally coarse and larger than in dispersion strengthen composites, typically in the order of few μm. The term "large" is used to indicate that particle–matrix interactions cannot be treated at the atomic scale. Here, the particles carry the majority of the load and particles are used to increase the modulus and decrease the ductility of the matrix.

### 2.5 Epoxy resin

The matrix materials also have influence on the characteristics of the composites. Vörös *et al.* [56] used two different matrices, low-density polyethylene (LDPE) and polyvinyl chloride (PVC) with the same limestone filler. The results showed the composites with the LDPE matrix improved in tensile strength as the percentage of filler increased while the tensile strength of PVC continuously decreased with increasing filler content. The author concluded that compatibility of limestone particles was higher in the LDPE matrix than in the PVC matrix. As a result, tensile strength in PVC resin reduced due to a decrease in the mobility of filler particles during tensile loading.

Synthetic epoxy or pure epoxy is the most commonly used thermoset matrix resin in the composites industry. Epoxy resin refers to molecules containing two or more epoxy groups. Epoxy resins are cured with the addition of a curing agent, which is commonly called a hardener. The most common type of curing agent is amine based. Hongwei *et al.* [57] showed that strengthening and toughening effects were achieved by adding nano limestone particles in epoxy matrix. Epoxy composites have very low shrinkage during curing and as a result can be fabricated with a relatively high degree of dimensional accuracy [58].

Currently around 75 % of the epoxy polymers worldwide are produced from the diglycidyl ether of bisphenol A (DGEBA) [59]. However, in the manufacturing process of epoxy from bisphenol A, hazardous toxic substances are produced that may be regulated in certain applications in the

future. Thus bio-sourcing of epoxy from plant and other natural sources would not only reduce the consumption of bisphenol A but would also produce more environmental friendly polymers. For these reasons, the bio-epoxy polymers recently received a great deal of attention. Different manufactures are producing different types of bio-epoxy with different properties. For example, commercially available bio-epoxy are; Change Climate bio-epoxy (77 % bio-content), Sicomin Greenpoxy (35-56 % bio-content), and ONE Epoxy by Entropy resin® (30 % bio-content). Overall, bio-epoxy has excellent chemical resistance, outstanding adhesion to a variety of fillers, remarkable resistance to corrosion, durability and dimension stability (low shrinkage) during curing [60]. François *et al.* [61] made bio-based epoxy from different plant based mononmers such as diglycidylether of iso-eugenol (DGE-isoEu) and diglycidyl ether of resorcinol (DGER) to replace DGEBA.

### 2.6 Chemical characterization of eggshell powder

To understand decomposition and phase change analysis of eggshell, Khemthong *et al.* [62] performed thermogravimetric analysis (TGA) and measured the weight loss between 25 °C to 1000 °C (Figure 2.4 (a)). The TGA curve showed a small weight loss around 100 °C due to evaporation of surface water and also between 400 °C-550 °C due to removal of trapped water and organic compounds. A major weight loss was found between 720 °C-830 °C (peak at 810 °C) as $CaCO_3$ began to convert into calcium oxide (CaO) due to loss of $CO_2$. They also observed the crystalline phase of the calcined sample using X-ray diffractometer (XRD) (Figure 2.4 (b)). As shown in Figure 2.4 (b), calcined CaO samples showed sharp defractions at (1 1 1), (2 0 0), (2 2 0), (3 1 1) and (2 2 2) orientations, which proved the calcined sample was well crystalized during the heat treatment process. Furthermore, Viriya empikul *et al.* [63], Cree *et al.* [4] and Park *et al.* [64] showed that calcination of eggshell at 850-950 °C completely converted $CaCO_3$ to CaO.

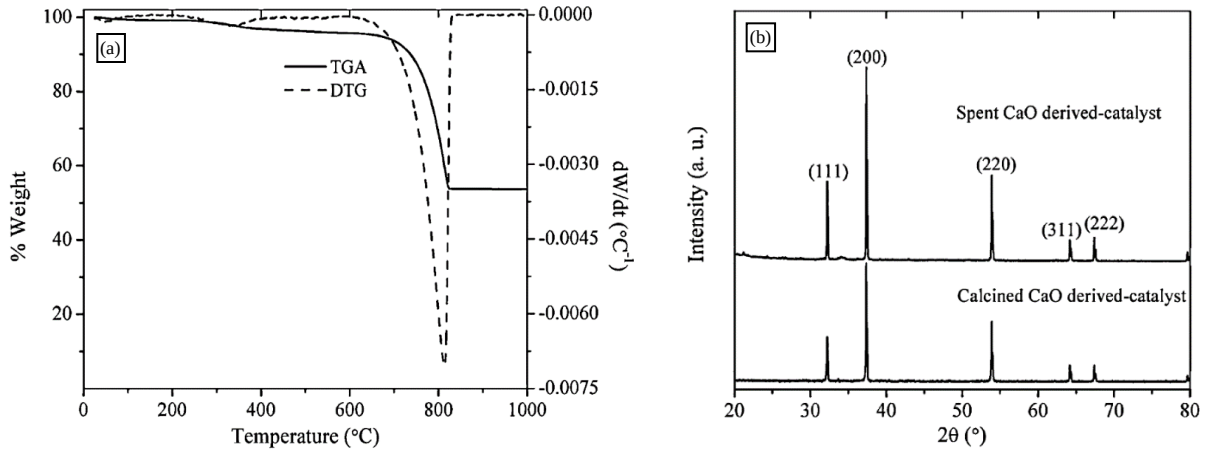


Figure 2.4 (a) eggshell TGA/DTG curve and (b) XRD pattern [62]

In addition to $CaCO_3$, trace elements in eggshell were examined by Kim *et al.* [65] which showed small concentrations of Zn, Cd, Pb, and Mn. Park *et al.* [64] compared the composition of pure eggshell with calcined eggshell. As shown in Table 2.1, pure eggshell contained 91.94 % calcium (Ca) which increased to 99.63 % when heated to 850 °C for 2 h. Besides Ca, other elements such Si, Al, Na, K and F were also found in small amounts in X-ray fluorescence (XRF) results. Different studies showed different trace elements in eggshell which could be due to the change in ambient and nourishment of a chicken [66].

Table 2.1. Composition of eggshell (natural and calcined) by XRF [64]

| Compound | Natural (%) | Calcined (%) | Compound | Natural (%) | Calcined (%) |
|---|---|---|---|---|---|
| Ca | 91.94 | 99.63 | P | 0.32 | 0.06 |
| Si | 4.30 | | Cl | 0.25 | |
| Al | 1.44 | | Sr | 0.16 | 0.16 |
| Na | 0.53 | | Fe | 0.09 | |
| K | 0.48 | 0.14 | Zn | 0.07 | |
| F | 0.42 | | Zr | 0.01 | |

In many applications where materials are subjected to periodic heating and cooling due to thermal cycling, some of the matrix materials can also be a major source of thermal failure, which can be understood by the glass transition temperature ($T_g$). The $T_g$ is one of the most important properties of polymer composites and is the temperature region where the polymer transitions from a rigid, glassy material to a soft, flexible material. Mohan *et al.* [67] studied the $T_g$ of epoxy composites containing nano eggshell particles with average particle size of 50 nm. Nano sized eggshell

particles were prepared by ultrasonic irradiation and mechanical attrition techniques [68]. Differential scanning calorimetry (DSC) results illustrated a $T_g$ of 68 °C for pure epoxy, which increased by 3, 4, 4 and 6 % at 2, 3, 4 and 5 wt. % of nano fillers, respectively. The authors suggested the increment of $T_g$ with increasing nano eggshell contents was due to particles restricting the matrix molecular movement at higher temperatures.

### 2.7 Eggshell filled composites

Limestone in the form of mineral rocks and derived from waste chicken eggshell or seashell have been added to different thermosets (epoxy and polyester) and thermoplastic polymers (polypropylene, PLA, polyethylene). Effect of eggshell and limestone fillers on mechanical and physical characteristics with various resins have been reviewed and are presented in this section.

#### 2.7.1 Epoxy matrix

Azman *et al.* [69] compared the properties of eggshell and limestone fillers with epoxy resin as matrix. They varied the filler particles of 500 µm size with amounts of 5, 10, 15 and 20 wt. % in the presence of a fixed amount of curing agent in epoxy composites. The eggshell fillers and epoxy was mixed using a magnetic stirrer at room temperature and the mixture was poured into a mold. The mold surface was covered with a sample-releasing wax for ease of sample pullout from the mold after the curing process (post-curing temperature and method was not reported). The tensile strength for pure epoxy was 39.0 MPa, whereas inclusion of 5, 10, 15 and 20 wt. % of eggshell particles showed decrements in tensile strengths by 13, 15, 23 and 33 %, respectively. Reductions in tensile strength were due to a weak ability of filler particles to transfer stress from the epoxy which ultimately led to poor adhesion of filler matrix and agglomeration of the eggshell. On the other hand, tensile modulus was observed to be 1.0 GPa for pure epoxy and increased by 2, 4 and 8 % for 5, 10 and 15 wt. % of fillers and then decreased by 1 % for 20 wt. % of fillers, respectively. The improvement in tensile modulus up to 15 wt. % loading was due to the presence of stiffer $CaCO_3$ particles from the eggshell which were able to absorb higher stresses with reduced deformation [70]. At a filler loading of 20 wt. % the decrement in tensile modulus was due to the aggregation of dense particles. Flexural strength for pure epoxy was 62.0 MPa and drastically reduced by 34 % for both 5 and 10 wt. % of eggshell fillers which was due to fact that the fillers may not disperse well in epoxy. However at 15 wt. % fillers, the composites showed nearly the

same tensile strength as pure epoxy but reduced by 13 % at 20 wt. % loading. Flexural modulus also showed the same trend with 1.5 GPa for pure epoxy and reductions of 28 and 23 % at 5 and 10 wt. % of fillers, respectively followed by a 10 % improvement at 15 wt. % and which again decreased by 13 % at 20 wt. % of eggshell fillers. Results showed that 15 wt. % of eggshell was the optimum loading for the best flexural strength and best tensile and flexural modulus. Therefore the authors compared the properties of eggshell and limestone composites containing 15 wt. % of fillers. Composites with limestone fillers showed slightly poorer tensile and flexural strengths as well as tensile and flexural modulus compared to eggshell filler composites. The differences may have been attributed to the tendency of a higher agglomeration of the inorganic limestone particles than eggshell particles [71]. This was a result of a better compatibility of eggshell particles in epoxy resin then limestone particles. This study suggested eggshell could be an ecological, environmentally friendly and low-cost alternative of some inorganic fillers. Mechanical properties of epoxy/eggshell composites in this study were generally lower than other research in the literature. This could be due to larger filler particle sizes [72].

In another work, Kaybal *et al.* [73] studied the influence of nano limestone particles on carbon fiber epoxy composite. They used as-purchased nano limestone powder with average particle size of 40 nm and varied the filler material from 0, 1, 2, 3, 4 and 5 wt. %. The filler material and resin was mixed using an ultra sonicator at room temperature. The composites were cured at 80 °C for 1 h, at 120 °C for 2 h and were slowly cooled to room temperature in an oven. They found pure epoxy with carbon fibers had a tensile strength of 53.5 MPa which improved by 20, 34 and 13 % when 1, 2 and 3 wt. % limestone particles were added, respectively, but reduced by 19 and 33 % for 4 and 5 wt. % filler loadings, respectively. Microscopic analyses of the fractured surfaces showed the improvement of tensile strengths were a result of better adhesion between fiber-matrix particles due to the presence of limestone particles. However, at higher loadings, limestone particles became predominant and reduced the strengthening effect of carbon fiber which ultimately reduced the tensile strength of the composites. Furthermore, Backes *et al.* [74] observed the effect of carbon nanotube (CNT) additions in limestone/epoxy composites. They varied the contents of CNT by 0.05 and 0.1 wt. % with fixed 1 wt. % of limestone particles. The results showed the flexure strength for pure epoxy was 96.0 MPa which improved by 3 % and 6 % for 0.05 and 0.1 wt. % of CNT, respectively. The flexure modulus was observed to be 2.7 GPa for pure epoxy which improved by 7 and 9 % for 0.05 and 0.1 wt. % of CNT, respectively. The authors

suggested improvements in flexural strength and modulus was due to the formation of epoxy/limestone interphase that restricted polymer chain mobility. This study suggested that low cost limestone fillers could be used to improve properties of epoxy composites.

Ji *et al.* [75] studied the possibility of adding eggshell as a filler material for epoxy composites by varying the eggshell filler content from 1-10 wt. % with average particle size of 10 µm. To remove membranes, washed eggshell powder was immerses in a 4.0 % NaOH solution for 72 h. Then it was dried in a vacuum oven at 60 °C for 3 h. An appropriate amount of eggshell filler and acetone were mixed at room temperature for 15 min, followed by ultrasonic stirring for 30 min at a frequency of 47 kHz. After the epoxy resin was added, the mixture was evacuated for 15 min to remove the solvent (acetone), and heated to 100 °C after stirring for 15 min at room temperature. The steel mold was initially preheated to 90 °C in which the mixture was carefully poured. Then, for degasification, the steel mold was placed into a vacuum oven for 10 min at 90 °C. The composites were post-cured in two stages; 90 °C for 2 h and at 150 °C for 5 h. The authors found an improvement in Charpy impact strength for epoxy composites with eggshell contents of 5 wt. % which reached a maximum value of 16.7 $kJ/m^2$ (cross section not reported) compared with 9.7 $kJ/m^2$ for pure epoxy resin. At 10 wt. %, the impact strength of the composites increased to 12.3 $kJ/m^2$ compared to pure epoxy. The improvement in impact strength was due to the presence of hard eggshell particles, however aggregation was present at higher filler loadings. The authors suggested that eggshell could be a potential source of filler to improve the epoxy resin toughness.

Shah *et al.* [76] treated eggshell with stearic acid to improve the dispersion and adhesion in an epoxy matrix. The crushed particles were soaked in ethanol at 15:1 ratio for 30 min to remove impurities. Eggshell particles (2-5 µm) were then dipped in a stearic acid solution, where the liquid solution was stirred at 300 rpm at different temperature stages (25 to 105 °C at 20 °C ramp) and time periods (20 to 60 min at 10 min intervals). The epoxy was heated to 80 °C and was mixed with the filler using the ultrasonicate mixture for 30 min. The samples were cured at ambient temperature for 24 h and post-cured at 90 °C for 2 h. Tensile strength for pure epoxy was 75 MPa, which decreased by 9 and 12 % for untreated eggshell particles, while reductions of 11 and 16 % were observed for treated eggshell particles with 15 and 20 wt. % loadings, respectively. The authors suggested decrements in tensile strength at higher filler loadings could be due to agglomeration of particles in the composites. Furthermore, FTIR results on the composites showed

the specimens contained lower organic compounds and higher carbonyl groups possible due to the stearic acid surface treatment interacting with eggshell proteins which could create weak intermolecular hydrogen bonding with the epoxy. While pure eggshell particles generated direct cross-linking of organic protein with epoxy [77]. This could be the reason for slightly higher tensile strengths of pure eggshell particles compared to the treated particles.

### 2.7.2 Polyester matrix

Hassan *et al.* [78] examined the mechanical performance of composites made with thermoset polyester resin with pure and carbonized eggshell particles (carbonization temperature not reported) having an average size of 20 µm with 0 to 50 wt. % of fillers. The polyester resin and eggshell filler was mixed by hand at room temperature. This mixture was then poured into a wooden mold, which was covered with a small layer of petroleum jelly to prevent the polyester from sticking to the mold during removal. The tensile strength for pure polyester was 90.0 MPa and increased by 7 % when 30 wt. % of uncarbonized eggshell particles were added, but remained constant at 7 % for 40 and 50 wt. % loadings, while carbonized eggshell composites showed steady improvements of 18 % at 30 wt. % filler loadings and then remained constant for 40 and 50 wt. % loadings. This research suggested that carbonized eggshell showed better strengthening effects due to a better compatibility between eggshell powder with the polyester resin. Flexural strengths increased steadily from 76.0 MPa for pure polyester to a maximum increment of 28 % at 40 wt. % loadings and then reduced to 9 % at 50 wt. % loadings for uncarbonized eggshell composites. However, for carbonized eggshell composites, a maximum increment of 40 % was observed at 20 wt. % of fillers. The decrement in flexural strength at higher loadings was due to weak interfacial bonding between dense filler particles and matrix. Charpy impact energy also increased from 0.1 J (20 J/cm$^2$ ) for pure polyester to a maximum increment of 250 % at 30 wt. % for uncarbonized eggshell and 350 % at 20 wt. % for carbonized eggshell due to the present of hard filler particles and better filler-matrix interface in the polyester resin. SEM observations showed the tensile and flexural strength improvements were attributed to the better interfacial bond between carbonized particles and the polyester resin.

Rahman *et al.* [79] studied the mechanical properties of various eggshell and limestone polyester composites. The filler particles of 1-8 µm size were varied by 5, 10, 15, 20 and 25 wt. %. Methyl

ethyl ketone peroxide as a catalyst was added to polyester resin at a standard ratio and the homogeneous mixture was poured into an aluminum frame at room temperature. The samples were post-cured at 70 °C for 10 min. They found pure polyester to have a tensile strength of 28 MPa which improved by 21 % for eggshell particles and 2 % for limestone particles at 5 wt. % of fillers. The composite strengths reached a maximum at 10 wt. % of fillers which translated to an 85 % and 71 % improvement for eggshell and limestone particles, respectively. However further increment in fillers (both eggshell and limestone) showed decrements in tensile strengths and decreased by 11 % and 10 % for 25 wt. % of eggshell and limestone filler loadings, respectively. The flexural strengths showed similar trends with a value of 74 MPa for pure polyester, which increased gradually and reached a maximum for both fillers at 10 wt. % loading with improvements of 37 % and 32 % for eggshell and limestone fillers, respectively. After this point, flexural strengths reduced by 35 % and 44 % at 25 wt. % of eggshell and limestone fillers, respectively. The strength decrements were due to increased void contents and uneven distribution of filler in matrix due to high percentage of fillers. Water absorption test showed that composite films with higher filler contents absorbed more water due to the formation of agglomeration which increased as a result of the nonhomogeneous dispersion of fillers at higher filler contents. After 4 h of soaking, water absorption values were 1.53 %, 1.96 % and 2.12 % for pure polyester, eggshell and limestone composites with 10 wt. % filler content, respectively. The composites with eggshell and limestone fillers absorbed more water than pure polyester because of the hydrophilic nature of calcium carbonate based particles [80].

### 2.7.3 Polypropylene matrix

Toro *et al.* [81] used thermoplastic polypropylene as the matrix and compared the tensile modulus of composites with eggshell and limestone fillers containing particle sizes of 1-20 μm. Initially, washed eggshell were dried at 90 °C for 8 h and then mechanically ground and sieved to achieve fine powders. The polypropylene and filler were mixed with 0.2 wt. % of an antioxidant in a nitrogen atmosphere at 75 rpm and at a temperature of 190 °C for 15 min. After blending, the composites were pelletized and pressed according to specific dimensions. Results revealed both eggshell and limestone improved in tensile modulus values as compare to pure polypropylene composites. Furthermore, the tensile modulus for pure polypropylene was 1.3 GPa which increased to 2.5 GPa (92 % higher) and 1.9 GPa (46 % higher) for 40 wt. % of eggshell and limestone filler

loadings, respectively. The tensile modulus increased with an increase in filler content due to the higher stiffness of eggshell and limestone particles compared to the pure polypropylene.

Another study by Kumar *et al.* [82] showed the effect of eggshell and limestone filler concentrations on polypropylene composites. The particle size of eggshell and limestone were 20 and 6-8 µm, respectively and varied by 5, 10, 20 and 30 wt. %. The particles were treated with isophthalic acid to increase the adhesion between the filler and matrix. To prevent degradation of the polymer during compounding, small amounts of antioxidants were added to the eggshell-polypropylene mixture. A twin screw extruder was used for homogeneous mixture of the fillers at 230 °C. The mixture was blended at a screw speed of 150 rpm under nitrogen atmosphere. The samples according to ASTM standards were prepared with an injection molding machine using Axxicon molds. The tensile strengths decreased for both filler types for all weight percentages due to agglomeration of eggshell and limestone particles in the polypropylene resin. Pure polypropylene showed a tensile strength of 35 MPa, which decreased by 12, 12, 14 and 20 % for eggshell and 6, 9, 14 and 14 % for limestone fillers with 5, 10, 20 and 30 wt. %, respectively. This was attributed to agglomeration of eggshell fillers in the polypropylene resin. However, treated eggshell with isophthalic acid showed slightly higher tensile properties. Tensile modulus for all composites increased considerably as compared to pure polypropylene and showed a maximum value for 30 wt. % of filler loadings. The tensile modulus for pure polypropylene was 0.4 GPa and improved by and 1, 2, 4 and 19 % for eggshell and 2, 6, 10 and 25 % for limestone with 5, 10, 20 and 30 wt. % respectively. Comparatively, treated eggshell showed the highest improvement of 1, 6, 24 and 31 % for same filler loadings, respectively. The flexure modulus (flexure strength was not reported) also showed the same trend as the tensile modulus with a value of 1.3 GPa for pure polypropylene which had improvements in the range of 2-40 % for eggshell and 4-48 % for limestone for the filler range of 5-30 wt. %. The researchers suggested the improvements in tensile and flexural modulus were due to better interfacial bonding of chemically treated filler particles.

### 2.7.4 Polyethylene biopolymer resin

Furthermore, to make environment friendly composites, Boronat *et al.* [83] used a bio-based polyethylene as a matrix material with different loadings of eggshell as fillers (0, 5, 10, 20, 30 and 40 wt. %). To increase the percentage of ecofriendly material in the composite, they used a petroleum matrix obtained from sugar cane ethanol. The eggshell from a local bakery were milled

and sieved to obtain particles within a 25 μm range. Polyethylene is a hydrophobic polymer, while eggshell are a hydrophilic filler [84]. To create a hydrophobic surface to the filler and to improve the interaction between the polymer resin and the filler particles, eggshell particles were titanate treated. Filler and matrix were mixed using a twin screw co-rotating extruder at a temperature of 180 °C. After blending, the composites were pelletized in order to be injection molded as per specific dimensions. The tensile strength results showed a maximum value of 20 MPa for pure polyethylene but decreased by 2, 5, 11, 15 and 25 % for 5, 10, 20, 30 and 40 wt. % of treated eggshell fillers, respectively. The authors suggested the reductions in strengths were due to an improper adhesion between the matrix and the filler at higher loadings. However, flexural strength for pure polyethylene was observed to be 24 MPa and improved by 1, 5, 6, 8 and 8 %, respectively. Pure polyethylene showed tensile and flexural modulus of 0.4 GPa and 0.8 GPa, respectively which increased by 6, 9, 18, 50, 65 % and 6, 9, 27, 29, 88 %, respectively for the same wt. % of treated eggshell. The flexural modulus evidently improved as the filler content increased which was due to the high density of the stiffer $CaCO_3$ in the composite. Charpy impact results showed pure polyethylene to have an impact energy of 0.28 $KJ/m^2$ which decreased by 38, 37, 42, 55 and 58 %, respectively. This decrement in impact energy with higher filler loading was due to the higher agglomeration which generated poor interfacial regions during impact. Furthermore, composites with 20 wt. % loadings were produced to compare the effect of untreated and treated eggshell and limestone fillers. The results showed pure polyethylene had a tensile strength of 20 MPa which reduced by 14, 11 and 14 % for limestone, eggshell and treated eggshell fillers, respectively. The decrease in tensile strengths for all composites, regardless of the eggshell treatment was due to adhesion of the filler-matrix and the agglomeration of filler particles in the composite. The tensile modules for pure polyethylene was 0.4 GPa and remained the same for limestone composites but improved by 8 % and 18 % for eggshell and treated eggshell at 20 wt. %, respectively. The treated eggshell particles showed higher modulus values due to the better particle-matrix bonding as a result of the chemical treatment.

### 2.7.5 Effect of particle size on eggshell composites

Zuiderduin *et al.* [85] showed the particle size had a large effect on composite properties. Similar to particle size, particle size distribution in a polymer matrix is equally important to characterize the properties of composite materials [86]. Nwanonenyi *et al.* [87] analyzed the effect on

mechanical properties of polyethylene/eggshell composites as a function of filler content (5, 10, 15, 20, 25 wt. %) with particle sizes of 75, 125 and 175 µm. Eggshell powder was mixed and melt blended with LDPE at 190 °C in a single screw injection molding machine. The samples were cooled at room temperature (post-curing details were not reported). Results showed that as particle size decreased, mechanical properties were improved due to the higher effective surface area. Furthermore, the increment in mechanical properties was also dependent on the wt. % of filler materials. At 10 wt. % loadings, composites with 75 µm showed 4 % and 6 % higher tensile and flexural strengths then 125 and 175 µm particles, respectively, which was increased to 16 % and 19 % at 25 wt. % of filler loading. It was also observed that the composites with higher filler contents and surface area had better water absorbing capacity. For instance, the composites with particle size of 75 µm had higher water absorption capacity than composites with 125 µm particle size due to higher surface area of the filler particles. In another article by same research team, Nwanonenyi *et al.* [88] showed when the incorporation of oyster shell powders as fillers were increased in LDPE, there was a reduction in the tendency of the composite to burn. This showed that calcium carbonate based composites can be used in the production of materials to provide sufficient escape time in case of a fire outbreak.

In a related study, Kamalbabu *et al.* [89] used cuttlebone (marine molluscs which contain mainly $CaCO_3$) particles as a reinforcement in commercially available DGEBA epoxy resin. The epoxy and fillers were mixed by hand for 15 min. The hardener was then added to the mixture and mixed slowly for 10 min to avoid air bubble formation. The mixture was then poured into the mold and cured for 8 h at room temperature. The samples were then post-cured at 80 °C for 3 h in a hot air oven. The composite materials were prepared at three different particle sizes of 75, 150 and 300 µm and five different weight-ratio (3, 6, 9, 12 and 15 wt. %). The cuttlebone reinforced epoxy composites with 75 µm particle size had higher tensile strengths than the other composites. For example, the tensile strength was maximum at 3 wt. % filler with values of 40 MPa, 38 MPa and 36 MPa for 75, 150 and 300 µm particle sizes, respectively and decreased at higher loadings due to poor bonding at the particle-matrix interface. Tensile modulus values were reduced by increased particle size because smaller particles tended to restrict the mobility of the polymer chains and in turn reduced the strain values. Furthermore, as the filler content increased, tensile and flexural strengths decreased due to difficulties of achieving a homogeneous dispersion of the filler at higher filler contents within the matrix.

## 2.8 Additional applications of eggshell

Aside from eggshell being used as filler materials in polymer composites, they have found uses in other applications. For example, eggshell organic membranes have been used in medical and pharmaceutical industries as they contain important compounds such as collagen, hyaluronic acid, glucosamine, and chondroitin sulphate [90]. These elements when extracted from other natural resources can have significant processing costs because they are rare in nature or it may be difficult to obtain the desired purity. Therefore, the extraction of these compounds from waste eggshell membranes is expected to reduce the cost considerably. US patent no. US 2008/0234195A1 held by Frank *et al.* [91], discussed an invention related to therapeutic, cosmetic and medical applications for eggshell membranes as well as an eggshell membrane separation method. The patent also discussed techniques where eggshell membranes can be used for skin wound healing as well as treatment and repair of tissues due to cuts, injuries and burns.

As mentioned earlier, limestone is the major composition of the eggshell accounting around 92 % of the total weight [38,43]. This waste eggshell could be transformed into a valuable source of calcium [92] for use as dietary supplements in animal feeds and toothpastes [93]. Deriving limestone from waste eggshell would not only decrease the pollution on landfills but would also serve as a potential alternative for mined limestone. In addition, limestone also finds widespread applications in the manufacturing of paper, bio-plastics and as components in ink jet paper coatings [94]. In addition, Anton *et al.* [95] showed that eggshell without membranes could be a cheap potential substitute of natural limestone for pharmaceutical companies which produce calcium related tablets.

## 2.9 Knowledge gap in earlier investigations

In the past, a number of research works reported on eggshell polymer composites, however most of the investigations were aimed at using eggshell in its original powdered form (e.g. washed and ground). There has been very little research on purifying eggshell to increase the concentration of limestone in eggshell by removing the organic membrane. In view of that, the following discusses methods to improve the quality of eggshell powders.

### 2.9.1 Membrane removal methods

eggshell membrane consist of highly cross-linked protein fibers which are deposited during the process of eggshell formation [96]. In this study, the possibility of developing a method to remove membrane from eggshell was investigated.

#### 2.9.1.1 Chemical treatments to remove membranes from eggshell

A literature review by Oliveira *et al.* [8] discussed different hypothetical processes in which eggshell could be purified and industrialized with both environmental and economic benefits. This study suggested sodium hypochlorite (e.g. bleach) or hydrochloric acid (HCl) treatments could be used to remove membranes from eggshell effectively. In order to obtain pure membranes, Cusack *et al.* [97] used different methods such as plasma ashing (etching), sodium hypochlorite and HCl treatments. In plasma etching, cleaned shells were placed in a plasma etching machine and organic membranes were removed by volatalization for 4 h. In another technique, the eggshell halves were first filled with sodium hypochlorite (37 % active chlorine) for 20 min or HCl (1 N) for 5 min and then rinsed with water. The results showed that due to oxidation of the membranes, sodium hypochlorite treatment removed the membrane in a simple and efficient manner compared to the acid and plasma etching methods. Although these treatments work well for removing the membranes, the removed membrane can no longer be used. Besides, these treatments are effective on a laboratory scale but not suitable on a large scale due to the cost and complexity of the treatments. The following section discusses different techniques to separate membrane as a main useful product.

#### 2.9.1.2 Mechanical processes to remove membranes from eggshell

The number of patents describing/developing methods for efficient separation of eggshell membranes has increased in the past decade. This is due to the presence of various bioactive compounds such as collagen, hyaluronic acid, or amino acids which could be extracted from the eggshell membranes and purified for various uses [98–101]. For instance, MacNeil (Pat. No. US 2003/0136711 A1) [102] developed a system for separation of membranes from the eggshell particles by passively dissociating them in a tank filled with liquid (preferably water). The abrasion was achieved by employing a reducing device where the cutting action diminished the size of the shell particles between 0.5 mm to 4.0 mm. The eggshell particles were then placed into a large

tank of water and allowed to settle to the bottom of the tank as shown in Figure 2.5. As they settled, the particles experienced turbulent forces in the water, which caused the membranes and shell portions to fully separate. The industrial set-up of the invention required gallons of the water with continuous recycling therefore adding to the production cost. In addition, this method functions in a batch manner only.

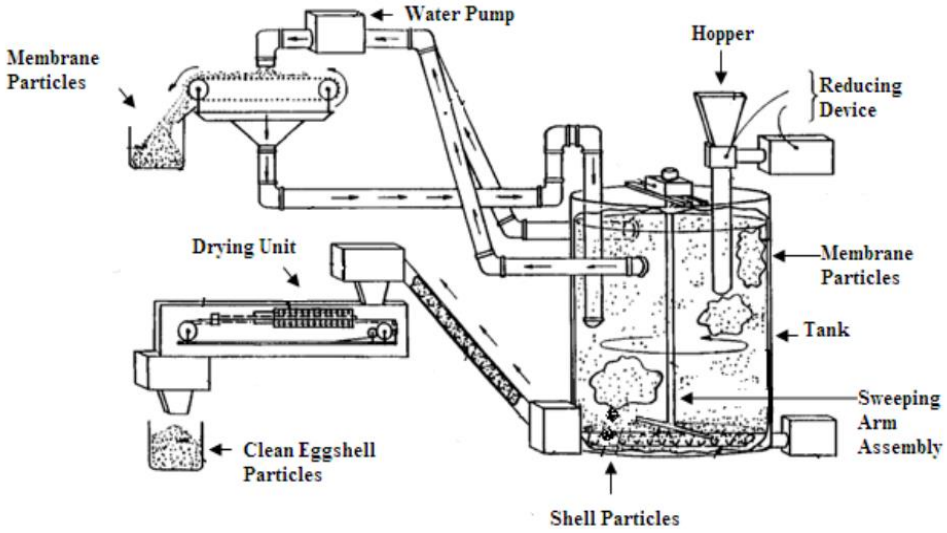


Figure 2.5 Apparatus for separation of eggshell and membrane [103]

Another invention by Roberto *et al.* (Pat. no. US 7,597,280 B2) [104] designed an apparatus for continuously separating the organic membranes from the non-organic mineral portion of broken eggshell. This apparatus works on the differences between the low specific gravity of the organic membrane portion (less than 1.0 g/cm$^3$) and the high specific gravity of the non-organic hard mineral portion which is typically, between 2.7 and 3.0 g/cm$^3$ without the necessity of turbulent flow or cavitation. When high density particles settled in the water tank, they were removed and dried while water with membrane particles from the top of the tank extracted the membrane materials.

However, it should be noted that the goal of the end applications of the two above methods were to extract pure membranes from eggshell and not the pure limestone particles. Therefore, in these techniques there may be small amounts of membrane in the cleaned eggshell powders, but this was not discussed in the patents.

### 2.9.1.3 Thermal decomposition to remove membranes from eggshell

Tsuboi *et al.* [103] studied the thermal decomposition of eggshell and showed eggshell could be used to produce pure CaO. During the TG−DTA analysis, to analyze the compound presence in gaseous part of the weight loss, outlet gas from the instrument was introduced to a mass spectrometer (MS, M-200QA, ANELVA) through a silica capillary tube (75 μm in internal diameter). TG/DTA− MS curves was generated by measuring the mass spectrum of the outlet gas at every 10 s at a mass range from m/z = 10 to m/z = 70. As shown in Figure 2.6 (a), water vapor and $CO_2$ were observed as the major gaseous products at m/z = 18 and m/z = 44, respectively. A well-shaped peak of $CO_2$ between 900-1000K (626-726 °C) was observed in Figure 2.6 (b) as $CaCO_3$ began to decompose into CaO. However, a small but visible peak for water vapor (m/z = 18) was also detected between 900-1000K (626-726 °C) where water vapor was released possibly due to the release of trapped water [105].

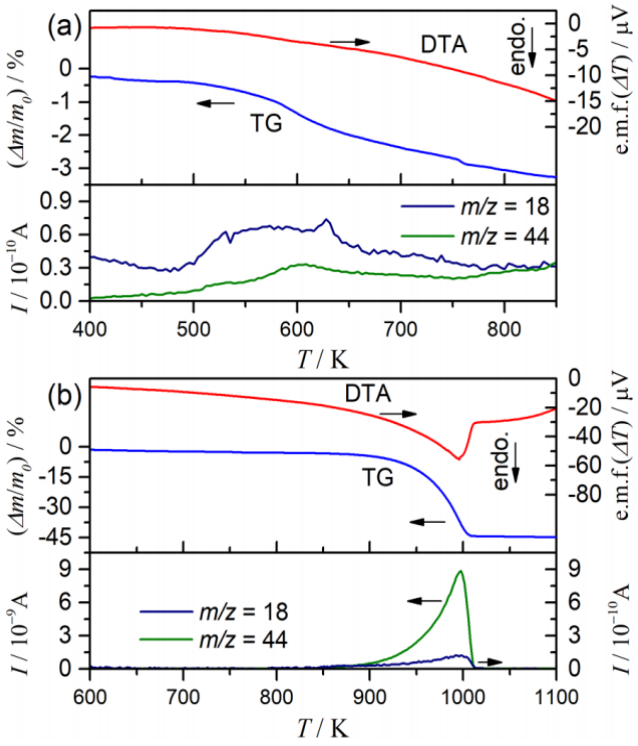


Figure 2.6 TG−DTA and MS curves of eggshell (a) for 400 to 850K (127 to 577 °C) and (b) for 600 to 1110K (327 to 837 °C) [103]

Furthermore, in the same study Tsuboi *et al.* [103] analyzed inner and outer membranes with SEM for eggshell heated to different temperatures. As shown in Figure 2.7 (a), holes can be observed

on the outer surface of the eggshell at 573K (300 °C). This was attributed to the release of water vapor during the initial period of heating. However, as shown in Figure 2.7 (b, d) no significant changes were observed on the inside surface of the eggshell. At the last stage of heating at 873K (600 °C), spherical calcite particles were observed on the inside surfaces (Figure 2.7 (f)). Here the fibrous structure made of protein decomposed completely and calcite particles appeared as shown in Figure 7 (f). However, TG/DTA results (Figure 2.6) could not detect other gases with larger molecular masses since the gases are in the fraction amount of $CO_2$.

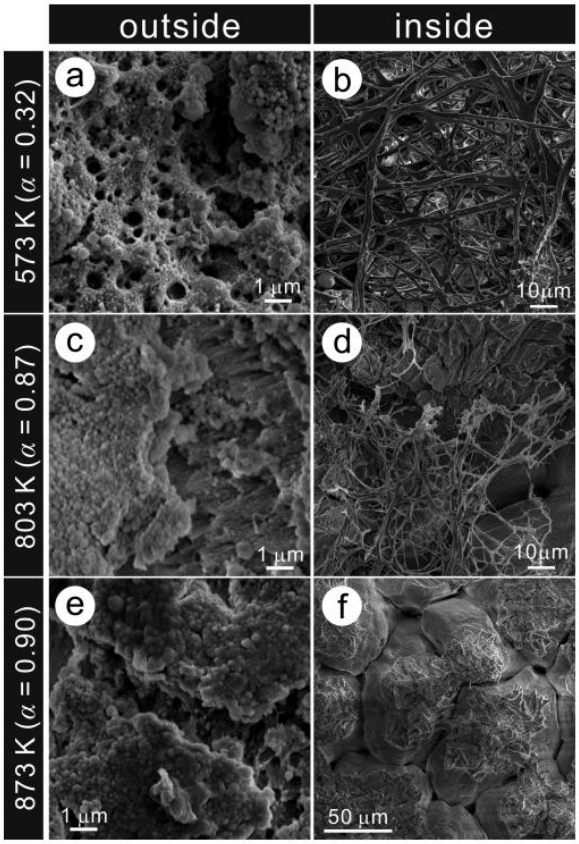


Figure 2.7 Typical SEM images for the heated eggshell (a, b) 573 K (300 °C), (c, d) 803 K (530 °C), and (e, f) 873 K (600 °C) [103]

Wei *et al.* [43] reported the calcination of eggshell heated to 600 °C and held for 2 h did not cause the eggshell to transform into CaO. Another similar study by Witoon *et al.* [42] analyzed the calcination behavior and elemental information of heated eggshell at a higher temperature of 900 °C. X-ray fluorescence results showed CaO was the most abundant component (97.4 %) of calcined eggshell with very small amounts of MgO, $P_2O_5$, $SO_3$, $K_2O$, SrO, $Fe_2O_3$, and CuO.

### 2.9.1.4 Calcium carbonate cycle

In view of the above research on the calcination of eggshell to CaO and complete removal of the organic membrane, the process to convert the CaO back into $CaCO_3$ is explained. Figure 2.8 shows how theoretically limestone changes into CaO when heated to around 700 °C. The addition of water to CaO transforms it into hydrated lime (calcium hydroxide- $Ca(OH)_2$). Finally, adding carbon dioxide ($CO_2$) to calcium hydroxide produces pure calcium carbonate ($CaCO_3$) as shown in Figure 2.8. In a closed system, the $CO_2$ produced from heating at 700 °C could be recuperated and used in the final cycle.

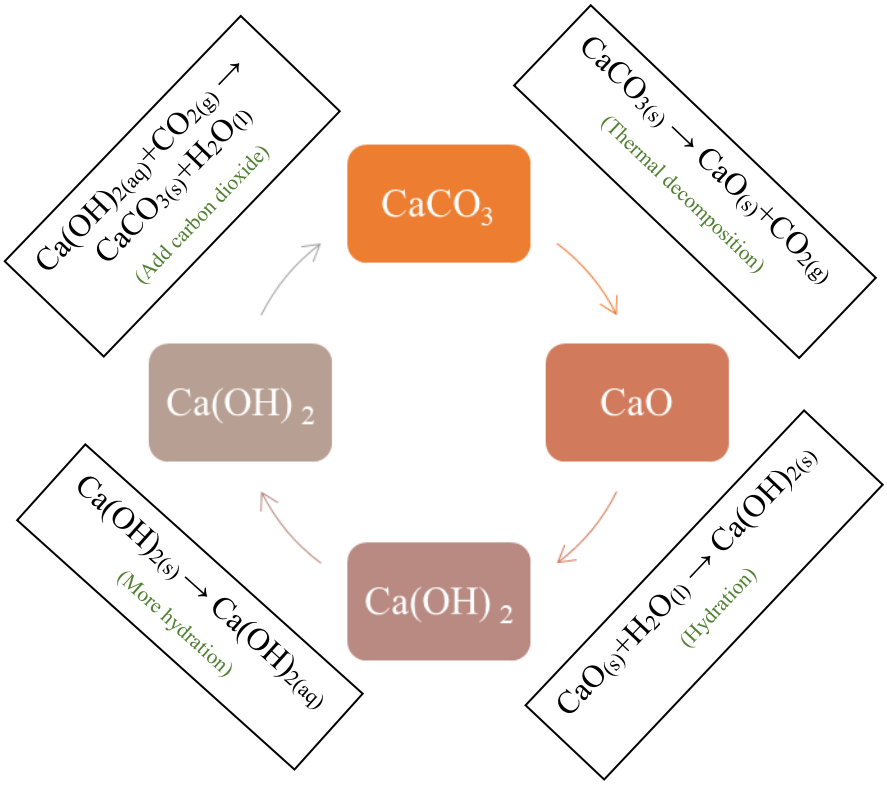


Figure 2.8 Calcium carbonate cycle

## 2.10 Summary

The literature review showed that eggshell fillers have a potential to be employed in polymer composite material. The mechanical and chemical characterization of different matrices with eggshell filler were evaluated. To understand the microstructure of eggshell, its organic membrane and its chemical composition, articles on these topics were reviewed and presented in this chapter. Different studies have shown eggshell powders used in composites also contained organic

membrane beside the limestone particles. Therefore, to address this issue, and use only purified eggshell particles (without membranes) in a polymer composite the calcium carbonate cycle to remove membranes was examined. The use of a plant-based bio-epoxy material is also discussed in order to produce an eco-friendly composite material. Many studies have utilized waste eggshell (with membrane) as fillers in polymer composite materials, but there are no studies that have been conducted to first purify the eggshell powders prior to using it as a filler material. This research gap was the main motivation to study the purification method using the calcium carbonate cycle and evaluate their effect on mechanical and chemical properties of eggshell composites.

# CHAPTER 3
# MATERIALS AND METHODS

The materials and experimental methods employed for processing and characterizing the composites are discussed in this chapter. It outlines and explains the tests procedures related to the physical, mechanical, microstructural and thermal characterization of the epoxy composites.

## 3.1 Materials

Raw eggshell were obtained from a local hatchery, Maple Lodge Farms Hatchery division based in Stratford, Ontario, Canada while limestone powder was obtained from Imasco Minerals Inc. Bio-epoxy resin and hardener for composite preparation was purchased from Super Sap, a leading manufacturer of thermoset bio-epoxy systems located in Michigan, USA. The properties of CPL/bio-epoxy were obtained from the manufacturers data sheet and are shown in Table 3.1. This epoxy contained 31 % bio-based content. The resin was mixed with hardener in a ratio of 100:40.

Table 3.1 Properties of Super Sap CPM bio-epoxy resin

| **Mechanical data** | |
|---|---|
| Tensile Modulus (ASTM D638) | 436,000 psi (3.0 GPa) |
| Tensile Strength (ASTM D638) | 8,990 psi (62.0 MPa) |
| Flexural Modulus (ASTM D790) | 412,510 psi (2.8 GPa) |
| Flexural Strength (ASTM D790) | 13,450 psi (92.7 MPa) |
| $T_g$ Ultimate (DSC, midpoint) | 154 ˚F/54 °C |
| Hardness (Shore D) | 70-80 |
| **Processing data** | |
| Component Density (specific density @ 77ºF/25ºC) | 1.13 (epoxy), 0.96 (hardener) |
| Mixed Density (specific density @ 77ºF/25ºC) | 1.08 |
| Viscosity (bio-epoxy/hardener/mixed @ 77 ºF/25 ºC) | 1300/450/880 |

Composites were made according to ASTM standards as shown in Figure 3.1 (c). Initially bio-epoxy and filler powder were mixed and stirred. Once the mixture was free from air bubbles, the hardener was added to the mixture and poured into a silicon mold. After that, composite samples were removed once the solution was solidified.


Figure 3.1 (a) bio-epoxy resin/hardener, (b) eggshell powdered filler and (c) bio-epoxy composites

### 3.1.1 Filler materials and grinding process

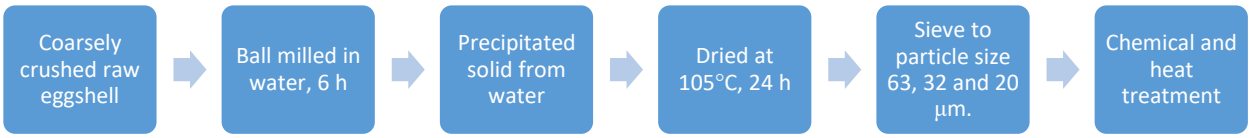


Figure 3.2 Raw eggshell preparation process

Initially eggshell powder was cleaned with water and dried at 105 °C for 24 h and then crushed in a ball mill with a rotation speed of 50 rpm for 24 h in a cylindrical ceramic jar as shown in Figure 3.3 (a). In this process the total number of alumina balls used in the ball mill were; 5 balls of 25 mm-diameter, 10 balls of 20 mm-diameter, and 15 balls of 12 mm-diameter. To obtain different particle size powders, the ground powders were sieved to different sizes (32 µm and 20 µm mesh size) using the sieving machine (RO-TAP) as shown in Figure 3.3 (b). This equipment performed vertical and circular vibrational motions which created three-dimensional sieving movements. Powder was sieved for 6 h in 10 different batches. All the sieves were cleaned frequently using an ultrasonic bath since the very fine holes of the 20 µm sieve were blocked repeatedly due to presence of larger particles in the samples.

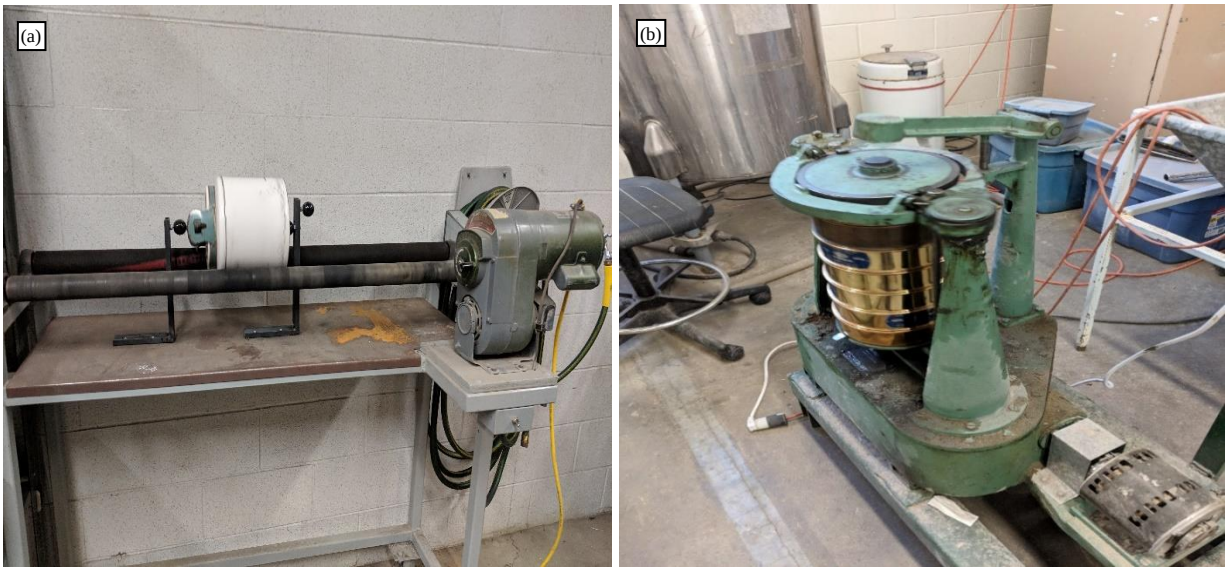


Figure 3.3 (a) Ball mill jar for grinding eggshell particles and (b) sieving machine

### 3.1.2 Particle size analysis

ImageJ software was used for the evaluation of the particle sizes and size distributions. ImageJ was developed at the National Institutes of Health (NIH), USA and is a Java-based package public domain image processing and analysis program, freely available, open source and is an independent platform that can be modified using coded plugins for specific applications [106]. The obtained images from microscopy analysis were inserted in ImageJ and a number of steps such as scale bar, dilate, fill holes and erode process were carried out to obtain better image. Figure 3.4 shows the sample process to calculate particle size and output summery from ImageJ software.

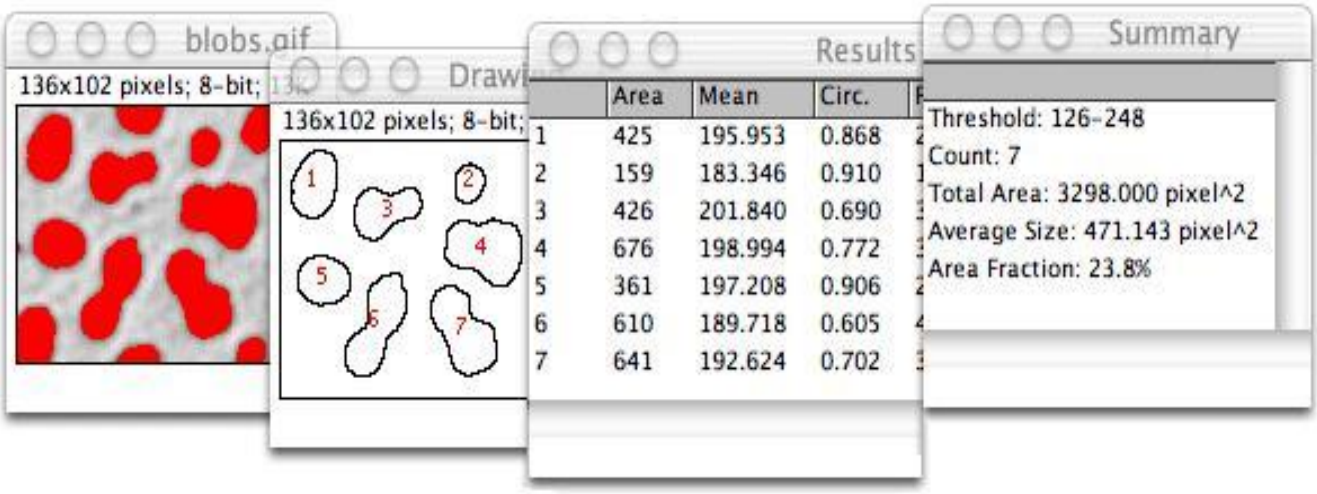


Figure 3.4 ImageJ software showing the process to calculate particle size and frequency

### 3.1.3 Heating and purification of eggshell powder

To remove membranes, sieved eggshell powders were first heated in air to different temperature (500 °C to 900 °C) for different times (0.5 to 2 h). As shown in the reaction of equation 3.1, limestone converts to pure CaO and carbon dioxide is generated, which can be stored and reused for reaction of equation 3.3 in an industrial mass production set-up. The addition of water to CaO transforms it into hydrated lime (e.g. calcium hydroxide- ($Ca(OH)_2$) as shown in the reaction of equation 3.2 (Figure 3.5). Finally, adding carbon dioxide ($CO_2$) to calcium hydroxide follows the reaction in equation 3.3 and converts it back into limestone, which in theory is pure $CaCO_3$. The pure limestone is heated to 105 °C for 12 h to remove all the water particles within the sample.

$$CaCO_3 \rightarrow CaO + CO_2 \quad (3.1)$$

$$CaO + H_2O \rightarrow Ca(OH)_2 \quad (3.2)$$

$$Ca(OH)_2 + CO_2 \rightarrow CaCO_3 + H_2O \text{ (drying at 105 °C)} \quad (3.3)$$

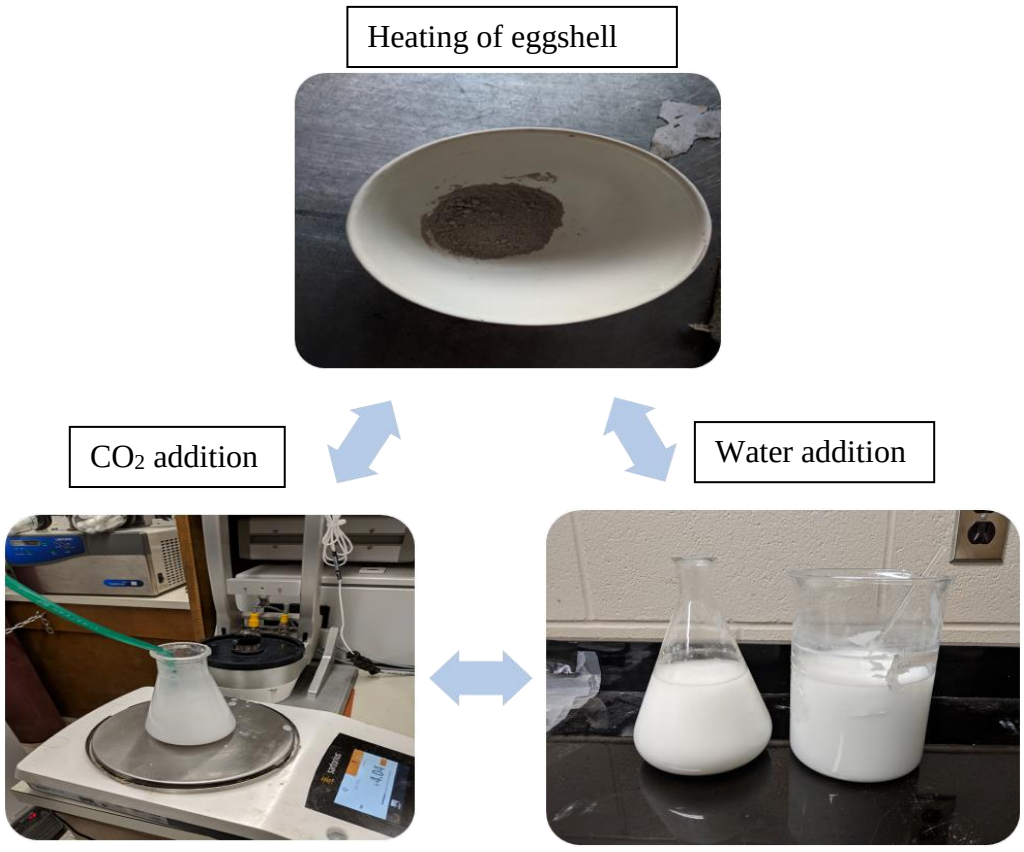


Figure 3.5 Calcium carbonate cycle on eggshell powder

As per equation 3, when one mole (100 gm) of limestone is heated to 750 °C, the reaction generates one mole of CaO (56 gm) and one mole of $CO_2$ (44 gm). Weight balances were performed for different temperatures and times to understand the weight loss in each reaction.

In the laboratory process, it is difficult to store carbon dioxide for reaction of equation 3.3. Therefore, carbon dioxide was produced using Kipp's apparatus, which is shown in Figure 3.6. The chemical reaction to produce carbon dioxide from Kipp's apparatus is given by equation 3.4 where the raw eggshell were used as $CaCO_3$ for the reaction. A 2 M concentrated HCl solution was added from the top chamber and the eggshell powder was placed into the middle chamber. This reaction generated $CO_2$ gas, which was drawn off through the stopcock as desired.

$$CaCO_3 + 2HCl + 2H_2O \rightarrow CaCl_2 + 3H_2O + CO_2 \quad (3.4)$$

As shown in reaction 3.4, calcium chloride ($CaCl_2$) was also produced as a byproduct which can be used in different ways in the chemical and pharmaceutical industries [107–109].


Figure 3.6 Kipp's apparatus for $CO_2$ generation

### 3.2 Composite preparation

#### 3.2.1 Mold preparation

Initially, polylactic acid (PLA) 3D printed tensile, flexural and Charpy specimens were fabricated according to ASTM D638-14 [110] , ASTM D6110-18 [111] and ASTM D790-17 [112] sizes, respectively. Silicon molds were made using Mold Max 10T, in which part A (epoxy) and part B (hardener) were mixed in a 100:10 ratio into a mixing container for 3 min. To remove any entrapped air in the mold, the mixture was degassed at a vacuum of 28 inches of Hg. The mixture was then poured carefully into a square container containing the 3D printed specimens. After 48 h of curing, the 3D specimens were removed which created cavities for producing the epoxy composite test specimens. Figure 3.7 shows an example of flexural specimens. The silicon molds were then post-cured at 65 ºC for 4 h to improve the cross-linking reactions and eliminate any residual moisture and alcohol that is a byproduct of the condensation reaction.

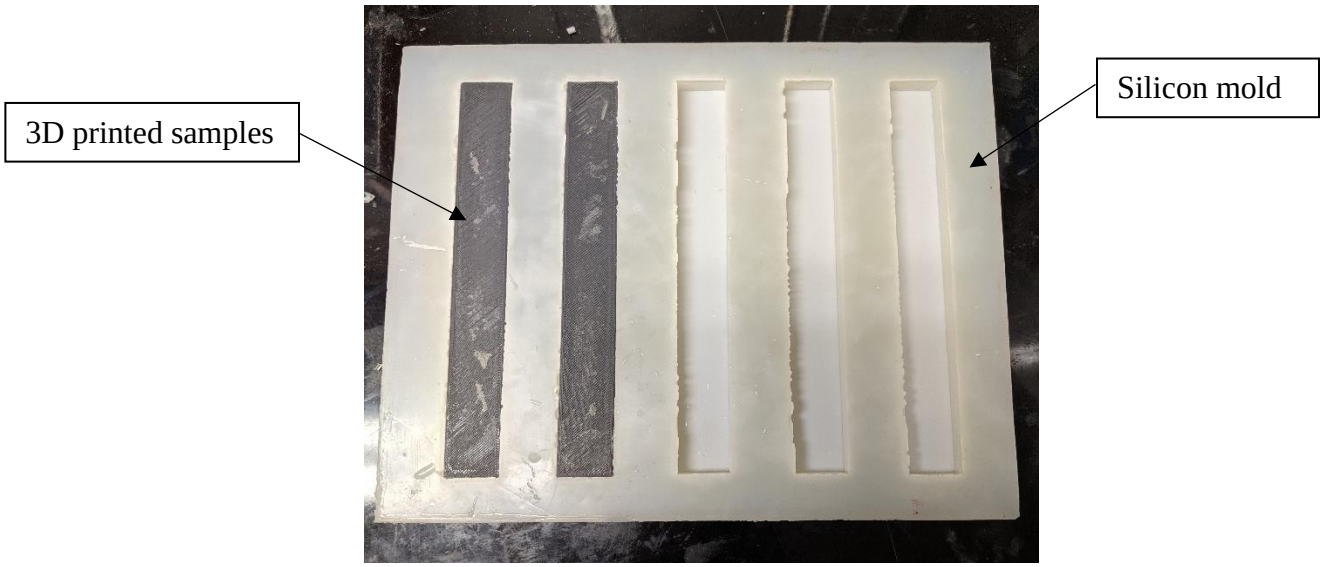


Figure 3.7 Example of silicone mold for flexural specimens as per ASTM standards

#### 3.2.2 Sample preparation

The bio-epoxy composite making process is illustrates in Figure 3.8. Initially, bio-epoxy and filler materials with different weight percentages (5, 10, 20 wt. %) were mixed in mixing container for 3 min. The mixture was then stirred with a magnetic stirring machine for 40 min. It was again mixed for 3 min in the ultrasonic sonicator to homogenize (Model FS 900N) the mixture as shown

in Figure 3.9. An ultrasonic probe was used to generate very high-energy waves in the mixture. This ultrasound brakes the inter-particle weak van der Walls bonds, which ultimately reduces agglomeration in the mixture [113]. The mixture was then degassed in a vacuum furnace (SHEL LAB Model SVAC1E) at a vacuum of 28 inches of Hg for 30 min to remove air bubbles. Once the air bubbles were removed, the mixture was carefully poured into the appropriate silicone mold. After 24 h of room temperature curing, the samples as shown in Figure 3.10 were removed from mold and post-cured at 82 °C for 40 min as suggested by manufactures' data sheet to improve the cross-linking density.

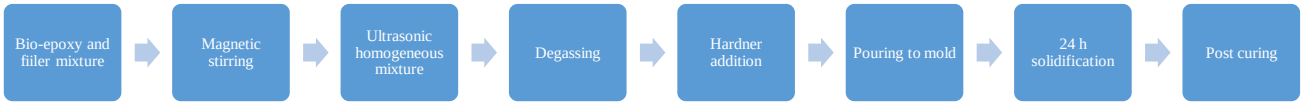


Figure 3.8 Epoxy composite making process

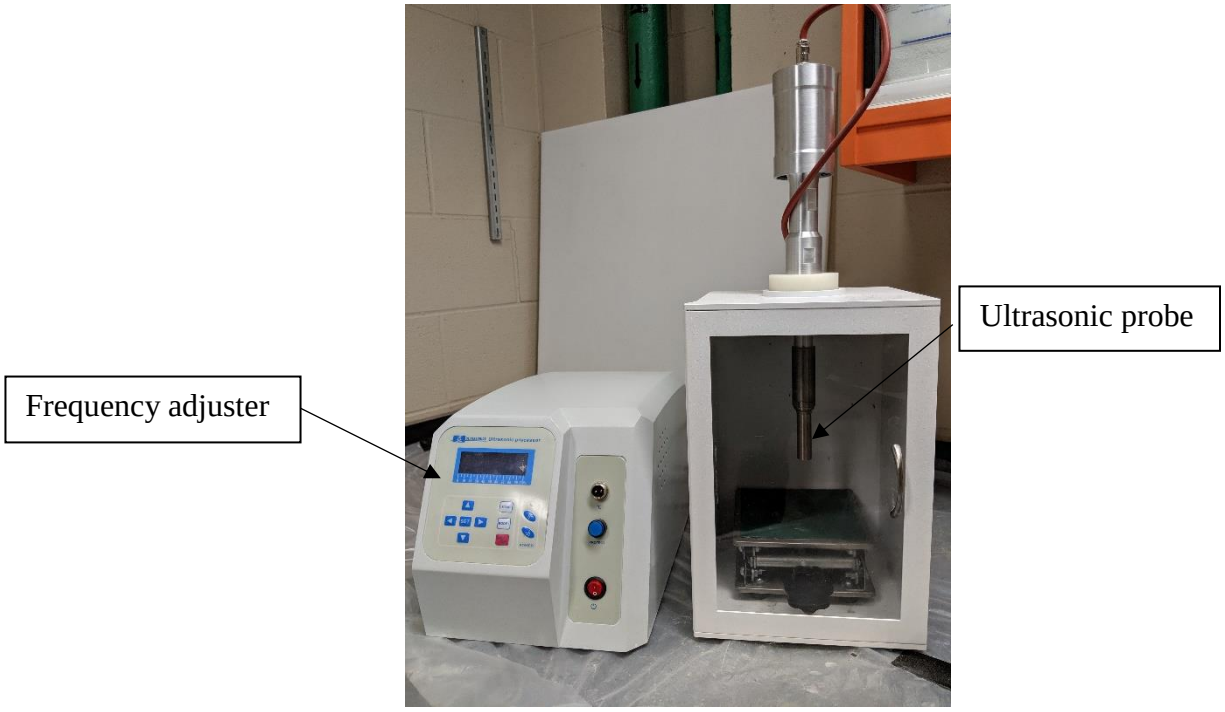


Figure 3.9 Ultrasonic sonicator homogeneous mixture

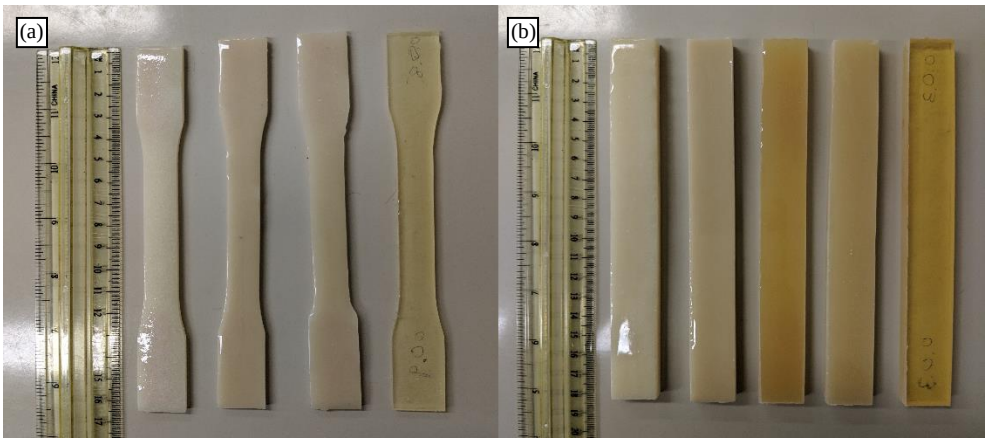


Figure 3.10 Composite samples according to ASTM standards (a) tensile and (b) flexural

The weight ratios for different fillers are shown in Table 3.2. For example, 10ES indicates composites made of 10 wt. % of eggshell filler with 32 µm particle size and remaining 90 wt. % is mixture of bio-epoxy and hardener. A 5LS_20µm indicates the samples are 5 wt. % of limestone filler with 20 µm particle size were mixed with 95 wt. % of bio-epoxy and hardener.

Table 3.2 Filler loading types in bio-epoxy composites

| Composite type | Bio-epoxy (wt. %) | Filler type | Filler (wt. %) |
|---|---|---|---|
| Bio-epoxy | 100 | -- | 0 |
| 5ES | 95 | Brown eggshell with 32 µm powder | 5 |
| 10ES | 90 | Brown eggshell with 32 µm powder | 10 |
| 20ES | 80 | Brown eggshell with 32 µm powder | 20 |
| 5PES | 95 | Purified eggshell with 32 µm powder | 5 |
| 10PES | 90 | Purified eggshell with 32 µm powder | 10 |
| 20PES | 80 | Purified eggshell with 32 µm powder | 20 |
| 5LS | 95 | Limestone with 32 µm powder | 5 |
| 10LS | 90 | Limestone with 32 µm powder | 10 |
| 20LS | 80 | Limestone with 32 µm powder | 20 |
| 5LS_20µm | 95 | Limestone with 20 µm powder | 5 |
| 10LS_20µm | 90 | Limestone with 20 µm powder | 10 |
| 20LS_20µm | 80 | Limestone with 20 µm powder | 20 |

### 3.3 Density analysis

The particle bulk density of filler (eggshell, purified eggshell and limestone) was calculated at room temperature using a gas pycnometer (Model-Micromeritics Accupyc 1340). The weight of the sample was measured with a high sensitivity weighing scale (Ohaus Precision Model TS400D) with a precision of 0.001g. The volume ($cm^3$) of the samples were determined by gas pycnometer based on non-destructive technique. The density of sample was determined by an equipment software, which works on Archimedes principle as shown in equation 3.5.

$$D_{sample} = \frac{M_{sample}}{V_{sample}} \tag{3.5}$$

where, $D_{sample}$ = density of sample ($g/cm^3$), $M_{sample}$ = mass of sample(g), $Vsample$ = volume of sample ($cm^3$).

Density of bio-epoxy composites were assessed based on the Archimedes principle which measures the actual density of the composites using the liquid displacement method. In this technique, the volume of the samples were estimated by the mass of the volume displaced when the sample is submerged in a liquid. The experimental setup for density measurement is shown in Figure 3.11. ASTM D792-13 [114] standard was used as a guideline for this experiment. The samples with a minimum size of 1 $cm^3$ at a temperature of 23 °C were submerged in distilled water of known density. The samples were weighted in air and in water with a precision nearest to 0.001 g. Application of Archimedes' principle leads to the following expression for the density ($\rho_m$) of the composites as given by equation 3.6:

$$\rho_m = \frac{m}{m - m_{cw}} \rho_w \tag{3.6}$$

where, $m$ is the dry weight (gm) of the composite sample in air, $m_{cw}$ is the mass (gm) of the same composite sample in distilled water and $\rho_w$ is the density of the distilled water (998 $kg/m^3$).

During the fabrication of the composites, some porosity was normal due to the increase in surface area in contact with the air during mixing. Mechanical properties of PMC are highly varied due to the volume fraction of porosity, its size and distribution in a composite [115–117]. Therefore, porosity levels must be kept to a minimum. Composites completely free of air bubbles are difficult to produce, but they can be controlled using different methods such as vacuum degassing [118],

heat curing [119] and a sonication procedure [120]. Porosity of the composites can be estimated using equation 3.7.

$$Porosity = \frac{\rho_{th} - \rho_m}{\rho_{th}} \tag{3.7}$$

where $\rho_{th}$ and $\rho_m$ are the theoretical and measured densities (g/cm$^3$), respectively.

The theoretical density of the composite ($\rho_{th}$) in terms of volume and weight (mass) fraction of the matrix ($w_m$) and filler ($w_f$) were calculated based on rule-of-mixture and shown in equation 3.8 and 3.9 respectively.

$$\rho_{th} = \rho_m * V_m + \rho_f * V_f \tag{3.8}$$

$$\rho_{th} = \frac{1}{\frac{w_m}{\rho_m} + \frac{w_f}{\rho_f}} \tag{3.9}$$

where ($\rho_m$) and ($\rho_f$) are the density (g/cm$^3$) and ($V_m$) and ($V_f$) are the volume fractions of the matrix and fillers, respectively.

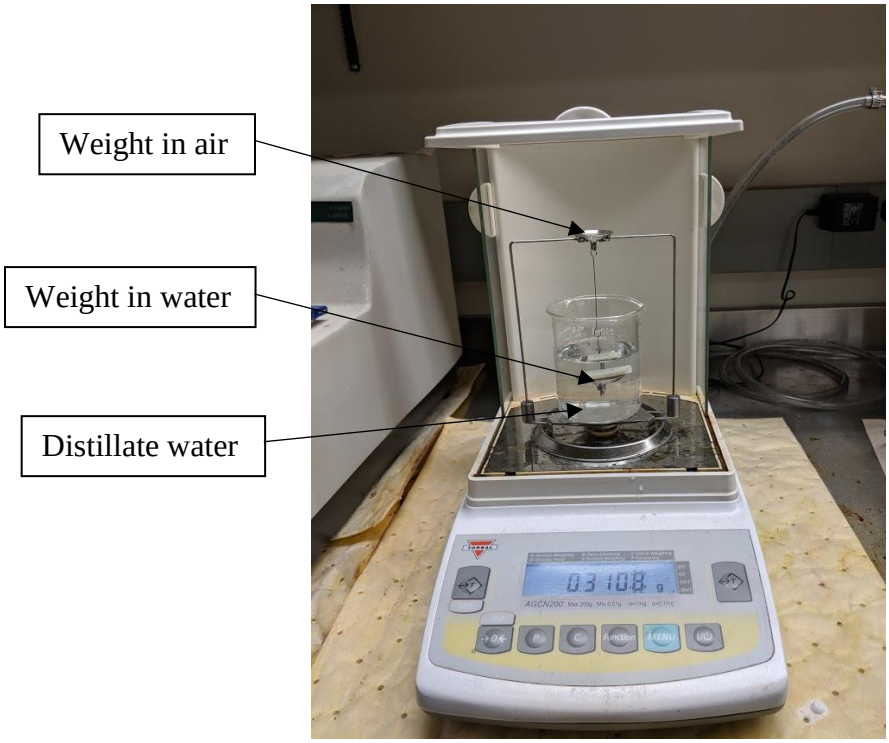


Figure 3.11 Composite density measurement by Archimedes method

### 3.4 Inductively coupled plasma mass spectrometry (ICP-MS) analysis

Inductively Coupled Plasma Mass Spectrometry (ICP-MS) is highly sensitive and capable of detecting metals and several nonmetals in materials, often at the level of parts-per-trillion. Trace elements can be analyzed on a variety of materials from super alloys to pure materials. An ICP-MS combines a high-temperature ICP source with a mass spectrometer. The ICP source converts the atoms of the elements in the test sample to ions which are subsequently detected and analyzed by the detector. Elements are separated depending upon the intensity and mass-charge ratio of ions.

The samples were digested via a CEM Corporation Mars 6 microwave digestion systems and analyzed on a Agilent 7700x ICP MS. For digestion, samples were placed in a closed vessel microwave with 65 % concentrated nitric acid at a temperature of 200 °C.

### 3.5 Water absorption analysis

Water absorption characteristics of epoxy composites may be affected by the addition of fillers (eggshell, purified eggshell and limestone) because these additives generally have an affinity to water. Test samples were cut in rectangular shapes with dimensions of 25.4 mm x 76.2 mm x 5 mm (l x w x t) were cut and immersed in a water container as shown in Figure 3.12. In order to analyze the water absorption characteristic of the composites, all samples were initially dried at 40 ºC for 3 h and then immersed in water for about 24 h at ambient conditions as defined in ASTM procedure D570 (ASTM D570 - 98(2018)) [121]. The weight change of each sample was recorded every 24 h until all the samples were 95 % saturated. Leftover water from sample surface was removed with a paper towel and immediately weighed to the nearest 0.0001 g. The percentage increase in mass during a specific time was calculated as follows:

$$\text{Percent Water Absorption } (\%) = \frac{W_t - W_o}{W_o} \text{x} 100 \tag{3.10}$$

where $W_o$ and $W_t$ denote the initial dry weight of composite and weight of the composite after a specific time t (days), respectively.

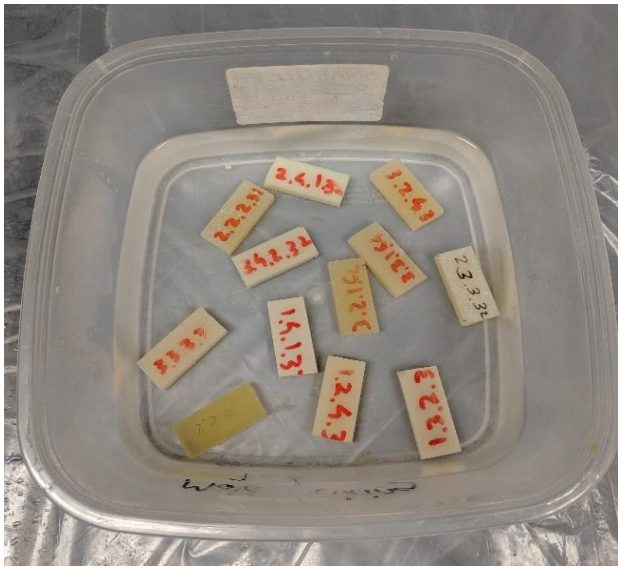

Figure 3.12 Water absorption test container with specimens

### 3.6 Microscopy preparation

The SEM model JEOL JSM-6010 LV (Tokyo, Japan) (Figure 3.13) was used for microstructural evaluation of fractured surfaces, and matrix-filler interface within the composites. Initially specimens were attached to cylindrical mounting stubs using a two-sided adhesive carbon tape. As the samples were non-conductive, they were gold coated to create a conductive layer which prevented samples from charging and reduced thermal damage to samples. The specimens were carefully examined using acceleration voltages ranging between 15 kV to 20 kV with a magnification of 500x to 1200x. The SEM equipment uses a high energy electron beam to generate a variety of signals depending upon specimens. A focused electron beam interacts with the specimen atoms and generates different wavelength signals. In SEM, mainly backscattered and the secondary electrons are used for imaging.

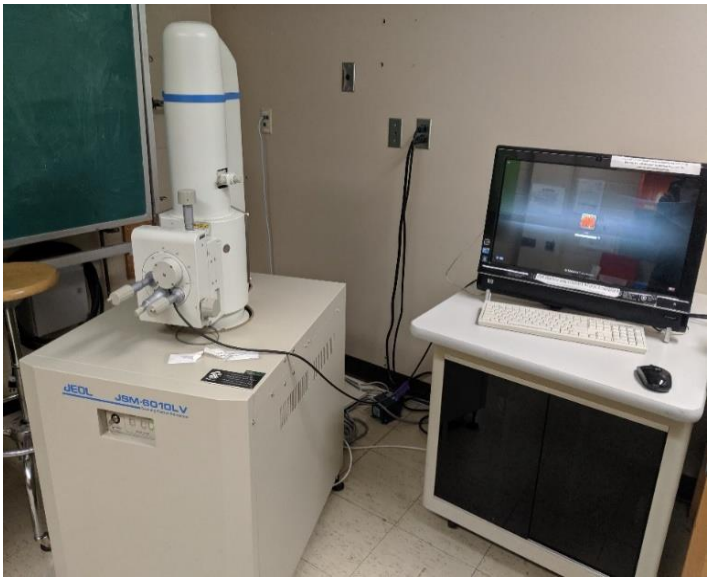


Figure 3.13 Digital image of the SEM model JEOL JSM-6010 LV

For the particle size distribution study, a Nikon 100 MA Eclipse inverted optical microscope was used to carry out images of filler powders. Images were captured and analyzed with the help of an image processing software called 'Pax-it'. Microscopic examination of filler powders were conducted using various magnifications lens (50x, 100x, 500x and 1000x).

### 3.7 Tensile test

Tensile test of any composite shows the maximum axial load it can withstand without failure, while the tensile modulus indicates the resistance of a material to elastic deformation under load. Fully cured dog-bone shaped composite samples of standard dimension (length 150 mm, width 20 mm and thickness 3 mm) were used for the tensile tests as per ASTM D638-14 standard [110]. A uniaxial load of 3 kN was applied through both ends using an Instron 600LX tensile machine equipped with an Instron advanced video extensometer (AVE 2663-821). The tests were carried out at a strain rate of 5 mm/min at room temperature with gauge lengths of 50 mm. The effect of filler type and percentage was investigated. Tensile properties for four different filler loadings (0, 5, 10 and 20 wt. %) of eggshell, limestone and purified eggshell were evaluated. The loading arrangement is shown in Figure 3.14. Tensile tests were repeated three times on individual samples and the mean value was calculated as the tensile strength of that composite.

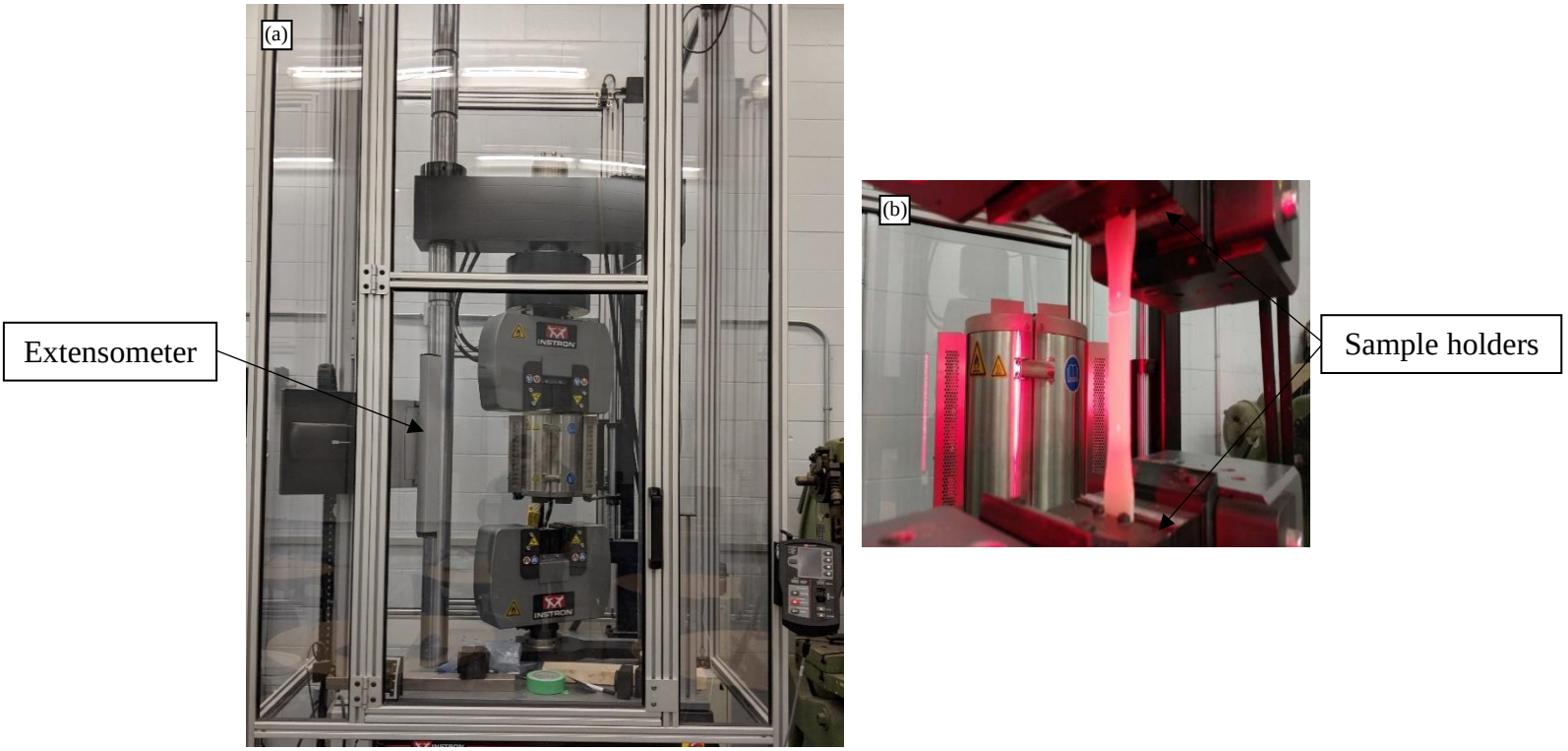


Figure 3.14 Digital images of the Instron tensile testing machine, (a) overall view and (b) tensile specimen in grips

### 3.8 Flexural test

The flexural strength of a composite is the maximum tensile stress that it can withstand during bending before reaching the breaking point. Three point bend tests were conducted on all bio-epoxy composites as per ASTM D790-17 standard [112] using an Instron 3366 testing machine. The set-up is shown in Figure 3.15. The cuboid-shaped specimens with dimensions of 50 mm x 15 mm x 3.2 mm (l x w x t) were used with a support span of 40 mm. The tests were conducted using a 10 kN load cell at a cross-head speed of 4 mm/min, which was determined using equation 3.11 [112].

$$cross\ head\ speed = \frac{ZL^2}{6d} \tag{3.11}$$

where Z which is a constant with a value of 0.01, while L and d are the support span (mm) and the thickness (mm) of the sample, respectively.

The deflection was measured by the software according to the cross-head position. The software collected all the data and generated a load-displacement curve from where the flexural stress and flexural modulus were calculated using equation 3.12 and 3.13. The flexural modulus is the slope of the initial linear portion of the stress versus strain curve, which is a measure of the specimen's stiffness.

$$\sigma_f = \frac{3\mathrm{PL}}{2\mathrm{b}d^2} \tag{3.12}$$

$$E_f = \frac{L^3 m}{4\mathrm{b}d^3} \tag{3.13}$$

Where: $\sigma_f$ = stress in outer fibers at midpoint, (MPa)

$E_f$ = flexural modulus of elasticity, (MPa)

P = load at a given point on the load deflection curve, (N)

D = maximum deflection of the center of the beam, (mm)

L = the support span, (mm)

b = width of test beam, (mm)

d = depth of tested beam, (mm) and

m = slope of the initial straight-line portion of the load deflection curve, (P/D), (N/mm).

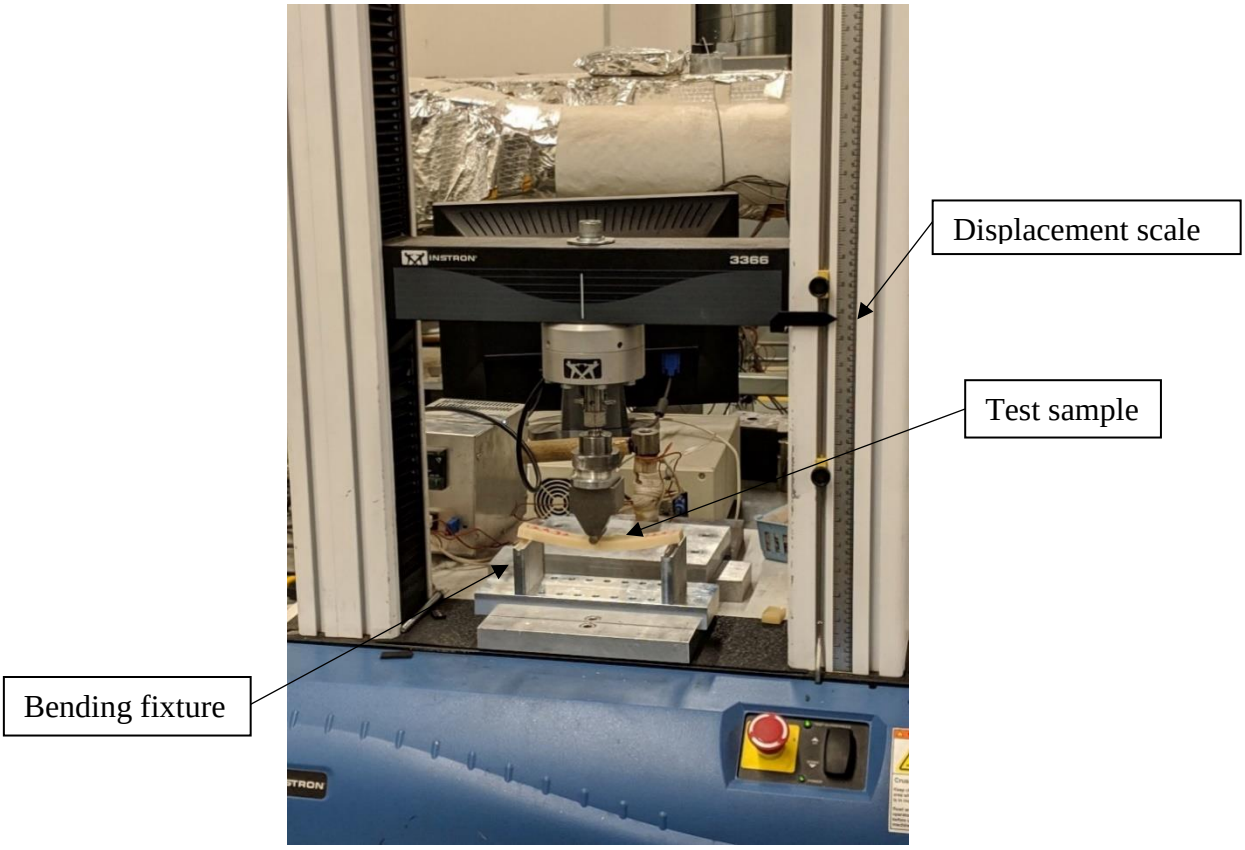


Figure 3.15 Digital image of Instron flexural test set-up

### 3.9 Charpy test

Toughness of polymeric materials can be evaluated by measuring the impact properties of such material. In general, the higher the ability to absorb energy, the higher the toughness. An Instron impact tester (Model 450 MPX) used to perform Charpy impact tests is shown in Figure 3.16. The tests were carried out according to ASTM D6110-18 standard [111] . Test samples measuring 55 mm x 10 mm x 7.5 mm (l x w x t) were placed in the specimen holder. The amount of energy absorbed by the material was calculated by measuring the height of the pendulum before and after collision. Five specimens were tested for each composite composition at room temperature. The energy absorbed per unit area ($E_i$) was calculated using equation 3.14 and averaged.

$$E_i = \frac{E_a}{b \times d} \tag{3.14}$$

where $E_a$, b and d are the total energy absorbed (J/cm$^2$), the width (mm) and thickness (mm) of each sample, respectively were measured and recorded.

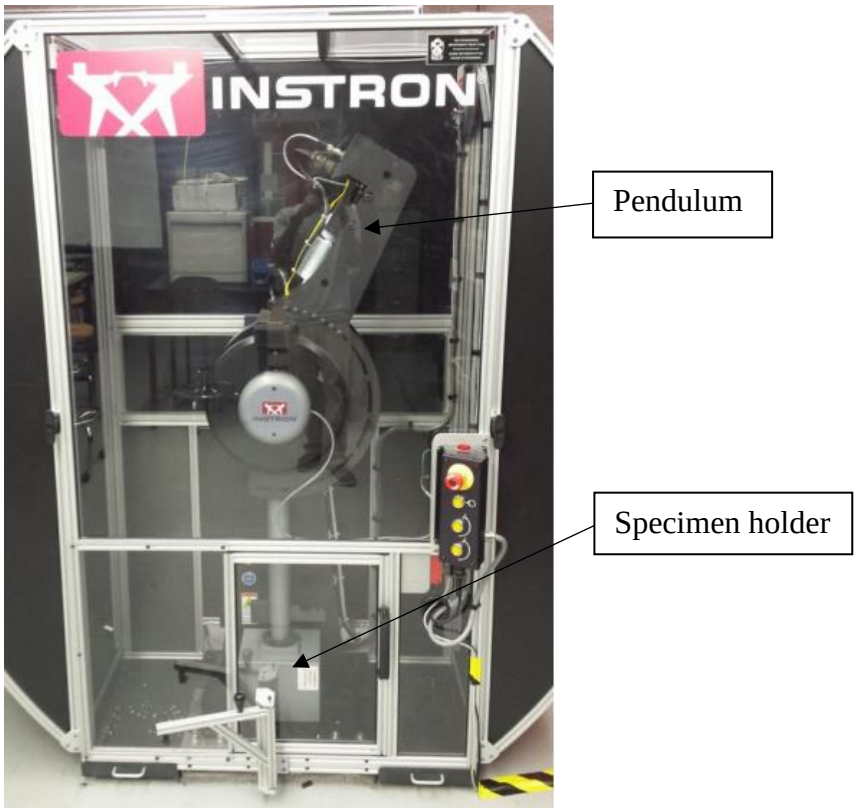


Figure 3.16 Digital image of the Instron Charpy testing machine

### 3.10 Thermogravimetric analysis (TGA)

TGA is a thermal analysis technique used to determine the weight change of a sample that is subjected to a steady increase of temperature. The weight change in a material is measured either as a function of specific temperature range or isothermally as a function of time in a controlled environment (nitrogen, helium, air, or in vacuum). The eggshell, purified eggshell and limestone powder samples were analyzed using a TGA Q5000 IR. 15 Build 263, universal V4.5A TA Instruments as shown in Figure 3.17. The samples were heated from 25 to 1000 ºC at a heating rate of 10 ºC/min in a nitrogen gas atmosphere. The experimental test conditions for the samples are given in Table 3.3.

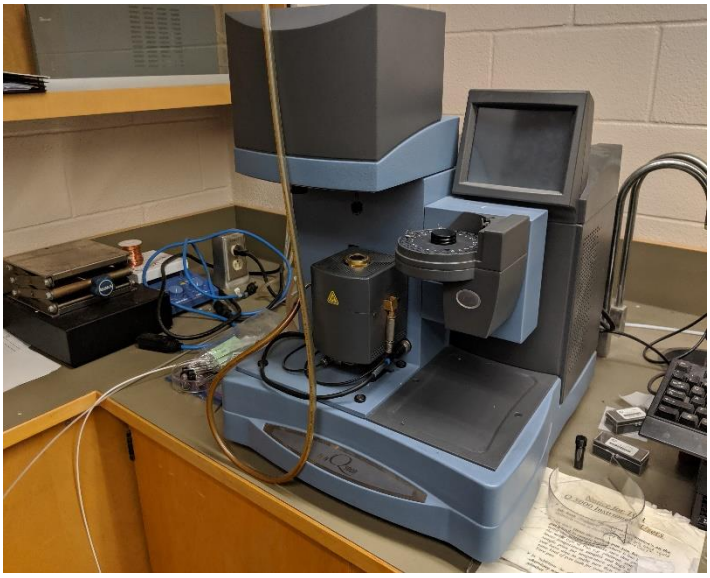

Figure 3.17 Digital image of TGA Q5000 IR machine for TGA tests

Table 3.3 Experiment test conditions for TGA

| Specimen type | Specimen size (mg) | Temperature range (ºC) | Sample gas flow rate (ml/min) | Balance gas flow rate (ml/min) |
|---|---|---|---|---|
| Eggshell | 30.8980 | 25 ºC to 1000 ºC | 25.0 ml/min | 10.0 ml/min |
| Purified eggshell | 49.7180 | 25 ºC to 1000 ºC | 25.0 ml/min | 10.0 ml/min |
| Limestone | 38.3910 | 25 ºC to 1000 ºC | 25.0 ml/min | 10.0 ml/min |

### 3.11 Differential scanning calorimetry (DSC) analysis

DSC is a thermo-analytical technique in which the behavior of a material is analyzed by measuring the amount of heat flow in a sample as a function of temperature or time. DSC results could be used to determine the best temperature performance, the $T_g$, and the melting or crystallization temperatures of material. The DSC instrument (Model 2910 V4.4E, TA instruments, New Castle, DE, USA) as shown in Figure 3.18 was used in this test. Composite samples containing different filler powders between 0.5 to 1 gm were placed in an aluminum pan and sealed with the crucible sealing press. The DSC tests were performed in a dynamic mode with a heating range of 25 to 150 ºC, and a heating rate of 10 ºC/min. A graph of heat flow versus temperature was produced.

Figure 3.18 Digital image of DSC machine

### 3.12 Statistical analysis

To examine the effect of different input variables (particle size, thermal treatment and filler loading) on composite properties (tensile strength, tensile modulus, flexural strength, flexural modulus and Charpy impact strength), statistical analysis was performed using analysis of variance (ANOVA) with aid of Sigmaplot 12.0. The level of confidence in this analysis was 95% (significance level of 0.05). This means the properties are dependent on input variable if the *p*-value calculated by the software were <0.05. However, if the *p*-value were >0.05, that suggests the input parameters did not create any significant influence on the output results. Two-way ANOVA was used in this test as there were two independent variables (filler type and wt. % of filler) in the composites. The tests were carried out in two different input models. In the first model, the significance of different fillers (eggshell, purified eggshell and limestone) with different loadings (5, 10 and 20 wt. %) were evaluated with fixed filler particle size of 32 µm. However, in the other model, the same limestone filler with varying particle sizes (20 and 32 µm) and filler percentages (5, 10 and 20 wt. %) were used as a variables.

# CHAPTER 4
# RESULTS AND DISCUSSION

## 4.1 Particle size analysis

To calculate the particle size using ImageJ software, original images from the optical microscope were converted into binary images made of black objects with a white background (Figure 4.1 (a)). Binary images were modified with different commands such as Erode, Dilate, Open, Close-, Fill Holes, Watershed, etc. Erode eliminates pixels from the edge of black entities and Dilate enhances the pixels of the edges of black objects. Open, performs an erosion operation that smoothens objects and removes isolated particles. Close, performs a dilation operation and fills in small holes. Due to some noise, white spots in the binary images were removed by the Fill Holes command. Watershed was used to separate or to cut touching particles as they could produce errors in the calculations. The software calculates the size of each particles and the number of particles in the sample as shown in Figure 4.1 (b).

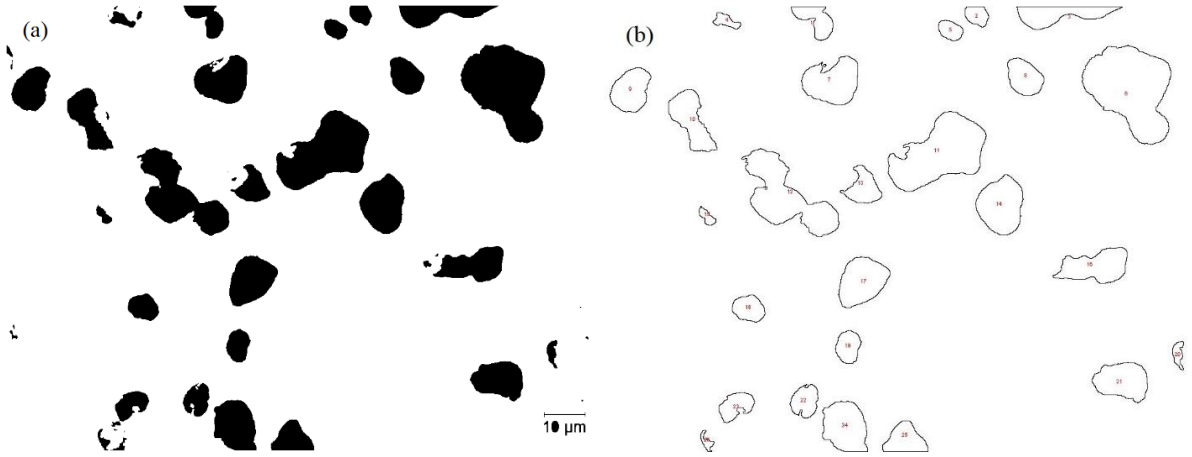


Figure 4.1 ImageJ (a) binary output (b) particle size and frequency output

In ImageJ analysis, Figure 4.1(b), the area of the particles and the number of particles can be used from 2-D images directly. In 2-D imaging, some errors may results since cylindrical shapes or length of the particles may not be calculated effectively. Rather projected particle length is calculated by 2-D imaging. In contrast, if the size of individual micro particles were measured manually, that would be a difficult and time consuming process [122]. Figure 4.2 and Figure 4.3 shows the output as a frequency of occurrence and average diameter of sample particles. The average output diameter from the software was 11.2 and 23.8 µm for 20 and 32 µm sieved sample powders, respectively. The average samples size was lower than the sieved size due to the fact that

there are some particles below the sieved size. Results showed there are some particles above 20 μm in the 20 μm sieved sample. This can be explained by the cylindrical shape of the particles and their high length to cross-sectional diameter ratio. During sieving, the particles, regardless of their lengths tend to slide on top of each other until they became perpendicular and pass through the square sieve openings. In addition, the hammer at the top of the sieving machine continuously impacts the sieves which makes the particles move up and down and pass through the openings regardless of their length.

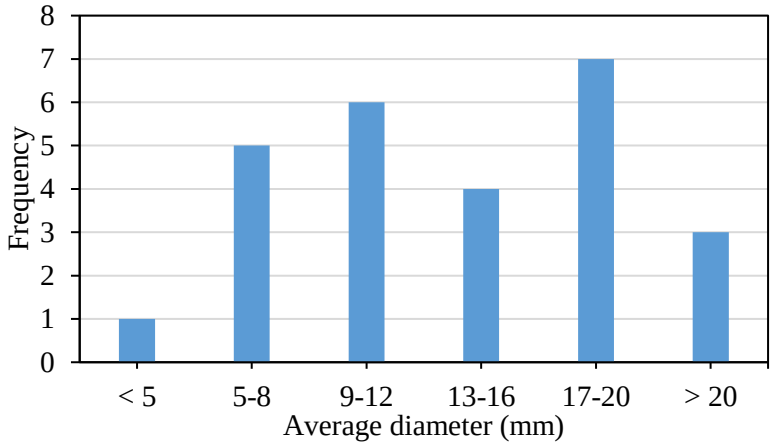


Figure 4.2 ImageJ output for 20-μm powder sample

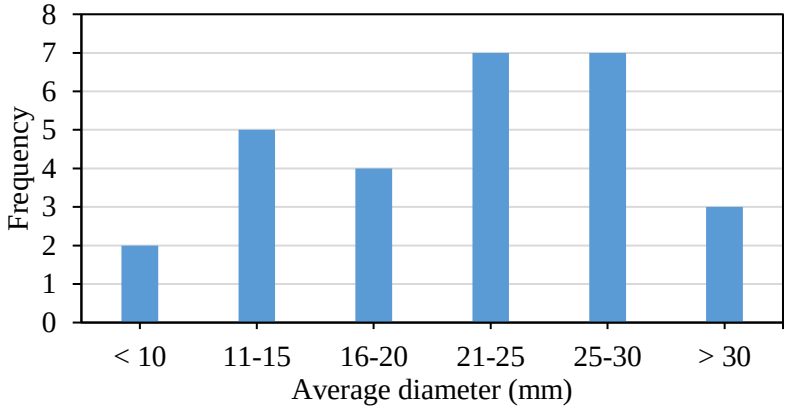


Figure 4.3 ImageJ output for 32-μm powder sample

### 4.2 Weight loss analysis

Particles of $CaCO_3$ begin to decompose into CaO when heated to 750-850 °C in air as shown in the reactions provided in Table 4.1[123]. Based on the law of conservation of mass, which states that matter is neither created nor destroyed in a chemical reaction, every chemical reaction has the

same elements in its reactants and products [124]. As shown in Table 4.1, when 1 mole of $CaCO_3$ (100 gm) is heated, it generates 1 mole of CaO (56 gm) and 1 mole (44 gm) of $CO_2$. In the laboratory, when eggshell powder was heated to 750 °C for 2 h it showed weight reductions of 28 % which was due to partial conversion of $CaCO_3$ to CaO. However, when the temperature increased to 800 °C, the weight loss of the samples increased to 32 %. Furthermore, powdered samples had a 33 and 47 % weight loss at 850 °C for 0.5 and 2 h, respectively. These results showed when eggshell and pure limestone powder was heated to 850 °C for 2 h, the eggshell powder had a 3 % higher weight loss compared to pure limestone powder. This was due to the decomposition of the organic membranes in the eggshell powders [103,125]. However, further increment in temperature and time did not show any improvement in weight loss which suggested that the optimum temperature and time for decomposition of organic membranes was reached at values of 850 °C for 2 h. Pure limestone powder (without membrane) showed the same theoretical weight loss of 56 gm at 850 °C for 2 h of heating time.

Table 4.1 Weight balance in $CaCO_3$ decomposition reactions

| | $CaCO_3$ → | CaO + | $CO_2$ |
|---|---|---|---|
| | Weight of $CaCO_3$ | Weight of CaO | Weight of $CO_2$ |
| Theoretical weight: | (100 gm)* | (56 gm)* | (44 gm)* |
| Eggshell at 750 °C for 2 h: | (100 gm) | (72 gm) | - |
| Eggshell at 800 °C for 2 h: | (100 gm) | (68 gm) | - |
| Eggshell at 850 °C for 0.5 h: | (100 gm) | (67 gm) | - |
| Eggshell at 850 °C for 2 h: | (100 gm) | (53 gm) | - |
| Eggshell at 900 °C for 2 h: | (100 gm) | (53 gm) | - |
| Limestone at 850 °C for 2 h: | (100 gm) | (56 gm) | - |

*Denotes theoretical values. For example,

Mass of $CaCO_3$ = Mass of 1 atom of Calcium (Ca)+Mass of 1 atom of Carbon (C)+Mass of 3 atoms of Oxygen (O).

Mass of 1 atom of Calcium = 1 × 40 g = 40 g

Mass of 1 atom of Carbon = 1 × 12 g = 12 g

Mass of 3 atoms of Oxygen = 3 × 16 g = 48 g

So total theoretical mass of $CaCO_3$ = 40 g + 12 g + 48 g = 100 g

### 4.3 Density analysis

#### 4.3.1 Filler density

The bulk density of eggshell powder was observed to be 2.59 g/cm$^3$, while both purified eggshell and limestone powders showed similar but higher densities of 2.87 and 2.78 g/cm$^3$, respectively. Eggshell organic membranes mainly consist of fibrous proteins [126], which have a significant lower density of 1.39 g/cm$^3$ [127] compared to the more rigid inorganic calcium carbonate mineral. Overall, as shown in Table 4.2, density of eggshell powder was lower than pure limestone powder. These results are in agreement with the earlier work of Hasan *et al.* [128] and Dwivedi *et al.* [129] which determined the density of 2.47 and 2.0 g/cm$^3$ for eggshell and 2.75 and 2.71 g/cm$^3$ for limestone respectively.

Table 4.2 Density of different fillers evaluated in this study

| Powder type | Bulk density (g/cm$^3$) |
|---|---|
| Eggshell | 2.59±0.03 |
| Purified eggshell | 2.87±0.06 |
| Limestone | 2.78±0.04 |

#### 4.3.2 Bio-epoxy composite density

Density results showed the bio-epoxy composite densities increased with all three filler additions. This was due to the $CaCO_3$ filler particles being more dense than the bio-epoxy polymer matrix. The density of the eggshell filler composites was slightly lower than that of the composites with purified eggshell and limestone fillers. This is due to the volatile components and some organic materials present in the eggshell powder which are of lower density [130]. The pure bio-epoxy composites showed a density of 1.130 g/cm$^3$, which improved as the filler loading was increased. Practical density of all composites were lower than theoretical density due to the presence of voids in the composite structure. As shown in Table 4.3, the percentage of voids slightly increased with higher filler contents. At higher filler loading, filler powder was mixed with the bio-epoxy resin at higher speed and time for better dispersion. This could lead to higher air bubbles at higher filler loading during the manufacturing process.

Table 4.3 Density of bio-epoxy composites in this study

| Composite type | Theoretical density ($g/cm^3$) | Practical density ($g/cm^3$) | Void (%) |
|---|---|---|---|
| Bio-epoxy | 1.150 | 1.130±0.006 | 1.770 |
| 5ES | 1.183 | 1.171±0.003 | 1.013 |
| 10ES | 1.218 | 1.188±0.008 | 2.495 |
| 20ES | 1.294 | 1.256±0.006 | 2.965 |
| 5PES | 1.186 | 1.170±0.003 | 1.311 |
| 10PES | 1.224 | 1.195±0.001 | 2.381 |
| 20PES | 1.307 | 1.268±0.002 | 3.016 |
| 5LS | 1.185 | 1.162±0.001 | 1.888 |
| 10LS | 1.222 | 1.194±0.006 | 2.268 |
| 20LS | 1.303 | 1.270±0.005 | 2.517 |

(Where ES-Eggshell, PES-Purified eggshell, LS-Limestone)

### 4.4 Inductively coupled plasma mass spectrometry (ICP-MS) analysis

ICP results showed $CaCO_3$ was the most abundant component in eggshell powder samples. Raw eggshell contained 87.5 ± 0.5 wt. % $CaCO_3$, which increased to 95.0 ± 0.5 wt. % for purified eggshell after the heat treatment. This improvement was due to burning of protein and organic membrane in the eggshell [103,125]. Similarly, the as-received limestone powder was 99.9 % of $CaCO_3$ as obtained from the manufacturer's data sheet. In addition to Ca, very small amounts of various elements such as Al, Cu, Fe, Mg, P, K and Na were found in the purified eggshell powder as shown in Table 4.4. These elements found in eggshell can be different in composition and amounts since they depend upon the ambient environment and nourishment of a chicken [131]. Trace minerals such as Zn, Cu, Fe and Mg in shells are essential nutrients required in small amounts for egg hardness, normal growth and development of the avian embryo. Heavy metals such as Fe, Cd, Cu, Mg, and V occur naturally in the environment and could be from plant nutrients [66]. The percentage of $CaCO_3$ and other elements for eggshell and purified eggshell at different temperature and time is included in Appendix A.

Table 4.4 Chemical results of elements for purified eggshell by ICP-MS

| Element | Weight percentage (µg per gram) |
|---|---|
| Ca | 38 % (380000 µg/g) |
| $CaCO_3$ | 95 % |
| Al | 0.0034 % (34 µg/g) |

| | |
|---|---|
| Cu | 0.0145 % (145 µg/g) |
| Fe | 0.0058 % (58 µg/g) |
| Mg | 0.2640 % (2640 µg/g) |
| P | 0.1300 % (1300 µg/g) |
| K | 0.0034 % (34 µg/g) |
| Na | 0.026 % (260 µg/g) |

### 4.5 Water absorption of bio-epoxy composites

The water absorption characteristics of the bio-epoxy composites varied with the type of fillers as shown in Figure 4.4. The results showed the water absorption of the specimens increased quickly with immersion time at the starting stage (0 to 20 days) and decreased until they were saturated after 65 days. Figure 4.4 shows water absorption ratio of bio-epoxy and bio-epoxy with 20 wt. % of eggshell, purified eggshell and limestone fillers. Pure bio-epoxy showed the lowest amount of water absorption due to absence of any $CaCO_3$ fillers. The water absorption for eggshell filled composites was higher than those filled with purified eggshell and limestone fillers. This could be due to the presence of various surface functional groups, such as amines, amides and carboxylic groups in the eggshell membranes [132]. These small chain functional groups are hydrophilic in nature and tend to create hydrogen bonds with water molecules [133]. Pure bio-epoxy composites absorbed 5.85 wt. % of water after 65 days, while eggshell filled composites showed 44 % higher water absorption for 20 wt. % of fillers. At the beginning and end of the water absorption test, the composites with 20 wt. % of purified eggshell and limestone fillers showed the same amount of water absorption, which was 17 % higher than bio-epoxy composites.

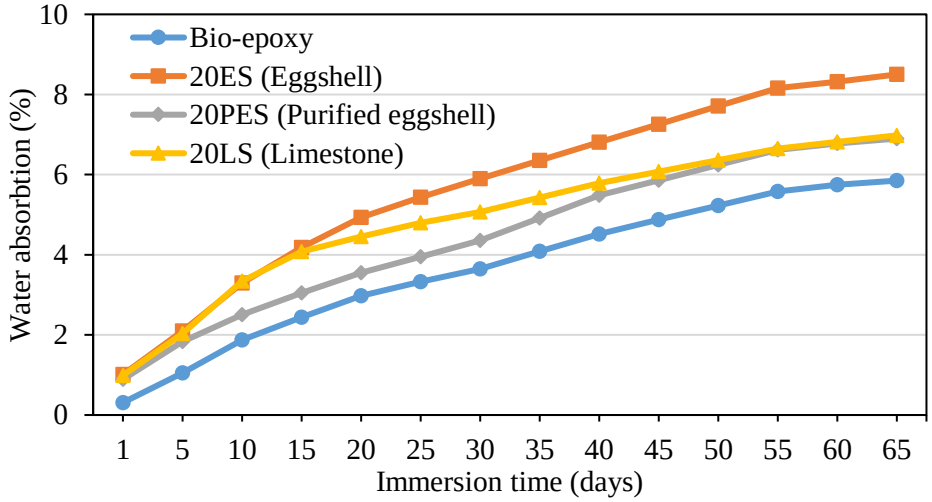


Figure 4.4 Effect of filler types on water absorption of bio-epoxy composites

For all three filler types, composites with higher filler loadings showed more water absorption. This may be due to the presence of greater amounts of filler particles that can absorb more water. At high filler loadings, there is a higher probability for the formation of agglomeration due to the electrostatic forces created between micro particles which hinders achieving a homogeneous dispersion of fillers in the epoxy matrix [134]. In addition, the agglomeration of particles at higher filler loadings may increase the void content in composites due to the difficulties of achieving a homogeneous dispersion at high filler loading which ultimately increases the water absorptivity of the composites [135]. The water absorption of bio-epoxy and bio-epoxy with 5, 10 and 20 wt. % eggshell are shown in Figure 4.5. Bio-epoxy composites showed 5.85 wt. % water absorption, which was increased by 2.5, 15.4 and 45.3 % for 5, 10 and 20 wt. % of eggshell fillers, respectively. Figure 4.6 shows the water absorption results for bio-epoxy and bio-epoxy containing 5, 10 and 20 wt. % purified eggshell, while Figure 4.7 illustrates the results for bio-epoxy and bio-epoxy containing 5, 10 and 20 wt. % limestone. Compared to the pure bio-epoxy, the addition of 5 wt. % purified eggshell or limestone fillers did not create any significant difference in water absorption. However, the amount of water absorbed by the composites increased by 6.0 and 17.9 % for purified eggshell, and 4.6 and 19.3 % for limestone fillers in loadings of 10 and 20 wt. % respectively. Overall, purified eggshell and limestone at all filler contents showed similar amounts of water absorption, which was lower than eggshell filled composites due to absence of membranes. Figure 4.8 showed composites with 20 µm fillers absorbed much more water than composites with 32 µm fillers. This is due to the fact that the smaller particle size of the fillers could produce a maximal interface contact with the water due to larger specific surface area. As a result, the ability to absorb water increased with reduction in particle size [136].

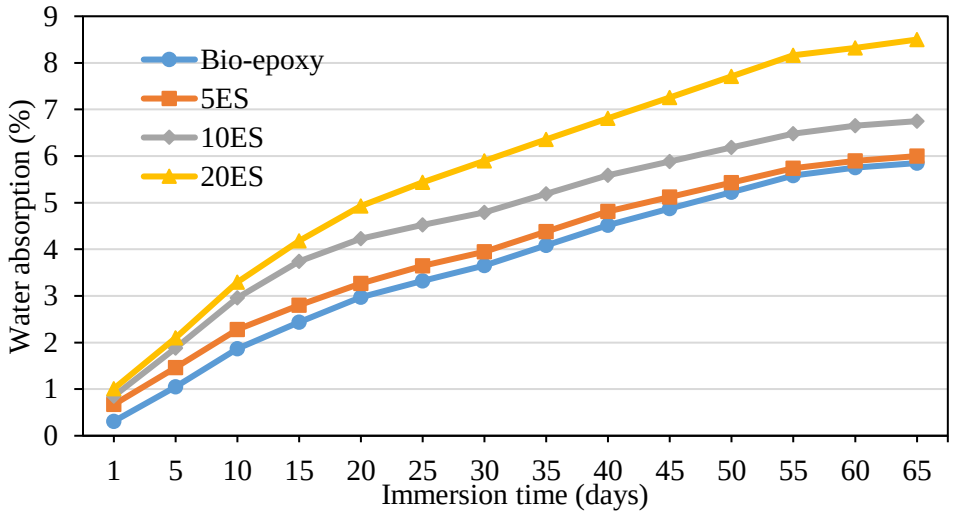


Figure 4.5 Water absorption of eggshell filled composite for 32 µm

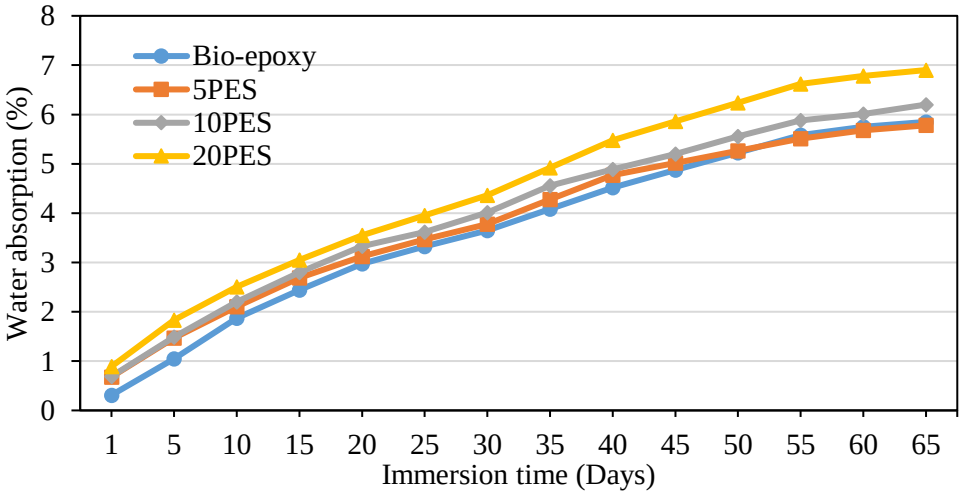


Figure 4.6 Water absorption of purified eggshell filled composite for 32 µm

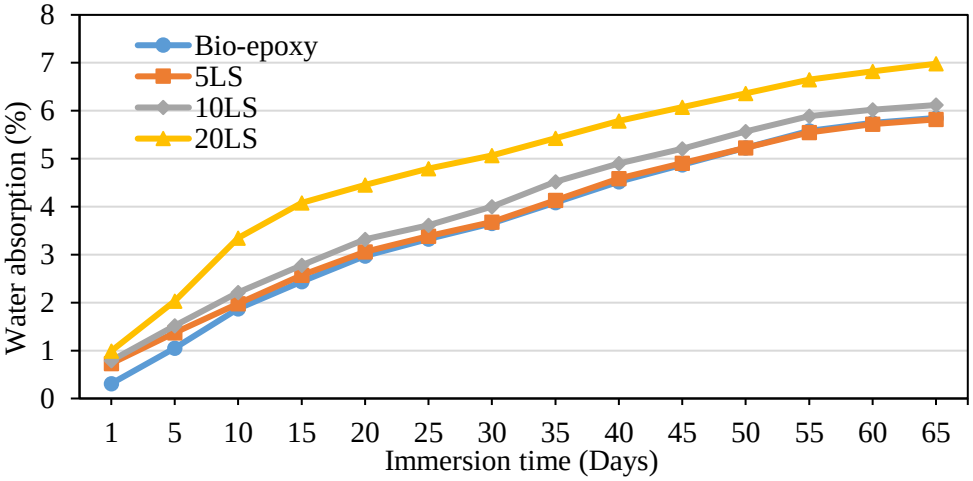


Figure 4.7 Water absorption of limestone filled composite for 32 µm

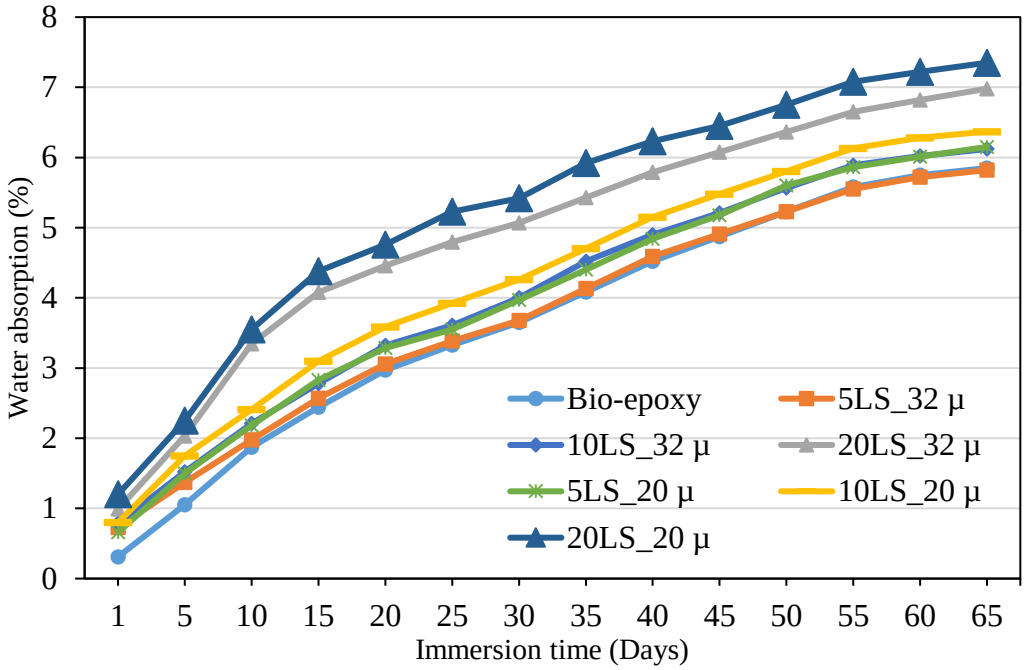


Figure 4.8 Water absorption of 32 and 20 µm limestone filled composite

### 4.6 Scanning electron microscopic (SEM) analysis

Morphological structures of eggshell, purified eggshell and limestone are outlined in Figure 4.9. As observed, all particles are irregular in shape with a wide range of particle sizes due to the crushing processes. The organic membranes on the surface of the eggshell particles can be observed in Figure 4.9 (a) which is absent in the purified eggshell and limestone samples of Figure 4.9 (b) and Figure 4.9 (c), respectively.

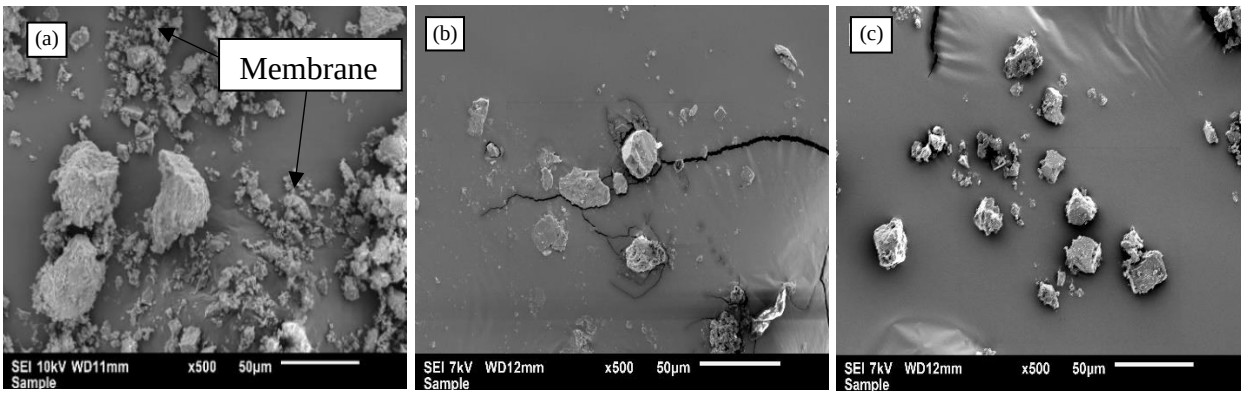


Figure 4.9 SEM images showing particle morphology of (a) eggshell (b) purified eggshell and (c) limestone

The tensile fractured surface morphologies of pure bio-epoxy, bio-epoxy filled with eggshell, purified eggshell and limestone under different filler loadings were taken at a magnification of X1000 and are shown in Figure 4.10. As observed in Figure 4.10 (a), pure bio-epoxy fractured surface showed uninterrupted crack paths propagated along the thickness direction. The nature of this surface suggests a brittle failure, as the surface is smooth and flat whiles the cracks are propagated uninterruptedly. However, at higher filler loading, as shown in Figure 4.10 (b-d), Figure 4.10 (e-g) and Figure 4.10 (h-j); the fractures showed rougher surfaces and contained river markings. These are indications of crack path deflection as a result of improved ductility of the matrix in the presence of harder filler particles. Filler particles bonded well within the matrix as can be seen in Figure 4.10 (b, c, f, g, h and i) as they are well embedded in the bio-epoxy matrix. At higher loadings, due to the higher concentration of $CaCO_3$ particles, stress transformation between $CaCO_3$ particles was predominant rather than the intended particle-to-polymer interaction [137]. This is attributed to the agglomeration, which is a collection of loosely bound particles, aggregates or a mixture of two small particles. The agglomerates behaves like a large particle holding smaller particles together with weak Van der Waals forces. These lower forces tend to create weaker filler-matrix interfaces and as a result some microvoids can be observed in Figure 4.10 (c, f) due to some particles being extracted when the load was applied. These flaws act as stress concentrations in the materials and lead to compromises in mechanical properties and unexpected failures. This also suggests that mechanical properties could be enhanced further if the flaws can be controlled. Cao *et al.* [138] used stearic acid to improve filler dispersion in the matrix, which, up to some extent, prevented the fillers from forming a network of aggregates in composite. These observations of the SEM analysis justified lower tensile properties at higher filler loadings compared to lower filler loadings.

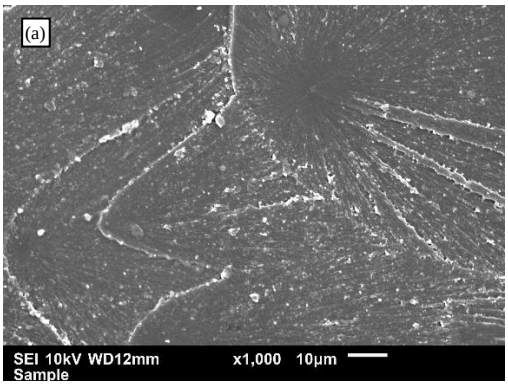

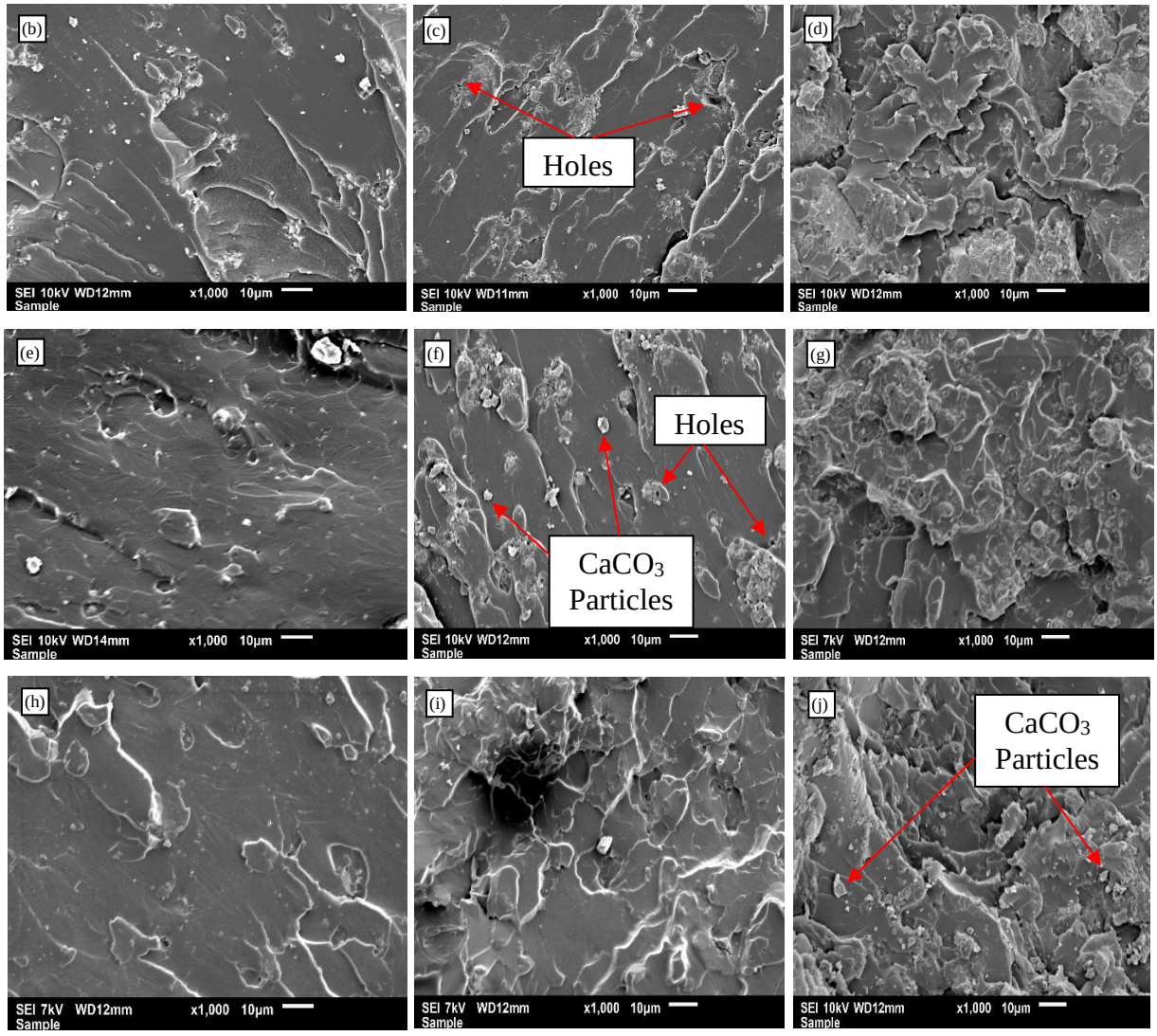


Figure 4.10 SEM fractured tensile surfaces for (a) bio-epoxy, (b) bio-epoxy/5ES, (c) bio-epoxy/10ES, (d) bio-epoxy/20ES, (e) bio-epoxy/5PES, (f) bio-epoxy/10PES, (g) bio-epoxy/20PES, (h) bio-epoxy/5LS, (i) bio-epoxy/10LS and (j) bio-epoxy/20LS

Fractured surfaces for flexural samples are shown in Figure 4.11 and showed similar behaviors to the tensile fractured surfaces. The unfilled bio-epoxy resin (Figure 4.11(a)) showed a flat, smooth mirror-like surface indicating brittle fracture. However, as given in Figure 4.11(b-j), the surface roughness increased as the filler loadings increased for all three fillers. This could be due to the presence of filler particles which act as a barriers and deviates the crack movement during deformation [139]. This uneven crack deviation from the presence of filler particles in the composites tended to generate rougher fractured surfaces as shown in Figure 4.11 (d, g, j).

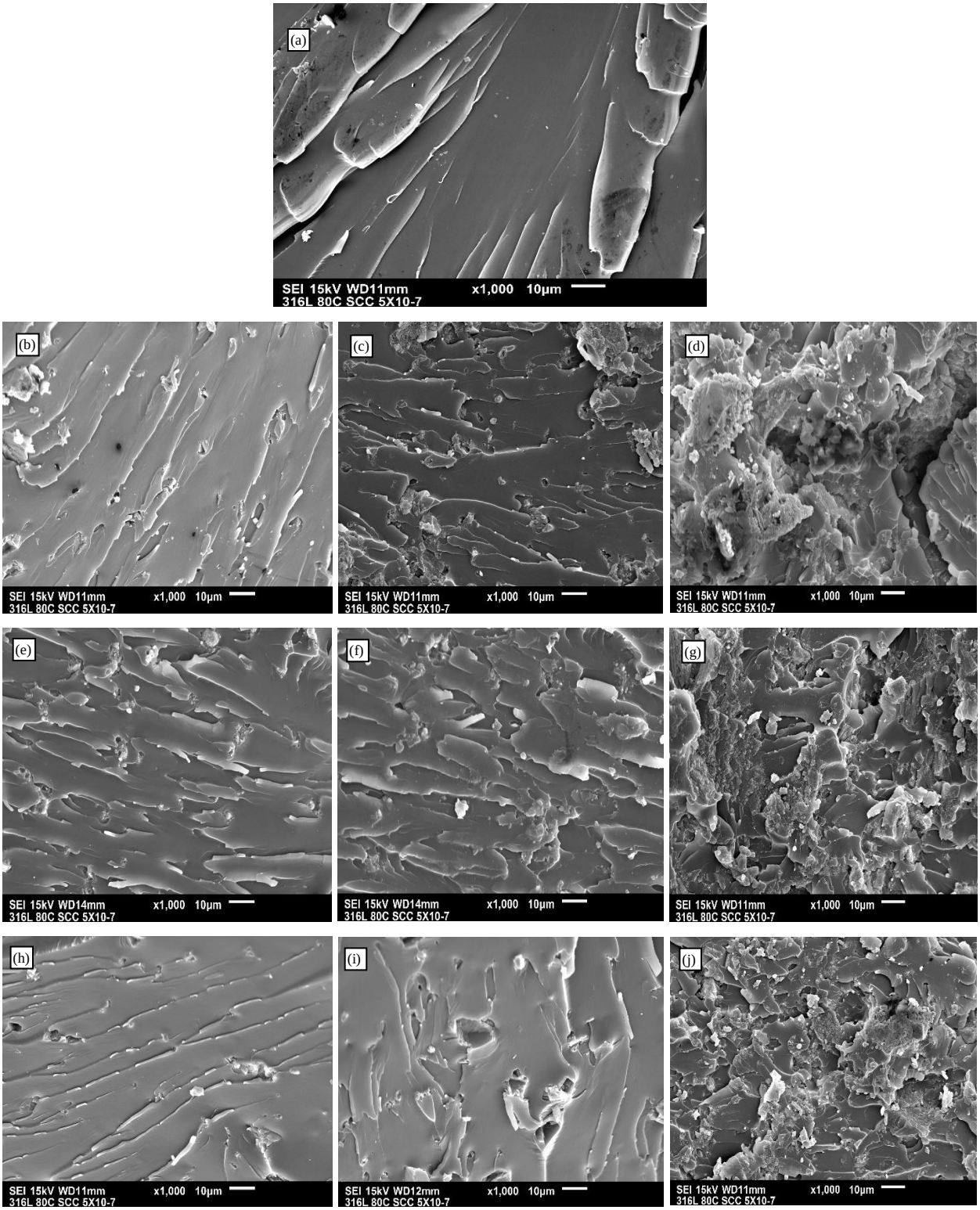


Figure 4.11 SEM fractured flexural surfaces for (a) bio-epoxy, (b) bio-epoxy/5ES, (c) bio-epoxy/10ES, (d) bio-epoxy/20ES, (e) bio-epoxy/5PES, (f) bio-epoxy/10PES, (g) bio-epoxy/20PES, (h) bio-epoxy/5LS, (i) bio-epoxy/10LS and (j) bio-epoxy/20LS

### 4.7 Tensile test

Figure 4.12 illustrates the typical bio-epoxy room temperature stress-strain curves derived from the load-displacement data obtained from the Instron test equipment. As the tensile force was applied by the hydraulic crosshead, the laser extensometer precisely measured the extension of the specimens. The tensile stress was calculated based on the force and displacement data obtained by tensile machine.

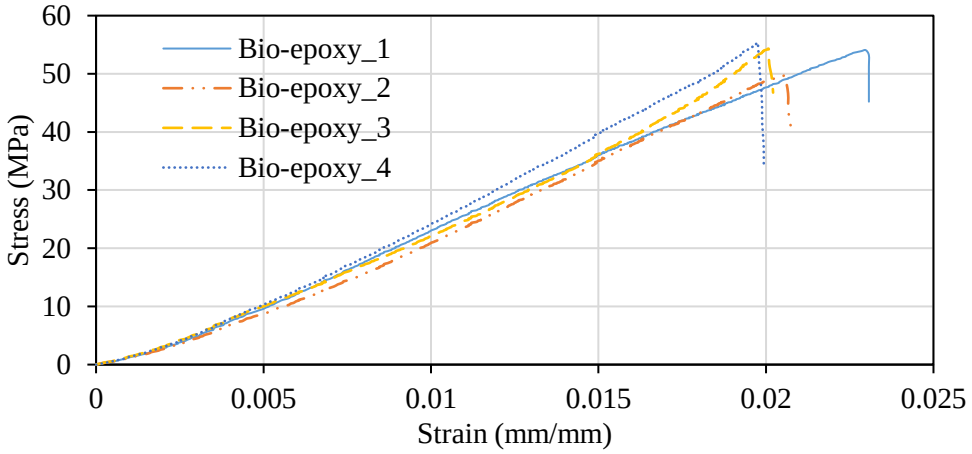


Figure 4.12 Output of stress-strain curve for bio-epoxy

The tensile strength of pure bio-epoxy and bio-epoxy with different filler types (eggshell, purified eggshell and limestone) and of filler loadings (5, 10 and 20 wt. %) are shown in Figure 4.13 for 32 µm particles. The pure bio-epoxy showed the maximum tensile strength of 55.9±2.1 MPa which was due to the absence of any filler materials. The value is comparable to the manufacturers data sheet of 62.0 MPa [140]. The tensile strength reduced by 10.3, 28.2 and 15.7 % when 5 wt. % of eggshell, purified eggshell and limestone were mixed with the bio-epoxy, respectively. Tensile strengths were highest when 10 wt. % fillers were added and reduced by 3.6, 17.0 and 14.1 % for eggshell, purified eggshell and limestone, respectively, but decreased by 19.5, 31.7 and 20.7 % at 20 wt. %, fillers, respectively. The reduction in strength at higher filler loadings were possibly due to particle agglomeration which limited the load transfer from the matrix to the fillers. This phenomenon can cause cracks to initiate and propagate easily [134,141]. Overall, composites with eggshell fillers showed higher tensile strengths compare to purified eggshell and limestone. This could be due to the presence of membranes on the eggshell particles, , which are a protein matrix with relatively high concentrations of polar amino acids [142]. These amino acids may promote better bonding between bio-epoxy and organic membrane which has been reported to adhere well

to the eggshell particles [143]. Hincke *et al.* [50] showed that the soluble matrix proteins of eggshell membranes can change the macroscopic performance of the resulting composite. The nature of the interactions between the mineral phase and eggshell matrix proteins has been intensely studied, but mechanistic behaviors remain unknown [50]. Composites with 20 µm limestone fillers showed slightly higher tensile strengths than 32 µm limestone fillers due to the higher effective surface area.

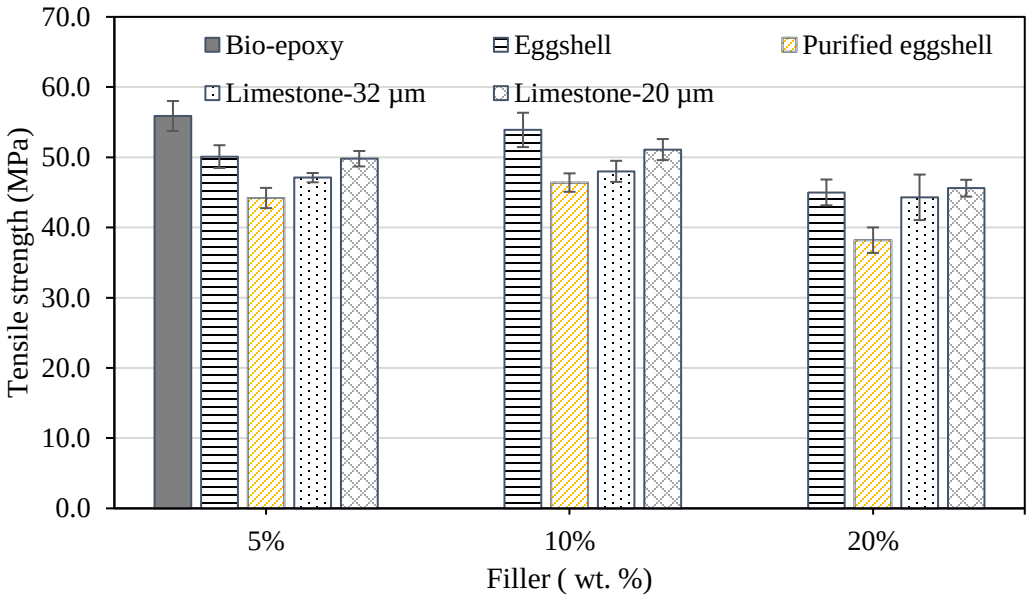


Figure 4.13 Effect of $CaCO_3$ filler type and loadings on tensile strength

Figure 4.14 shows the tensile modulus results for different fillers with different loadings. Pure bio-epoxy showed the lowest tensile modules of 2.5±0.2 GPa which was similar to the manufacturers data sheet of 2.8 GPa [140]. Tensile modulus increased steadily for all filler types as the percentage of filler increased. The highest modules was recorded at 20 wt. % loading where the modulus increased by 68.0, 96.0 and 63.9 % for eggshell, purified eggshell and limestone, respectively compared to pure bio-epoxy composites. The improvement of stiffness with filler increments was attributed to the presence of harder limestone particles than the polymer matrix.

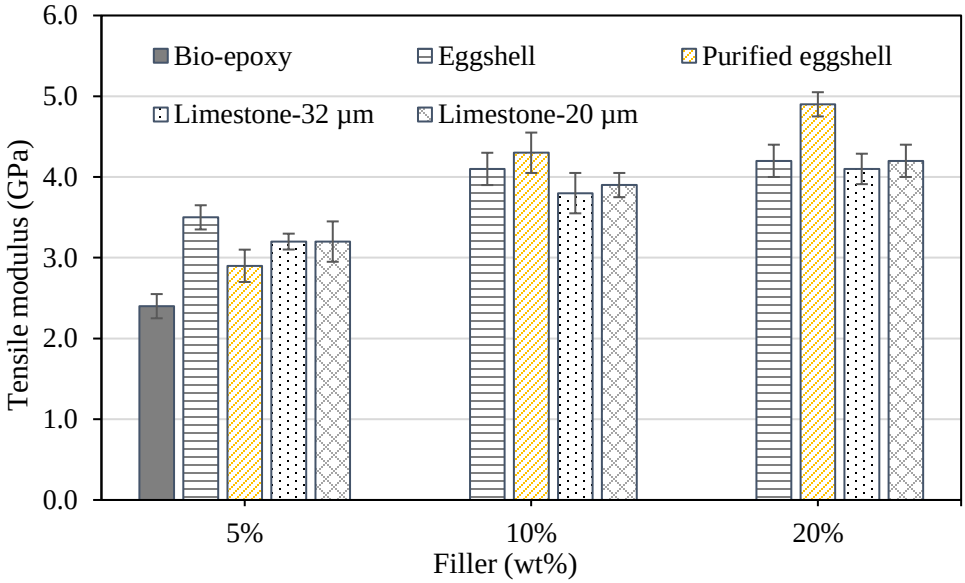


Figure 4.14 Effect $CaCO_3$ filler type and loadings on tensile modulus

### 4.8 Flexural test

The flexural strength of the bio-epoxy composite materials with different types (eggshell, purified eggshell and limestone) and filler loadings are shown in Figure 4.15. The pure bio-epoxy had a maximum flexural strength of 86.0±3.2 MPa, which was comparable to the manufacturers value of 92.7 MPa [140]. Generally, composites containing eggshell particles showed the highest flexural strengths, but tended to decrease by 13.4, 16.7 and 37.6 % at 5, 10 and 20 wt. %, respectively as compared to pure bio-epoxy composites. At lower filler loadings, there may be less particle agglomeration which suggests better load transfer from the matrix to the filler particles. The purified eggshell and limestone performed similarly with limestone having slightly better strengths. For example, flexural strengths reduced by 26.1, 31.3 and 36.7 % for purified eggshell and 23.2, 29.0 and 31.5 % for limestone fillers, respectively. Similar to the tensile properties, composites with 20 µm limestone fillers showed slightly higher flexural properties (both strength and modulus) than 32 µm limestone fillers as a result of higher effective surface area for smaller particles.

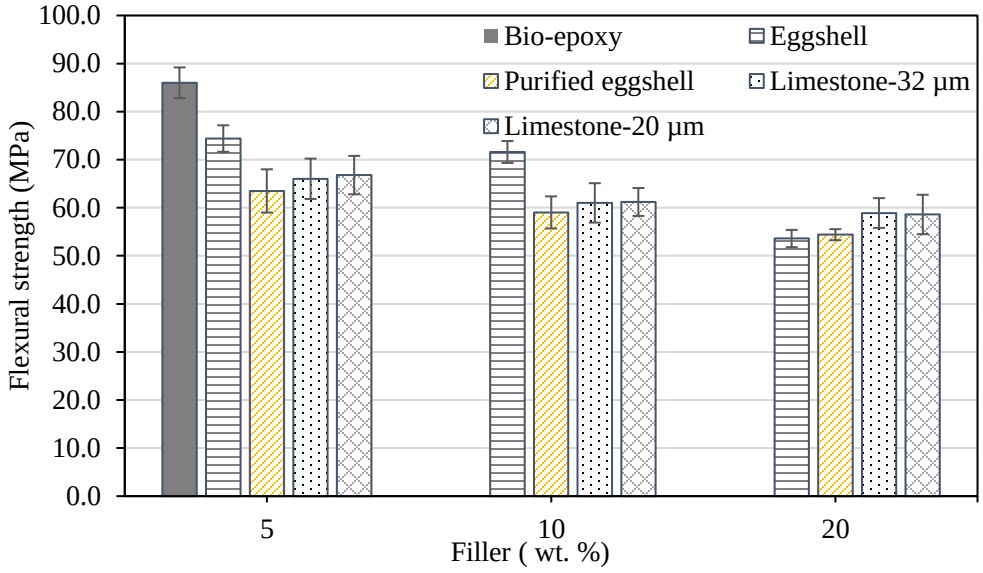


Figure 4.15 Effect of 32 µm $CaCO_3$ filler type and loadings on flexural strength

The flexural modulus results are given in Figure 4.16. The flexure modulus recorded 3.8±0.25 GPa (compared to 2.8 GPa from manufacturers data sheet) for pure bio-epoxy composites which increased sharply by 60.5, 36.8 and 34.2 % for bio-epoxy, purified eggshell and limestone containing 20 wt. %, respectively. This higher flexural modulus could be due to the presence of stiffer limestone particles, which increased the stiffening effect in the composites [144]. The results obtained from these tests were in-line with other researchers such as Leong *et al.* [145] and Timob *et al.* [146].

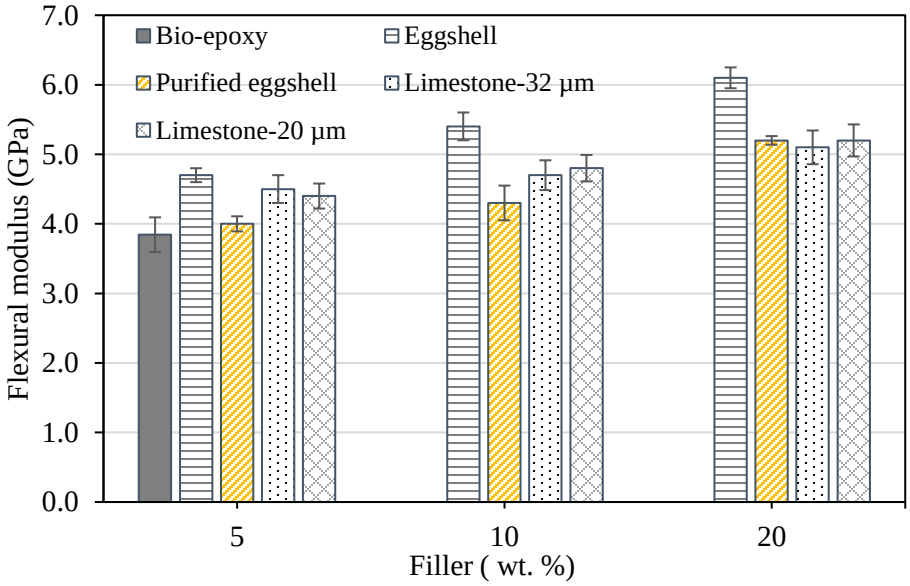


Figure 4.16 Effect of 32 µm $CaCO_3$ filler type and loadings on flexural modulus

### 4.9 Charpy impact test

Room temperature Charpy impact toughness results are shown in Figure 4.17. Impact test results showed there was a gradual decrease in impact energy with increase in filler contents for all three fillers (eggshell, purified eggshell and limestone). This could be due to the higher tendency of agglomeration at higher filler loadings which generates poor interfacial regions during impact. Toro *et al.* [147] indicated when a crack is generated due to an impact it propagates towards the poor interfacial regions. As a result, impact strengths tend to decrease gradually when filler contents increase. Pure bio-epoxy produced an impact strength of 82 J/cm$^2$, which reduced by 16, 25, and 31 % for eggshell; 25, 31 and 39 % for purified eggshell and 22, 28 and 36 % for limestone fillers with 5, 10 and 20 wt. %, respectively. Large particle sizes lead to greater stress concentration, therefore limestone particles with 20 µm sizes showed higher impact strengths than 32 µm sizes which is typical. Bio-epoxy composites with 20 µm limestone fillers showed 4, 5 and 4 % higher impact strengths than 32 µm fillers at 5, 10 and 20 wt. %, respectively. Furthermore, eggshell fillers showed a slight enhancement in impact strengths for the same content of filler loadings in purified eggshell and limestone composites. This could be due to presence of membranes on eggshell particles, which may promote better bridging between the bio-epoxy matrix and $CaCO_3$ particles in eggshell fillers.

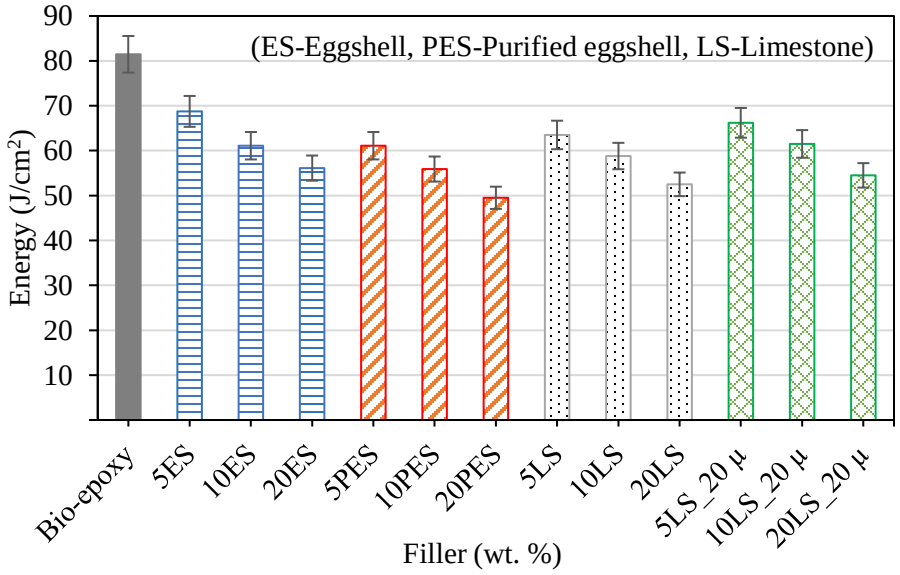


Figure 4.17 Effect of different $CaCO_3$ fillers and loadings on Charpy impact energy

### 4.10 Thermogravimetric analysis (TGA)

The thermal decomposition of eggshell, purified eggshell and limestone was studied by TGA and experimental results are shown in Figure 4.18 for samples heated from 25 to 1000 °C. Figure 4.19 illustrated a magnified version for a section of Figure 4.18 from 200 to 600 °C. The results showed very little surface moisture was present in the samples as no weight loss can be observed in Figure 4.18 around 100 °C. This was predicted as the sample had been dried prior to testing.

A small amount of weight loss can be observed in Figure 4.19 between 200 to 600 °C for both eggshell and purified eggshell due to removal of trapped water from the boundary of calcite crystals [148]. However, eggshell powder showed higher weight loss due to the presence of organic membranes which are not present in purified eggshell. Although purified eggshell does not contain an organic membrane, it did have a weight loss within this temperature range. This could be due to the breakdown of other chemical compounds present in the eggshell as shown in ICP-MS results of Table 4.4. These observations were similar to the results of Tsuboi *et al.* [103] which showed that fibrous proteins in organic membranes decomposed totally at 600 °C. Furthermore, eggshell membranes are organic materials containing collagen, amines, amides of proteins and carboxylic acids. [149]. To understand the thermal degradation of collagen protein, León-Mancilla *et al.* [150] performed TGA and DSC studies. TGA results showed a weight loss of 75.4 % at 700 °C due to combustion of collagen. DSC results showed an exothermic peak of collagen in a temperature range between 350 °C to 425 °C, corresponding to the combustion of the collagen fibers. Around 600 °C, $CaCO_3$ particles begin to decompose into CaO by producing $CO_2$ [64]. As a result, a major weight loss is seen in the range of 600-820 °C for all samples.

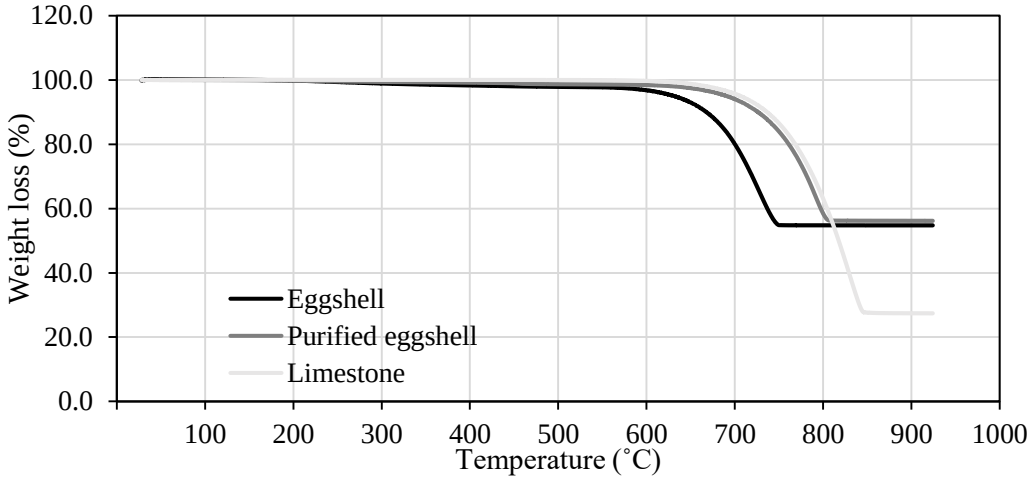


Figure 4.18 TGA result of eggshell, purified eggshell and limestone powders (25 to 1000 °C)

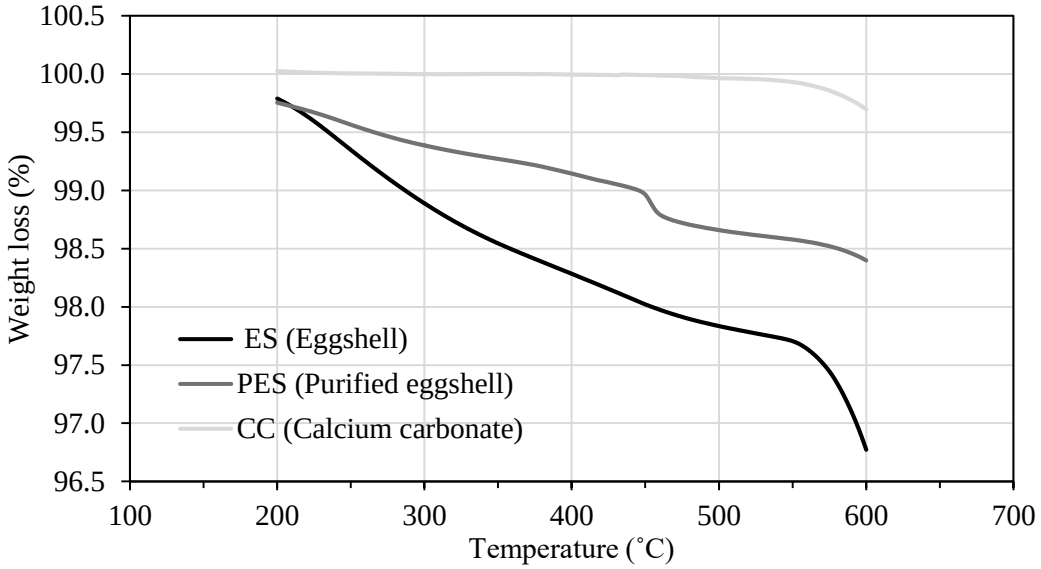


Figure 4.19 TGA result of eggshell, purified eggshell and limestone powders (200 to 600 °C)

### 4.11 Differential scanning calorimetry (DSC) analysis

Figure 4.20 shows the graph of DSC for different composites with 20 wt. % of filler loadings for eggshell, purified eggshell and limestone. Pure bio-epoxy composites showed a $T_g$ value of 54.0 ºC which increased by 53 % for composites containing all three filler types. This significant improvement in $T_g$ clearly indicated that the presence of $CaCO_3$ particles in bio-epoxy resin increased its rigidity and restricted the mobility of the polymer chains. Lorenzo *et al.* [151] also observed a similar behavior when limestone particles at 10 wt. % loading were added to polyethylene terephthalate resin. The composites showed a 21 % improvement in $T_g$ which was attributed to the chain mobility restrictions.

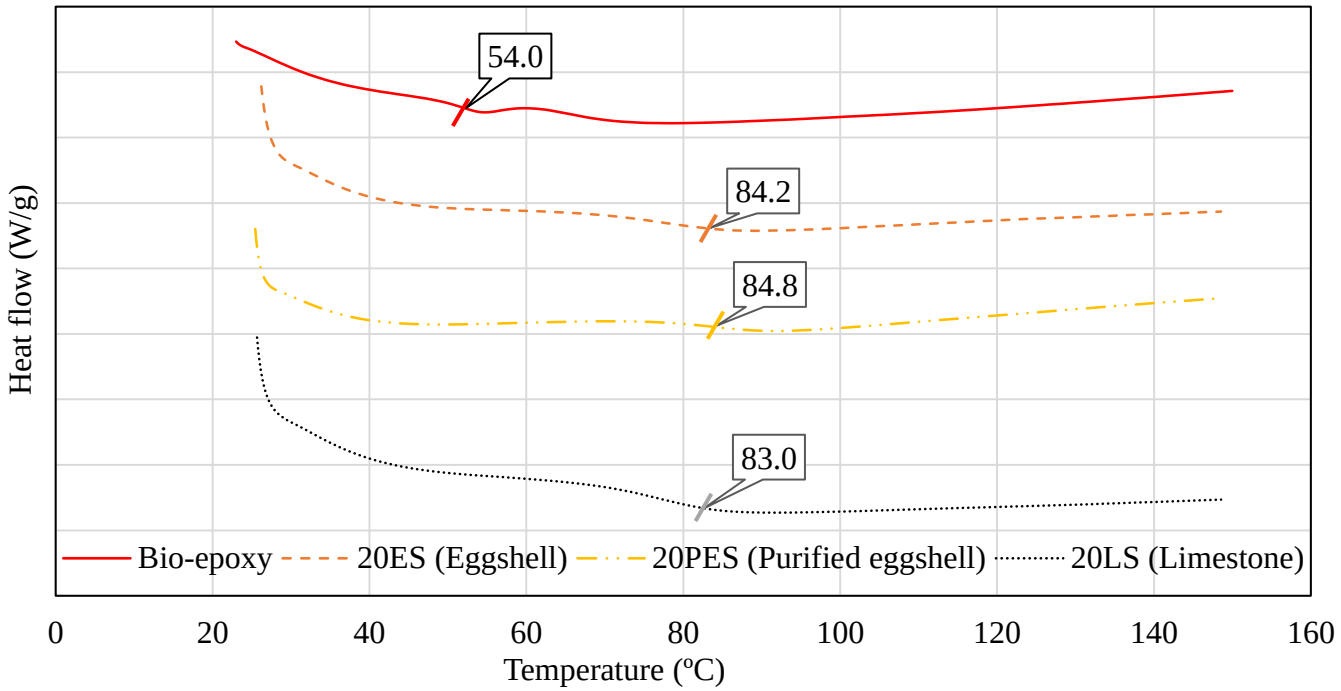


Figure 4.20 DSC result of bio-epoxy composites containing 20 wt. % eggshell, purified eggshell and limestone

### 4.12 Statistical analysis

The ANOVA result on the different mechanical properties (tensile strength, tensile modulus, flexural strength, flexural modulus and Charpy impact strength) are shown in Table 4.5 and Table 4.6. Table 4.5 provides the results for varying filler loadings and types with fixed 32 µm particles, while Table 4.6 provides varying filler loadings and particle sizes with fixed limestone filler. Two-way ANOVA results suggest that all mechanical properties were significantly dependent on filler loadings, filler types and particle size since the *p*-values were less than 0.05.

Table 4.5 ANOVA results for mechanical properties with varying filler loadings (5, 10 and 20 wt. %) and filler types (eggshell, purified eggshell and limestone) with fixed particle size (32 µm)

| Property | Composite Variation | DF | SS | MS | F | P |
|---|---|---|---|---|---|---|
| Tensile strength | Filler load | 2 | 273.59 | 136.79 | 35.96 | <0.001 |
| | Filler type | 3 | 592.52 | 197.50 | 51.92 | <0.001 |
| | Filler load x Filler type | 6 | 99.48 | 16.58 | 4.35 | 0.004 |
| | Residual | 24 | 91.29 | 3.80 | | |
| | Total | 35 | 1056.88 | 30.19 | | |
| Tensile modulus | Filler load | 2 | 14.12 | 7.06 | 469.69 | <0.001 |
| | Filler type | 3 | 18.38 | 6.12 | 407.60 | <0.001 |
| | Filler load x Filler type | 6 | 4.88 | 0.81 | 54.09 | <0.001 |
| | Residual | 24 | 0.36 | 0.015 | | |
| | Total | 35 | 37.75 | 1.078 | | |
| Flexural strength | Filler load | 2 | 1135.32 | 567.66 | 63.98 | <0.001 |
| | Filler type | 3 | 3813.64 | 1271.21 | 143.27 | <0.001 |
| | Filler load x Filler type | 6 | 513.55 | 85.59 | 9.64 | <0.001 |
| | Residual | 24 | 212.94 | 8.87 | | |
| | Total | 35 | 5675.45 | 162.15 | | |
| Flexural modulus | Filler load | 2 | 3.18 | 1.58 | 23.51 | <0.001 |
| | Filler type | 3 | 6.82 | 2.274 | 33.64 | <0.001 |
| | Filler load x Filler type | 6 | 1.18 | 0.196 | 2.90 | 0.028 |
| | Residual | 24 | 1.62 | 0.067 | | |
| | Total | 35 | 12.80 | 0.36 | | |
| Charpy impact strength | Filler load | 2 | 936.18 | 468.09 | 84.86 | <0.001 |
| | Filler type | 3 | 4848.62 | 1616.20 | 293.02 | <0.001 |
| | Filler load x Filler type | 6 | 316.65 | 52.77 | 9.56 | <0.001 |
| | Residual | 24 | 132.37 | 5.51 | | |
| | Total | 35 | 6233.83 | 178.11 | | |

DF = degree of freedom, SS = sum of squares, MS = mean square, F = F-test statistic, *p*-value = calculated probability

Table 4.6. ANOVA results for mechanical properties with varying filler loadings (5, 10 and 20 wt. %) and particle sizes (20 and 32 μm) with fixed limestone filler

| Property | Source of Variation | DF | SS | MS | F | P |
|---|---|---|---|---|---|---|
| Tensile strength | Filler load | 2 | 121.78 | 60.88 | 16.02 | <0.001 |
| | Filler type | 2 | 489.29 | 244.64 | 64.37 | <0.001 |
| | Filler load x Filler type | 4 | 62.45 | 15.61 | 4.10 | 0.015 |
| | Residual | 18 | 68.41 | 3.8 | | |
| | Total | 26 | 741.93 | 28.53 | | |
| Tensile modulus | Filler load | 2 | 7.96 | 3.98 | 328.83 | <0.001 |
| | Filler type | 2 | 15.75 | 7.87 | 650.72 | <0.001 |
| | Filler load x Filler type | 4 | 3.98 | 0.99 | 82.24 | <0.001 |
| | Residual | 18 | 0.22 | 0.012 | | |
| | Total | 26 | 27.91 | 1.07 | | |
| Flexural strength | Filler load | 2 | 157.58 | 78.79 | 5.86 | 0.011 |
| | Filler type | 2 | 3608.30 | 1804.14 | 134.32 | <0.001 |
| | Filler load x Filler type | 4 | 197.25 | 49.31 | 3.672 | 0.023 |
| | Residual | 18 | 241.76 | 13.43 | | |
| | Total | 26 | 4204.89 | 161.72 | | |
| Flexural modulus | Filler load | 2 | 1.58 | 0.79 | 11.34 | <0.001 |
| | Filler type | 2 | 7.84 | 3.92 | 56.21 | <0.001 |
| | Filler load x Filler type | 4 | 0.81 | 0.203 | 2.90 | 0.048 |
| | Residual | 18 | 1.26 | 0.069 | | |
| | Total | 26 | 11.49 | 0.44 | | |
| Charpy impact strength | Filler load | 2 | 539.36 | 269.68 | 33.75 | <0.001 |
| | Filler type | 2 | 3780.02 | 1890.01 | 236.53 | <0.001 |
| | Filler load x Filler type | 4 | 270.17 | 67.54 | 8.45 | <0.001 |
| | Residual | 18 | 143.82 | 7.99 | | |
| | Total | 26 | 4733.38 | 182.05 | | |

### 4.13 Economic analysis

The amount of eggs produced by different countries are discussed in Chapter 2 (Figure 2.3). The shell alone covers around 11 wt. % of the whole egg which weights approximately 6.8 gm [40]. To calculate the cost saving from recycling waste eggshell, the egg processing plant in Lethbridge, Alberta (EggSolutions EPIC Inc.) was selected as a base model. This plant handles around 103,68 thousands of tons of eggs per year (e.g. 180,000 dozens of eggs per week) [152], which could be a source of 705,000 kg of $CaCO_3$. In Calgary, Alberta it costs around $ 200 to dispose 1 ton (1000 kg) of waste to the landfills [153]. Based on these values, it would cost approximately $ 140,000 annually to dispose eggshell waste to landfills. In contrast, mined limestone powder price varies from $ 200 to $ 500 per ton depending upon the fineness and purity of powder. Assuming the eggshell powder processing location is located near the egg processing plant (neglecting transportation cost) and a market value of $ 250 per ton of limestone, this plant could produce $ 175,000 worth of limestone annually. Therefore, the total saving from this one plant alone could reach to $315,000 per year by recycling waste eggshell. However, in this analysis the cost of grinding, cleaning and packaging was not considered.

# CHAPTER 5
# CONCLUSIONS AND RECOMMENDATIONS

## 5.1 Conclusion

Effective thermal and chemical treatments of bio-waste eggshells and their utilization in composite materials can benefit our society both in the environment and economically. This work presented one method to recover pure $CaCO_3$ from waste eggshell and utilize them as fillers to produce new composite materials.

In this study, three types of fillers were prepared: unpurified eggshell, purified eggshell and mineral limestone. The fillers were added to a bio-epoxy composite using a solution mixing technique. The powders were evaluated for particle size, optical microscopy, density, scanning electron microscopy (SEM), Inductively Coupled Plasma Mass Spectrometry (ICP-MS) analysis, Thermogravimetric (TGA) analysis, and Differential scanning calorimetry (DSC) analysis. New bio-epoxy composites with different filler loadings of eggshell with and without any treatment were produced and compared against limestone fillers. The composite results were investigated by means of density measurement, water absorption analysis, tensile properties, flexural properties and Charpy impact properties. The significance of the results were analyzed using two-way analysis of variance (ANOVA) system.

The following conclusions can be drawn from experimental results and analysis of the data:

- ICP-MS analysis showed the purified eggshell contained slightly more $CaCO_3$ than raw eggshell due to the removal of the organic membranes. Weight loss analysis showed eggshell powders decreased more than the theoretical values when heated to 850ºC for 2 h due to the removal of membranes.
- Particle size analysis showed the average particle size was below the sieve size. i.e. average of 11.2 µm and 23.8 µm when sieved with 20 and 32 µm size standard sieves, respectively, possibly due to the presence of lower size particles in samples.
- Eggshell powder showed lower density than purified eggshell and limestone due to the percent of low-density (1.39 $g/cm^3$) membrane particles on the eggshell particles and within the sample. The density of the composites increased with increasing filler contents due to the presence of denser $CaCO_3$ (2.78 $g/cm^3$) particles.

- Pure bio-epoxy composites absorbed 5.85 wt. % water after 65 days of being immersed, which increased by 44 % for bio-epoxy containing 20 wt. % eggshell and 17 % for both bio-epoxy composites with purified eggshell and limestone fillers at 20 wt. % loadings.
- The TGA curve showed small weight losses between 250-600 °C due to the presence of organic membranes in the eggshell. It also showed that $CaCO_3$ began to decompose into CaO at 800ºC.
- SEM images of both fractured tensile and flexural surfaces showed a number of holes at the fractured surface for higher filler loadings due to agglomeration of filler particles.
- Overall, the tensile and flexural strengths decreased when the addition of filler materials were increased from 5 wt. % to 20 wt. % for all three filler types (eggshell, purified eggshell and limestone). However, the tensile and flexural modulus improved with the increase of filler loadings compared to the pure bio-epoxy. For composites subjected to tensile and flexural applications, the addition of not more than 10 wt. % and 5 wt. % eggshell, respectively in the bio-epoxy is recommended.
- The Charpy impact energy decreased with increase in filler contents for all three fillers. This could be due to presence of agglomeration and voids created during manufacturing at higher filler loadings.
- Generally, 20 µm powders showed higher mechanical properties than 32 µm powders which may be attributed to finer particles having a maximal interface contact with the polymer chains due to their larger specific surface areas of the particles.
- ANOVA results proved that composite properties such as tensile strength, tensile modulus, flexural strength, flexural modulus and Charpy impact strengths were significantly dependent on filler loadings, filler types and filler size.
- Economy analysis for an egg breaking plant located in Lethbridge, Alberta showed that around 705,000 kg of $CaCO_3$ could be produced from this egg processing plant annually by recycling waste eggshell.
- In conclusion, eggshell could be an alternative to mineral limestone as a filler material for the plastics industry.

## 5.2 Recommendations for future work

Based on the research conducted, some recommendations that could be performed in future studies are:

- Coating of purified eggshell particles with stearic acid to improve dispersion of particles and interfacial bonding with the matrix.
- Size of filler particles was found to affect the dispersion and the agglomeration of the composites. Nano-particles as filler materials at lower than 5 wt. % loadings are recommended for further investigation.
- An attempt should be made to remove other trace metals presence in purified eggshell to achieve pure limestone powder from eggshell for use as a pharmaceutical grade limestone.
- Calcium carbonate tablets could be fabricated using purified eggshell powders and the treatment response as a medication could be analyzed with current tablets on the market. This could potentially reduce the price of calcium related supplements in the medical and pharmaceutical industries.

## REFERENCES


[1] E. Papargyropoulou, R. Lozano, J. Steinberger, N. Wright, and Z. Ujang, "The food waste hierarchy as a framework for the management of food surplus and food waste," *J. Clean. Prod.*, 2014.

[2] J. Gertsakis and H. Lewis, "Sustainability and the waste management hierarchy," *A Discuss. Pap. Waste Manag. Hierarchy its Relatsh. to Sustain.*, 2003.

[3] M. A. Martin-Luengo *et al.*, "Biomaterials from beer manufacture waste for bone growth scaffolds," *Green Chem. Lett. Rev.*, 2011.

[4] D. Cree and A. Rutter, "Sustainable bio-inspired limestone eggshell powder for potential industrialized applications," *ACS Sustain. Chem. Eng.*, vol. 3, no. 5, pp. 941–949, 2015.

[5] I. Abdulrahman *et al.*, "From garbage to biomaterials: an overview on egg shell based hydroxyapatite," *J. Mater.*, 2014.

[6] M. Shahbandeh, "Global egg production from 1990 to 2017" - Available online: https://www.statista.com/statistics/263972/egg-production-worldwide-since-1990/. (Accessed on November 25, 2019).

[7] A. Laca, A. Laca, and M. Díaz, "Eggshell waste as catalyst: A review," *Journal of Environmental Management.*, 2017.

[8] D. Oliveira, P. Benelli, and E. Amante, "A literature review on adding value to solid residues: Egg shells," *J. Clean. Prod.*, 2013.

[9] M. Baláž, "Eggshell membrane biomaterial as a platform for applications in materials science," *Acta Biomaterialia.*, 2014.

[10] H. Faridi and A. Arabhosseini, "Application of eggshell wastes as valuable and utilizable products: A review," *Res. Agric. Eng.*, 2018.

[11] S. A. Ghani, A. Zakaria, A. Y. M. Shakaff, M. N. Ahmad, and A. H. Abdullah, "Enhancing conductive polymer performance using eggshell for ammonia sensor," *J. Phys. Sci.*, 2012.

[12] S. Ummartyotin, P. Pisitsak, and C. Pechyen, "Eggshell and bacterial cellulose composite membrane as absorbent material in active packaging," *Int. J. Polym. Sci.*, 2016.

[13] S. Sulaiman and N. I. F. Ruslan, "A heterogeneous catalyst from a mixture of coconut waste and eggshells for biodiesel production," *Energy Sources, Part A Recover. Util. Environ. Eff.*, 2017.

[14] M. J. Quina, M. A. R. Soares, and R. Quinta-Ferreira, “Applications of industrial eggshell as a valuable anthropogenic resource,” *Resour. Conserv. Recycl.*, 2017.

[15] C. M.M. Cordeiro and M. T. Hincke, “Recent Patents on Eggshell: Shell and membrane applications,” *Recent Patents Food, Nutr. Agric.*, 2012.

[16] J. Rovenský, M. Stančíková, P. Masaryk, K. Švík, and R. Ištok, “Eggshell calcium in the prevention and treatment of osteoporosis,” *International Journal of Clinical Pharmacology Research.*, 2003.

[17] T. Yamamoto, L. R. Juneja, H. Hatta, and M. Kim, "Hen Eggs: Their Basic and Applied Science," *Crc Press.*, 1996.

[18] S. Teir, S. Eloneva, and R. Zevenhoven, “Production of precipitated calcium carbonate from calcium silicates and carbon dioxide,” *Energy Convers. Manag.*, 2005.

[19] Y. Karaduman, H. Ozdemir, N. S. Karaduman, and G. Ozdemir, “Interfacial modification of hemp fiber–reinforced composites,” in *Natural and Artificial Fiber-Reinforced Composites as Renewable Sources.*, pp. 17–18, 2018.

[20] B. F. Boukhoulda, E. Adda-Bedia, and K. Madani, “The effect of fiber orientation angle in composite materials on moisture absorption and material degradation after hygrothermal ageing,” *Compos. Struct.*, 2006.

[21] R. F. Gibson, “Principles of composite material mechanics,” *McGraw-Hill Sci.*, pp. 3–7, 1994.

[22] M. Rosso, “Ceramic and metal matrix composites: Routes and properties,” *J. Mater. Process. Technol.*, 2006.

[23] S. Rawal, “Metal-matrix composites for space applications,” *JOM.*, 2001.

[24] Y. B. Liu, S. C. Lim, L. Lu, and M. O. Lai, “Recent development in the fabrication of metal matrix-particulate composites using powder metallurgy techniques,” *J. Mater. Sci.*, 1994.

[25] R. L. Deuis, J. M. Yellup, and C. Subramanian, “Metal-matrix composite coatings by PTA surfacing,” *Compos. Sci. Technol.*, 1998.

[26] J. Goni, I. Mitxelena, and J. Coleto, “Development of low cost metal matrix composites for commercial applications,” *Mater. Sci. Technol.*, 2013.

[27] E. Lester, S. Kingman, K. H. Wong, C. Rudd, S. Pickering, and N. Hilal, “Microwave heating as a means for carbon fibre recovery from polymer composites: A technical

feasibility study," *Mater. Res. Bull.*, 2004.

[28] J. D. Muzzy and A. O. Kays, "Thermoplastic vs. thermosetting structural composites," *Polym. Compos.*, 1984.

[29] G. Greenwood, "The mechanisms of phasetransformations in crystalline solids," *I. M. Monogr., No. 33*, pp. 103, 1963.

[30] S. Schmidt, S. Beyer, H. Knabe, H. Immich, R. Meistring, and A. Gessler, "Advanced ceramic matrix composite materials for current and future propulsion technology applications," in *Acta Astronautica.*, 2004.

[31] J. George, M. S. Sreekala, and S. Thomas, "A review on interface modification and characterization of natural fiber reinforced plastic composites," *Polym. Eng. Sci.*, 2001.

[32] S. R. Dyer, L. V. J. Lassila, M. Jokinen, and P. K. Vallittu, "Effect of fiber position and orientation on fracture load of fiber-reinforced composite," *Dent. Mater.*, 2004.

[33] O. Faruk, A. K. Bledzki, H. P. Fink, and M. Sain, "Biocomposites reinforced with natural fibers: 2000-2010," *Progress in Polymer Science*. 2012.

[34] P. Wambua, J. Ivens, and I. Verpoest, "Natural fibres: Can they replace glass in fibre reinforced plastics?," *Compos. Sci. Technol.*, 2003.

[35] S. Luo and A. N. Netravali, "Mechanical and thermal properties of environment-friendly 'green' composites made from pineapple leaf fibers and poly(hydroxybutyrate-co-valerate) resin," *Polym. Compos.*, 1999.

[36] J. Ogin, S. Brondsted, S. Zangenberg, "Modeling damage, fatigue and failure of composite materials," *Woodhead Publishing.*, pp. 3–9, 2016.

[37] C. L. Wu, M. Q. Zhang, M. Z. Rong, and K. Friedrich, "Silica nanoparticles filled polypropylene: Effects of particle surface treatment, matrix ductility and particle species on mechanical performance of the composites," *Compos. Sci. Technol.*, 2005.

[38] T. Ghabeer, R. Dweiri, and S. Al-Khateeb, "Thermal and mechanical characterization of polypropylene/eggshell biocomposites," *J. Reinf. Plast. Compos.*, 2013.

[39] T. Nakano, N. I. Ikawa, and L. Ozimek, "Chemical composition of chicken eggshell and shell membranes," *Poult. Sci.*, 2003.

[40] Minister of Industry, Poultry and egg statistics. Available online: http://publications.gc.ca/Collection/Statcan/23-015-XIE/23-015-XIE2005001.pdf. (Accessed on November, 25, 2019).

[41] W. J. Stadelman, “Eggs and egg products.,” *Encycl. Food Sci. Technol. 2nd ed; Fr. F. J., Ed.; John Wiley Sons New York.*, pp. 593−599, 2000.

[42] T. Witoon, “Characterization of calcium oxide derived from waste eggshell and its application as $CO_2$ sorbent,” *Ceram. Int.*, 2011.

[43] Z. Wei, C. Xu, and B. Li, “Application of waste eggshell as low-cost solid catalyst for biodiesel production,” *Bioresour. Technol.*, 2009.

[44] M. N. Freire and J. N. F. Holanda, “Characterization of avian eggshell waste aiming its use in a ceramic wall tile paste,” *Cerâmica.*, 2007.

[45] D. Thakre, P. Dixit, S. Waghmare, N. Manwar, N. Labhsetwar, and S. S. Rayalu, “Synthesis optimization and fluoride uptake properties of high capacity composite adsorbent for defluoridation of drinking water,” *Environ. Prog. Sustain. Energy.*, 2015.

[46] P. Intharapat, A. Kongnoo, and K. Kateungngan, “The potential of chicken eggshell waste as a bio-filler filled epoxidized natural rubber (ENR) composite and its properties,” *J. Polym. Environ.*, 2013.

[47] M. M. Bain *et al.*, “Enhancing the egg’s natural defence against bacterial penetration by increasing cuticle deposition,” *Anim. Genet.*, 2013.

[48] X. Chen *et al.*, “Impact of cuticle quality and eggshell thickness on egg antibacterial efficiency,” *Poult. Sci.*, 2019.

[49] C. G. Belyavin and K. N. Boorman, “The influence of the cuticle on egg-shell strength,” *Br. Poult. Sci.*, 1980.

[50] M. T. Hincke, Y. Nys, J. Gautron, K. Mann, A. B. Rodriguez-Navarro, and M. D. McKee, “The eggshell: structure, composition and mineralization.,” *Front. Biosci. (Landmark Ed.*, pp. 1271–1272, 2012.

[51] H.-W. Windhorst, B. Grabkowsky, and A. Wilke, “Atlas of the global egg industry,” 2013.

[52] W. Wu, T. He, J. feng Chen, X. Zhang, and Y. Chen, “Study on in situ preparation of nano calcium carbonate/PMMA composite particles,” *Mater. Lett.*, 2006.

[53] M. Balasubramanian, “Polymer matrix composites,” in *Composite Materials and Processing.*, 2013.

[54] J. R. Potts, D. R. Dreyer, C. W. Bielawski, and R. S. Ruoff, “Graphene-based polymer nanocomposites,” *Polymer.*, 2011.

[55] S. M. Sapuan, M. Harimi, and M. A. Maleque, “Mechanical properties of epoxy/coconut shell filler particle composites,” *Arab. J. Sci. Eng.*, 2003.

[56] J. Móczó and B. Pukánszky, “Particulate fillers in thermoplastics,” in *Encyclopedia of Polymers and Composites.*, 2015.

[57] H. He, Z. Zhang, J. Wang, and K. Li, “Compressive properties of nano-calcium carbonate/epoxy and its fibre composites,” *Compos. Part B Eng.*, 2013.

[58] S. T. Peters, “Hand book of composites, second edition,” *Chapman Hall.*, pp. 48–49, 1998.

[59] Admin3Coxy, “Bio-based epoxy resins,” *ECOXY*, 2019. Available online: https://ecoxy.eu/news/bio-based-epoxy-resins/. (Accessed on November, 25, 2019).

[60] J. L. Massingill and R. S. Bauer, “Epoxy resins,” in *Applied Polymer Science: 21st Century.*, 2000.

[61] C. François *et al.*, “Design and synthesis of biobased epoxy thermosets from biorenewable resources,” *Comptes Rendus Chim.*, 2017.

[62] P. Khemthong *et al.*, “Industrial eggshell wastes as the heterogeneous catalysts for microwave-assisted biodiesel production,” *Catal. Today.*, 2012.

[63] N. Viriya-empikul, P. Krasae, B. Puttasawat, B. Yoosuk, N. Chollacoop, and K. Faungnawakij, “Waste shells of mollusk and egg as biodiesel production catalysts,” *Bioresour. Technol.*, 2010.

[64] H. J. Park, S. W. Jeong, J. K. Yang, B. G. Kim, and S. M. Lee, “Removal of heavy metals using waste eggshell,” *J. Environ. Sci.*, 2007.

[65] J. Kim and J. M. Oh, “Trace element concentrations in eggshells and egg contents of black-tailed gull (Larus crassirostris) from Korea,” *Ecotoxicology.*, 2014.

[66] F. A. Al-Obaidi, “Comparative study of egg morphology, components and chemical composition of some pheasant groups reared in Baghdad,” *J. Genet. Environ. Resour. Conserv. J. Gene c Environ. Resour. Conserv.*, 2017.

[67] T. P. Mohan and K. Kanny, “Thermal, mechanical and physical properties of nanoegg shell particle-filled epoxy nanocomposites,” *J. Compos. Mater.*, 2018.

[68] K. A. Iyer and J. M. Torkelson, “Green composites of polypropylene and eggshell: Effective biofiller size reduction and dispersion by single-step processing with solid-state shear pulverization,” *Compos. Sci. Technol.*, 2014.

[69] N. A. N. Azman, M. R. Islam, M. Parimalam, N. M. Rashidi, and M. Mupit, “Mechanical, structural, thermal and morphological properties of epoxy composites filled with chicken eggshell and inorganic $CaCO_3$ particles,” *Polym. Bull.*, 2019.

[70] J. W. de L. Souza, N. G. Jaques, M. Popp, J. Kolbe, M. V. L. Fook, and R. M. R. Wellen, “Optimization of epoxy resin: An investigation of eggshell as a synergic filler,” *Materials (Basel).*, 2019.

[71] L. Jiang, J. Zhang, and M. P. Wolcott, “Comparison of polylactide/nano-sized calcium carbonate and polylactide/montmorillonite composites: Reinforcing effects and toughening mechanisms,” *Polymer (Guildf).*, 2007.

[72] J. Cho, M. S. Joshi, and C. T. Sun, “Effect of inclusion size on mechanical properties of polymeric composites with micro and nano particles,” *Compos. Sci. Technol.*, 2006.

[73] H. B. Kaybal, H. Ulus, and A. Avci, “Influence of Nano-$CaCO_3$ Particles on Shear Strength of Epoxy Resin Adhesives,” *Uluslararası Muhendis. Arastirma ve Gelistirme Derg.*, 2017.

[74] E. H. Backes, T. S. Sene, F. R. Passador, and L. A. Pessan, “Electrical, thermal and mechanical properties of epoxy/ENT/calcium carbonate nanocomposites,” *Mater. Res.*, 2017.

[75] G. Ji, H. Zhu, C. Qi, and M. Zeng, “Mechanism of interactions of eggshell microparticles with epoxy resins,” *Polym. Eng. Sci.*, pp. 1383–1387, 2009.

[76] A. H. Shah *et al.*, “Reinforcement of stearic acid treated egg shell particles in epoxy thermosets: Structural, thermal, and mechanical characterization,” *Materials (Basel).*, vol. 11, no. 10, 2018.

[77] K. Riew, C. Gillham, “Rubber-modified thermoset resins,” *J. Polym. Sci. Part C Polym. Lett.*, pp. 388, 1986.

[78] S. B. Hassan, V. S. Aigbodion, and S. N. Patrick, “Development of polyester/eggshell particulate composites,” *Tribol. Ind.*, 2012.

[79] G. M. Shafiur Rahman, H. Aftab, M. Shariful Islam, M. Z. Bin Mukhlish, and F. Ali, “Enhanced physico-mechanical properties of polyester resin film using $CaCO_3$ filler,” *Fibers Polym.*, 2016.

[80] K. Oksman and C. Clemons, “Mechanical properties and morphology of impact modified polypropylene-wood flour composites,” *J. Appl. Polym. Sci.*, 1998.

[81] P. Toro, R. Quijada, M. Yazdani-Pedram, and J. L. Arias, “Eggshell, a new bio-filler for polypropylene composites,” *Mater. Lett.*, 2007.

[82] R. Kumar, J. S. Dhaliwal, G. S. Kapur, and Shashikant, “Mechanical properties of modified biofiller-polypropylene composites,” *Polym. Compos.*, 2014.

[83] T. Boronat, V. Fombuena, D. Garcia-Sanoguera, L. Sanchez-Nacher, and R. Balart, “Development of a biocomposite based on green polyethylene biopolymer and eggshell,” *Mater. Des.*, 2015.

[84] H. Huang, “Structure development and property changes in high density polyethylene during pan-milling,” *J. Appl. Polym. Sci.*, 2000.

[85] W. C. J. Zuiderduin, C. Westzaan, J. Huétink, and R. J. Gaymans, “Toughening of polypropylene with calcium carbonate particles,” *Polymer (Guildf).*, 2002.

[86] H. P. Schlumpf and W. Bilogan, “Natural calcium carbonate as polymer filler, new developments in filled thermoplastics, duroplastics and elastomers,” *Kunstoffe.*, 1983.

[87] S. C. Nwanonenyi and C. O. Chike-Onyegbula, “Water absorption, flammability and mechanical properties of linear low density polyethylene/egg shell composite,” *Acad. Res. Int.*, 2013.

[88] S. C. Nwanonenyi, M. U. Obidiegwu, T. S. Onuchukwu, and I. C. Egbuna, “Studies on the properties of linear low density polyethylene filled oyster shell powder,” *Int. J. Eng. Sci.*, 2013.

[89] P. Kamalbabu and G. C. M. Kumar, “Effects of particle size on tensile properties of marine coral reinforced polymer composites,” *Procedia Mater. Sci.*, 2014.

[90] R. Kevin, “Methods for treating metabolic disorders,” *United States Pat.*, 2015.

[91] D. P. Frank Daniel Long, Neosho. ; Randall, Gene Adams; Carthage, C. DeVore, and M. R. Franklin, “Therapeutic, nutraceutical and cosmetic applications foreggshell membrane and processed eggshell membrane preparations,” *United States Pat.*, 2008.

[92] M. Gaonkar and P. Chakraborty, “Application of eggshell as fertilizer and calcium supplement tablet,” *Int. J. Innov. Res. Sci. Eng. Technol.*, 2016.

[93] G. B. Dafal and N. K. Khare, “Formulation and evaluation of toothpaste by using eggshells,” *World J. Pharm. Res.*, 2017.

[94] S. Yoo, J. S. Hsieh, P. Zou, and J. Kokoszka, “Utilization of calcium carbonate particles from eggshell waste as coating pigments for ink-jet printing paper,” *Bioresour. Technol.*,

2009.

[95] M. Anton, F. Nau, and Y. Nys, “Bioactive egg components and their potential uses,” *Worlds. Poult. Sci. J.*, pp. 62, 2006.

[96] X. Guo *et al.*, “Layered double hydroxide/eggshell membrane: An inorganic biocomposite membrane as an efficient adsorbent for Cr(VI) removal,” *Chem. Eng. J.*, 2011.

[97] M. Cusack and A. C. Fraser, “Eggshell membrane removal for subsequent extraction of intermineral and intramineral proteins,” *Cryst. Growth Des.*, 2002.

[98] K. J. Ruff, A. Winkler, R. W. Jackson, D. P. DeVore, and B. W. Ritz, “Eggshell membrane in the treatment of pain and stiffness from osteoarthritis of the knee: A randomized, multicenter, double-blind, placebo-controlled clinical study,” *Clin. Rheumatol.*, 2009.

[99] K. J. Ruff, D. P. DeVore, M. D. Leu, and M. A. Robinson, “Eggshell membrane: a possible new natural therapeutic for joint and connective tissue disorders. Results from two open-label human clinical studies.,” *Clin. Interv. Aging.*, 2009.

[100] G. D. Mogoşanu and A. M. Grumezescu, “Natural and synthetic polymers for wounds and burns dressing,” *Int. J. Pharm.*, 2014.

[101] M. K. Sah and S. N. Rath, “Soluble eggshell membrane: A natural protein to improve the properties of biomaterials used for tissue engineering applications,” *Materials Science and Engineering C.*, 2016.

[102] J. MacNeil, “Method and apparatus for separating a protein membrane and shell material in waste egg shells,” *United States Pat.*, 2003.

[103] Y. Tsuboi and N. Koga, “Thermal decomposition of biomineralized calcium carbonate: correlation between the thermal behavior and structural characteristics of avian eggshell,” *ACS Sustain. Chem. Eng.*, 2018.

[104] L. J. Roberto, V. Floh; Sergio, “Apparatus for separating the organic membrane portion and the mineral portion of broken egg shells,” *United States Pat.*, 2009.

[105] N. Koga, D. Kasahara, and T. Kimura, “Aragonite crystal growth and solid-state aragonite-calcite transformation: A physico-geometrical relationship via thermal dehydration of included water,” *Cryst. Growth Des.*, pp. 2237–2245, 2013.

[106] W. S. Rasband, “ImageJ, U.S. national institutes of health, Bethesda, Maryland, USA,” Available online: https://imagej.nih.gov/ij/. (Accessed on November, 25, 2019).

[107] I. Haq, A. Rab, and M. Sajid, “Foliar application of calcium chloride and borax enhance the fruit quality of litchi cultivars,” *J. Anim. Plant Sci.*, vol. 23, no. 5, pp. 1385–1390, 2013.

[108] Y. Wang, S. Krishna, and J. Golledge, “The calcium chloride-induced rodent model of abdominal aortic aneurysm,” *Atherosclerosis*. 2013.

[109] A. Ajisawa, “Dissolution aqueous of silk fibroin with calciumchloride/ethanol solution,” *J. Sericultural Sci. Japan.*, 1997.

[110] ASTM, “D638-14-standard test method for tensile properties of plastics,” *ASTM Stand.*, 2014.

[111] ASTM, "D790-17 standard test method for determining the charpy impact resistance of notched specimens of plastics," *ASTM Stand.*, 2018.

[112] ASTM, “D790-17-standard test method for flexural properties of unreinforced and reinforced plastics and electrical insulation materials,” *ASTM Stand.*, 2017.

[113] E. I. Akpan, X. Shen, B. Wetzel, and K. Friedrich, “Design and Synthesis of Polymer Nanocomposites,” in *Polymer Composites with Functionalized Nanoparticles.*, 2019.

[114] ASTM, “D792 − 13: Standard Test Methods for Density and Specific Gravity (Relative Density) of Plastics by Displacement,” *ASTM Stand.*, 2013.

[115] D. S. Prasad, C. Shoba, and N. Ramanaiah, “Investigations on mechanical properties of aluminum hybrid composites,” *J. Mater. Res. Technol.*, 2014.

[116] M. L. Costa, S. F. M. d. Almeida, and M. C. Rezende, “The influence of porosity on the interlaminar shear strength of carbon/epoxy and carbon/bismaleimide fabric laminates,” *Compos. Sci. Technol.*, 2001.

[117] K. J. Bowles and S. Frimpong, “Void Effects on the interlaminar shear strength of unidirectional graphite-fiber-reinforced composites,” *J. Compos. Mater.*, 1992.

[118] N. Yu, Z. H. Zhang, and S. Y. He, “Fracture toughness and fatigue life of MWCNT/epoxy composites,” *Mater. Sci. Eng. A.*, 2008.

[119] K. C. Richardson, L. Jarett, and E. H. Finke, “Embedding in epoxy resins for ultrathin sectioning in electron microscopy,” *Biotech. Histochem.*, 1960.

[120] W. Liu, S. V. Hoa, and M. Pugh, “Fracture toughness and water uptake of high-performance epoxy/nanoclay nanocomposites,” *Compos. Sci. Technol.*, 2005.

[121] ASTM, “D570-98 (2018)-standard test for water absorption of plastics,” *ASTM Stand.*,

2018.

[122] L. Banta, K. Cheng, and J. Zaniewski, “Estimation of limestone particle mass from 2D images,” *Powder Technol.*, vol. 132, pp. 184–189, 2003.

[123] S. Lin, T. Kiga, Y. Wang, and K. Nakayama, “Energy analysis of $CaCO_3$ calcination with $CO_2$ capture,” in *Energy Procedia.*, 2011.

[124] R. S. Treptow, “Conservation of mass: Fact or fiction?,” *J. Chem. Educ.*, 2009.

[125] D. Cree and P. Pliya, “Effect of elevated temperature on eggshell, eggshell powder and eggshell powder mortars for masonry applications,” *J. Build. Eng.*, 2019.

[126] F. Yi, Z. X. Guo, P. Hu, Z. X. Fang, J. Yu, and Q. Li, “Mimetics of eggshell membrane protein fibers by electrospinning,” *Macromol. Rapid Commun.*, 2004.

[127] W. T. Tsai, J. M. Yang, C. W. Lai, Y. H. Cheng, C. C. Lin, and C. W. Yeh, “Characterization and adsorption properties of eggshells and eggshell membrane,” *Bioresour. Technol.*, 2006.

[128] S. B. Hassan and V. S. Aigbodion, “Effects of eggshell on the microstructures and properties of Al–Cu–Mg/eggshell particulate composites,” *J. King Saud Univ. - Eng. Sci.*, 2015.

[129] S. P. Dwivedi, S. Sharma, and R. K. Mishra, “A comparative study of waste eggshells, $CaCO_3$ , and SiC-reinforced AA2014 green metal matrix composites,” *J. Compos. Mater.*, 2017.

[130] M. T. Hincke, “The eggshell: structure, composition and mineralization,” *Front. Biosci.*, 2012.

[131] M. P. Richards, “Trace mineral metabolism in the avian embryo,” *Poult. Sci.*, 1997.

[132] Y. Zhang, W. Wang, L. Li, Y. Huang, and J. Cao, “Eggshell membrane-based solid-phase extraction combined with hydride generation atomic fluorescence spectrometry for trace arsenic(V) in environmental water samples,” *Talanta.*, 2010.

[133] D. W. Ball, J. W. Hill, and R. J. Scott, "Introduction to Chemistry: General, Organic, and Biological". *Creative Commons.*, pp. 770–782, 2011.

[134] J. Ervina, M. Mariatti, and S. Hamdan, “Effect of filler loading on the tensile properties of multi-walled carbon nanotube and graphene nanopowder filled epoxy composites,” *Procedia Chem.*, 2016.

[135] S. Shuhadah and S. Ghani, “LDPE-Isophthalic acid-modified egg shell powder,” *J. Phys.*

*Sci.*, 2009.

[136] H. Nasution, A. Tantra, and P. Arista, "The effect of filler content and particle size on the impact strength and water absorption of epoxy/cockleshell powder (anadora granosa) composite," *ARPN J. Eng. Appl. Sci.*, 2016.

[137] H. Salmah, S. C. Koay, and O. Hakimah, "Surface modification of coconut shell powder filled polylactic acid biocomposites," *J. Thermoplast. Compos. Mater.*, pp. 809–819, 2013.

[138] Z. Cao *et al.*, "Chemical surface modification of calcium carbonate particles with stearic acid using different treating methods," *Appl. Surf. Sci.*, 2016.

[139] C. M. Vu, L. H. Sinh, H. J. Choi, and T. D. Pham, "Effect of micro/nano white bamboo fibrils on physical characteristics of epoxy resin reinforced composites," *Cellulose*, 2017.

[140] Entropy resins, Technical data sheet-SUPER SAP® CPM system. Available online: https://wjayc3fs2tlk6mip9ccjq208-wpengine.netdna-ssl.com/wp-content/uploads/CPM-TDS-v2.pdf (Accessed on November, 25, 2019).

[141] Y. S. Song and J. R. Youn, "Influence of dispersion states of carbon nanotubes on physical properties of epoxy nanocomposites," *Carbon N. Y.*, 2005.

[142] F. Yi, Z. X. Guo, L. X. Zhang, J. Yu, and Q. Li, "Soluble eggshell membrane protein: Preparation, characterization and biocompatibility," *Biomaterials.*, 2004.

[143] Vladimir Vlad and V. Vlad, "Avian eggshell membrane polypeptide extraction via fermentation process," *United States Pat.*, 2007.

[144] W. Qiu, K. Mai, and H. Zeng, "Effect of silane-grafted polypropylene on the mechanical properties and crystallization behavior of Talc/polypropylene composites," *J. Appl. Polym. Sci.*, 2000.

[145] Y. W. Leong, M. B. Abu Bakar, Z. A. M. Ishak, A. Ariffin, and B. Pukanszky, "Comparison of the mechanical properties and interfacial interactions between talc, kaolin, and calcium carbonate filled polypropylene composites," *J. Appl. Polym. Sci.*, 2004.

[146] B. J. Tiimob, S. Jeelani, and V. K. Rangari, "Eggshell reinforced biocomposite - An advanced 'green' alternative structural material," *J. Appl. Polym. Sci.*, 2016.

[147] P. Toro, R. Quijada, J. L. Arias, and M. Yazdani-Pedram, "Mechanical and morphological studies of poly(propylene)-filled eggshell composites," *Macromol. Mater. Eng.*, 2007.

[148] M. Fridland and R. Rosado, “Mineral trioxide aggregate (MTA) solubility and porosity with different water-to-powder ratios,” *J. Endod.*, 2003.

[149] S. F. D’Souza, J. Kumar, S. K. Jha, and B. S. Kubal, “Immobilization of the urease on eggshell membrane and its application in biosensor,” *Mater. Sci. Eng. C.*, 2013.

[150] B. H. León-Mancilla, M. A. Araiza-Téllez, J. O. Flores-Flores, and M. C. Piña-Barba, “Physico-chemical characterization of collagen scaffolds for tissue engineering,” *J. Appl. Res. Technol.*, 2016.

[151] M. L. Di Lorenzo, M. E. Errico, and M. Avella, “Thermal and morphological characterization of poly(ethylene terephthalate)/calcium carbonate nanocomposites,” *J. Mater. Sci.*, 2002.

[152] Alberta Egg Industry, Available online: http://eggs.ab.ca/about/press-releases/alberta-egg-industry-celebrates-opening-of-egg-breaking-plant/. (Accessed on November, 25, 2019).

[153] Landfill rates, Available online: https://www.calgary.ca/UEP/WRS/Pages/Landfill-information/Landfill-Rates.aspx. (Accessed on November, 25, 2019).

**APPENDIX A**

ICP-MS results of elements in eggshell and purified eggshell at different temperature and time

| Powder type | Analyte | Weight of element- µg/gm |
|---|---|---|
| Pure eggshell | Calcium ($CaCO_3$) | 349000 (87.3%) |
| Purified eggshell at 500 °C for 2 h | Calcium ($CaCO_3$) | 331000 (82.8%) |
| Purified eggshell at 600 °C for 2 h | Calcium ($CaCO_3$) | 351000 (87.8%) |
| Purified eggshell at 850 °C for 1 h | Calcium ($CaCO_3$) | 380000 (95%) |
| Purified eggshell at 850 °C for 1 h | Barium | 14 |
| Purified eggshell at 850 °C for 1 h | Boron | 31 |
| Purified eggshell at 850 °C for 1 h | Chromium | 0.23 |
| Purified eggshell at 850 °C for 1 h | Cobalt | 1.5 |
| Purified eggshell at 850 °C for 1 h | Copper | 145 |
| Purified eggshell at 850 °C for 1 h | Iron | 58 |
| Purified eggshell at 850 °C for 1 h | Lead | 0.76 |
| Purified eggshell at 850 °C for 1 h | Magnesium | 2640 |
| Purified eggshell at 850 °C for 1 h | Manganese | 0.62 |
| Purified eggshell at 850 °C for 1 h | Nickel | 0.33 |
| Purified eggshell at 850 °C for 1 h | Phosphorus | 1300 |
| Purified eggshell at 850 °C for 1 h | Potassium | 34 |
| Purified eggshell at 850 °C for 1 h | Sodium | 260 |
| Purified eggshell at 850 °C for 1 h | Strontium | 176 |
| Purified eggshell at 850 °C for 1 h | Zinc | 57 |

## APPENDIX B

Copyright permission for the images used in literature review (chapter 2).



**ELSEVIER LICENSE**
**TERMS AND CONDITIONS**

Sep 13, 2019

This Agreement between Gaurang Golakiya ("You") and Elsevier ("Elsevier") consists of your license details and the terms and conditions provided by Elsevier and Copyright Clearance Center.

| | |
|---|---|
| License Number | 4667170556076 |
| License date | Sep 13, 2019 |
| Licensed Content Publisher | Elsevier |
| Licensed Content Publication | Catalysis Today |
| Licensed Content Title | Industrial eggshell wastes as the heterogeneous catalysts for microwave-assisted biodiesel production |
| Licensed Content Author | P. Khemthong,C. Luadthong,W. Nualpaeng,P. Changsuwan,P. Tongprem,N. Viriya-empikul,K. Faungnawakij |
| Licensed Content Date | Aug 1, 2012 |
| Licensed Content Volume | 190 |
| Licensed Content Issue | 1 |
| Licensed Content Pages | 5 |
| Start Page | 112 |
| End Page | 116 |
| Type of Use | reuse in a thesis/dissertation |
| Intended publisher of new work | other |
| Portion | figures/tables/illustrations |
| Number of figures/tables/illustrations | 1 |
| Format | both print and electronic |
| Are you the author of this Elsevier article? | No |
| Will you be translating? | No |
| Original figure numbers | Figure 1 |
| Title of your thesis/dissertation | Mechanical Engineering |
| Publisher of new work | University of Saskatchewan |
| Expected completion date | Sep 2019 |
| Estimated size (number of pages) | 1 |
| Requestor Location | Gaurang Golakiya<br>307, 714 Appleby drive<br><br>Saskatoon, SK S7M 4N7<br>Canada<br>Attn: |

**ELSEVIER LICENSE**
**TERMS AND CONDITIONS**

Sep 13, 2019

This Agreement between Gaurang Golakiya ("You") and Elsevier ("Elsevier") consists of your license details and the terms and conditions provided by Elsevier and Copyright Clearance Center.

| | |
|---|---|
| License Number | 4667171173746 |
| License date | Sep 13, 2019 |
| Licensed Content Publisher | Elsevier |
| Licensed Content Publication | Journal of Environmental Sciences |
| Licensed Content Title | Removal of heavy metals using waste eggshell |
| Licensed Content Author | Heung Jai PARK,Seong Wook JEONG,Jae Kyu YANG,Boo Gil KIM,Seung Mok LEE |
| Licensed Content Date | Jan 1, 2007 |
| Licensed Content Volume | 19 |
| Licensed Content Issue | 12 |
| Licensed Content Pages | 6 |
| Start Page | 1436 |
| End Page | 1441 |
| Type of Use | reuse in a thesis/dissertation |
| Intended publisher of new work | other |
| Portion | figures/tables/illustrations |
| Number of figures/tables/illustrations | 1 |
| Format | both print and electronic |
| Are you the author of this Elsevier article? | No |
| Will you be translating? | No |
| Original figure numbers | Table 2 |
| Title of your thesis/dissertation | Mechanical Engineering |
| Publisher of new work | University of Saskatchewan |
| Expected completion date | Sep 2019 |
| Estimated size (number of pages) | 1 |
| Requestor Location | Gaurang Golakiya<br>307, 714 Appleby drive<br><br>Saskatoon, SK S7M 4N7<br>Canada<br>Attn: |
| Publisher Tax ID | GB 494 6272 12 |

## RE: Permission to cite image from US 20030136711 A1 patent

Swope, Bradley <bas101@psu.edu>
Mon 7/29/2019 7:59 AM
**To:** Golakiya, Gaurang <gaurang.golakiya@usask.ca>

Hi Gaurang,

Thanks for checking.

You may the image for your master's thesis.

Brad

---

Bradley A. Swope
Associate Director
Penn State Office of Technology Management
bradswope@psu.edu
(814) 863-5987 (direct)
(814) 865-6277 (main office #)
(814) 865-3591 (fax)
113 Technology Center
University Park, PA 16802
[www.research.psu.edu/offices/otm]www.research.psu.edu/offices/otm

Protecting Your Penn State Invention: https://www.research.psu.edu/otm/inventors
PSU Technologies Available for Licensing: https://invent.psu.edu/program/intellectual-property-navigator/

---

**From:** Golakiya, Gaurang <gaurang.golakiya@usask.ca>
**Sent:** Friday, July 26, 2019 4:02 PM
**To:** Swope, Bradley <bas101@psu.edu>
**Subject:** Permission to cite image from US 20030136711 A1 patent

Hello Bradley,

This is Gaurang Golkaiya doing MSc in Mechanical Engineering from University of Saskatchewan, Saskatoon, Canada. In my thesis writing, I want to reuse one figure from Penn State patent article. The details of the patent is given below.

Title: Method and apparatus for separating a protein membrane and shell material in waste egg shells.
Image on first page (Attached screenshot for you reference)
Document Number: US 20030136711 A1

As per our university policy, I need approval from author (or publishing organization) before reusing in any article. And I saw your name on Penn state website as Licensing Officer. So can you please provide me a permission to use this image for my master's thesis.

Thank you

Gaurang Golakiya

| | |
|---|---|
| **Title:** | Thermal Decomposition of Biomineralized Calcium Carbonate: Correlation between the Thermal Behavior and Structural Characteristics of Avian Eggshell |
| **Author:** | Yoji Tsuboi, Nobuyoshi Koga |
| **Publication:** | ACS Sustainable Chemistry & Engineering |
| **Publisher:** | American Chemical Society |
| **Date:** | Apr 1, 2018 |



**PERMISSION/LICENSE IS GRANTED FOR YOUR ORDER AT NO CHARGE**

This type of permission/license, instead of the standard Terms & Conditions, is sent to you because no fee is being charged for your order. Please note the following:

- Permission is granted for your request in both print and electronic formats, and translations.
- If figures and/or tables were requested, they may be adapted or used in part.
- Please print this page for your records and send a copy of it to your publisher/graduate school.
- Appropriate credit for the requested material should be given as follows: "Reprinted (adapted) with permission from (COMPLETE REFERENCE CITATION). Copyright (YEAR) American Chemical Society." Insert appropriate information in place of the capitalized words.
- One-time permission is granted only for the use specified in your request. No additional uses are granted (such as derivative works or other editions). For any other uses, please submit a new request.

If credit is given to another source for the material you requested, permission must be obtained from that source.

BACK CLOSE WINDOW